

Development of Laser-Induced Breakdown Spectroscopy as a Rapid Diagnostic
Tool for Bacterial Infection

By

Alexandra E. Paulick

A Thesis
Submitted to the Faculty of Graduate Studies
through the **Department of Physics**
in Partial Fulfillment of the Requirements for
the Degree of **Master of Science**
at the University of Windsor

Windsor, Ontario, Canada

2018

© 2018 Alexandra E. Paulick

Development of Laser-Induced Breakdown Spectroscopy as a Rapid Diagnostic
Tool for Bacterial Infection

By

Alexandra E. Paulick

APPROVED BY:

A. V. Hubberstey
Department of Biological Sciences

D. Xiao
Department of Physics

S. J. Rehse, Advisor
Department of Physics

December 13, 2018

Declaration of Originality

I hereby certify that I am the sole author of this thesis and that no part of this thesis has been published or submitted for publication.

I certify that, to the best of my knowledge, my thesis does not infringe upon anyone's copyright nor violate any proprietary rights and that any ideas, techniques, quotations, or any other material from the work of other people included in my thesis, published or otherwise, are fully acknowledged in accordance with the standard referencing practices. Furthermore, to the extent that I have included copyrighted material that surpasses the bounds of fair dealing within the meaning of the Canada Copyright Act, I certify that I have obtained a written permission from the copyright owner(s) to include such material(s) in my thesis and have included copies of such copyright clearances to my appendix.

I declare that this is a true copy of my thesis, including any final revisions, as approved by my thesis committee and the Graduate Studies office, and that this thesis has not been submitted for a higher degree to any other University or Institution.

Abstract

A rapid elemental analysis technique known as laser-induced breakdown spectroscopy (LIBS) has been shown to be a promising tool for detection and identification of pathogens. The aim of this work was to demonstrate the feasibility of the LIBS technique as a point-of-care diagnostic tool for bacterial infection. A size-based technique for separating bacteria from unwanted material that could be present in a clinical specimen was developed using a custom-built centrifuge tube insert device. Tungsten powder was used to simulate unwanted contaminants in a bacterial suspension, all of which was removed from suspension while ~90% of the bacteria were successfully separated from the contaminant. A new bacterial mounting procedure was developed by designing and constructing a small aluminum cone for use with the centrifuge tube insert. The bacterial limit of detection for this new mounting procedure was calculated to be ~5000 CFU per laser shot location – an order of magnitude improvement from previous mounting procedures. Methods to reduce the measured shot-to-shot variation assumed to be caused by uneven deposition of the bacteria using either the detergent Tween 20 or growth of bacteria in a liquid culture medium were investigated. No significant effect was observed. The ability to detect bacteria that were collected using common pathology swabs to more closely simulate the collection of some clinical specimens was also investigated. The efficiency of bacterial cell pick-up with a swab and subsequent shake-off prior to LIBS testing was determined. Protocols for collecting bacteria from swabs were developed and a study of the resulting LIBS emission as a function of bacterial coverage was conducted using the new mounting procedure.

Acknowledgements

This thesis is the result of contributions from various people and would not have been possible without their help.

Most importantly, I would like to thank my advisor, Dr. Steven Rehse, for his hours spent teaching me; his guidance with this research; and for always offering advice, whether it was related to this research or not. None of this would have been possible without him.

I would also like to thank our group's previous Master's student, Dylan Malenfant for bringing me up to speed on this project and showing me what to do. Thank you to Mark Armstrong, Kevin Beaugrand, and Doris Rusu who performed most of the experiments for Chapter 7.

In addition, I would like to thank the other members of this research group as well as friends and family who have offered suggestions and supported me during the best and worst times over the course of my graduate studies.

Table of Contents

Declaration of Originality.....	iii
Abstract.....	iv
Acknowledgements.....	v
List of Tables.....	x
List of Figures.....	xi
List of Abbreviations.....	xvi
Chapter 1: Introduction.....	1
1.1 Motivation.....	1
1.2 Laser-Induced Breakdown Spectroscopy.....	2
1.3 Overview of Previous Results for LIBS on Bacterial Samples.....	3
1.4 Scope of Thesis.....	8
References.....	10
Chapter 2: Laser-Induced Breakdown Spectroscopy and Apparatus.....	12
2.1 Laser-Induced Breakdown Spectroscopy.....	12
2.1.1 Atomic Transitions.....	12
2.1.2 Plasma Formation.....	13
2.1.3 Plasma Emissions.....	14
2.1.4 Plasma Parameters.....	16
2.2 LIBS Apparatus.....	19
2.2.1 Delivery of Laser Pulse to Target.....	19
2.2.2 Detection of Light from the Plasma.....	22
2.2.3 Steel Calibration.....	26

References.....	29
Chapter 3: Bacterial Physiology and Sample Preparation.....	30
3.1 Bacterial Physiology.....	30
3.2 Bacterial Species used in this work for LIBS Testing.....	33
3.3 Bacterial Sample Preparation.....	35
3.3.1 Preparation of Growth Media and Harvesting of Bacteria.....	35
3.3.2 Target Preparation.....	36
3.3.2.1 Well-Plate.....	37
3.3.2.2 Insert.....	39
References.....	45
Chapter 4: Technique to Separate a Contaminant from a Bacterial Suspension.....	46
4.1 Introduction.....	46
4.2 Method.....	46
4.3 Experiments and Results.....	48
References.....	52
Chapter 5: Effect of Metal Cone in Target Preparation.....	53
5.1 Motivation.....	53
5.2 Design.....	54
5.3 Bacterial Concentration.....	54
5.4 Comparison of LIBS Signal from Targets Prepared with Metal Cone, Well-plate, and Insert.....	56
5.5 Limit of Detection.....	58
5.5.1 Introduction.....	58
5.5.2 Experiment and Results.....	60

References.....	63
Chapter 6: Effects of Tween 20 and Growth in Liquid Culture on the LIBS Analysis of <i>E. coli</i> Cells.....	64
6.1 Introduction.....	64
6.1.1 Motivation.....	64
6.1.2 Tween 20.....	65
6.1.3 Liquid Culture.....	66
6.2 Experiments and Results.....	66
6.2.1 Investigation of the Effect on the LIBS Bacterial Signal of <i>E. coli</i> Cells Treated with Tween 20.....	66
6.2.2 Effect of Growing <i>E. coli</i> in Liquid Medium to Reduce Inconsistencies in the LIBS Bacterial Signal.....	73
6.3 Conclusion.....	76
References.....	78
Chapter 7: LIBS Analysis of Bacteria Collected with Swabs.....	79
7.1 Introduction.....	79
7.1.1 Motivation.....	79
7.1.2 Flocked Swabs.....	79
7.2 Determination of Vortex Time Required for Maximum Release of Sample from Swab.....	80
7.3 Determination of Amount of Cells Released from Swab.....	82
7.4 Absorbance Values and LIBS Intensity.....	84
7.5 LIBS Analysis of Samples Collected from Swabbing Bacteria off a Metal Plate.....	85
References.....	91
Chapter 8: Conclusions and Future Work.....	92

8.1 Conclusions.....	92
8.2 Future Work.....	94
Vita Auctoris.....	99

List of Tables

Table 3.1: Regularly observed spectral lines in bacterial LIBS spectra in this work.....	31
Table 3.2: A list of bacterial species investigated in LIBS experiments to date.....	41
Table 7.1: Absorbance values for the different dilutions of <i>E. coli</i>	86

List of Figures

Figure 1.1: Typical LIBS spectrum of <i>M. smegmatis</i> (Adapted from Rehse et al., reference 20).....	5
Figure 1.2: DFA of 669 LIBS spectra classified into: (a) five groups according to genus and (b) thirteen groups according to taxonomic classification. Each data point represents one spectrum. The symbols of the thirteen groups in (b) are the same as the symbols for their genus classification in (a). (Adapted from Mohaidat et al., reference 21).....	7
Figure 2.1: Schematic of the formation of a LIBS plasma. (a) Target is rapidly heated by absorbing the incident laser energy. (b) Target material is vaporized, leaving behind a crater in the target and generating a cloud of atoms above the target surface. (c) The cloud of atoms absorbs the remaining part of the laser pulse, ionizing the atoms and creating a plasma. (d) The plasma cools and emits photons which are characteristic of the elements vaporized in the target material.....	14
Figure 2.2: Temporal evolution of a LIBS plasma.....	15
Figure 2.3: Spectrum from emission from bacterial plasma (black) overlaid with spectrum from emission from fish otolith (red) zoomed in on the Ca 393 line. Stark broadening is apparent in the emission line for the otolith spectrum.....	18
Figure 2.4: (a) Overhead schematic of the optical train used to direct laser pulses to the target. (b) Schematic side view of laser pulses emerging from the iris and directed to a target which is mounted on a steel piece.....	20
Figure 2.5: Side view of an échelle grating. The quantities α , β , and d are described below.....	22
Figure 2.6: (a) Échellogram for the emissions from a steel target piece. (b) Zoomed-in section of the échellogram. (c) Resultant spectrum.....	24
Figure 2.7: Schematic of the Échelle spectrometer ¹¹	25

Figure 2.8: ROI view from ESAWIN software. The line plot in red is the intensity as a function of the X-pixel coordinates for 60 pixels. The vertical green line depicts the center of the peak according to ESAWIN, and the blue line below and to the right of the vertical green line shows the expected location of an emission line according to the NIST atomic database. The horizontal green lines designate the background and the FWHM. The text in the upper left corner denotes the element. The numbers in the upper right, from top to bottom, denote the ratio of the peak area to some reference line (not used in this work) and the peak area. Numbers below the window are wavelengths in nm. Below the window shows the portion of the échellogram corresponding to that ROI.....27

Figure 3.1: TSA plate: (a) before addition of bacteria (*E. coli*) and (b) after incubation with bacteria. Bacteria grow in an even layer across the surface of the TSA medium. The black markings in (b) are from the labeling of the bottom of the petri dish.....36

Figure 3.2: (a) Well-plate sitting on top of a filter paper with bacterial suspension in each of the three wells. (b) Filter paper after well-plate is removed. Three bacterial lawns are evident.....37

Figure 3.3: (a) Typical LIBS spectrum acquired from a blank filter. (b) Typical LIBS spectrum acquired from a filter with *E. coli* on it.....38

Figure 3.4: 3-D printed insert. (a) Main body and base of insert. (b) Filter paper sitting on top of the base. (c) The base screwed into the bottom of the main body. (d) The insert sitting inside a centrifuge tube.....40

Figure 4.1: Centrifuge tube insert device with the main body of the insert alongside two base pieces in (a), all pieces screwed together in (b) and sitting inside a centrifuge tube in (c). Black lines in (b) show approximate location of where filter papers sit inside the insert.....47

Figure 4.2: (a) Images of the filter papers after centrifugation through the insert device. Black spots on 5 μm filter are tungsten powder. (b) Spectrum from 5 μm filter (black)

overlaid with spectrum from 0.45 μ m filter (red). Tungsten emission lines in 5 μ m filter are evident and bacterial emission lines in 0.45 μ m filter are evident.....48

Figure 4.3: Average total LIBS intensity of the 5 μ m and 0.45 μ m filters for three bacterial suspensions. Error bars represent one standard deviation in the measurements.....50

Figure 5.1: (a) Metal cone. (b) Insert with filter paper placed on the base. (c) Metal cone inside the insert which is inside a centrifuge tube. (d) Cap of centrifuge tube presses metal cone into filter paper sitting on the base of the insert.....54

Figure 5.2: After centrifugation with the metal cone, a bacterial lawn is observed near the center of the filter.....55

Figure 5.3: (a) Colour map depicting total LIBS intensity as a function of position on the filter. Each black dot represents a data point corresponding to a single laser shot. The black circle indicates the approximate location of the cone hole on the filter. (b) Image of the filter after data acquisition. The four trapezoidal indentations are again evident.....56

Figure 5.4: Average total LIBS intensity of bacteria deposited using three different methods. Error bars represent one standard deviation in the measurements.....57

Figure 5.5: (a) Plot of average total LIBS intensity as a function of CFU. Error bars represent one standard deviation in the measurements. (b) Linear fit to the linear dynamic range in (a).....61

Figure 6.1: Two overlapped *E. coli* spectra taken side-by-side on the same filter paper, showing evidence of non-uniform laser ablation. Black spectrum exhibits high bacterial signal and blue spectrum exhibits signal comparable to a blank filter which is shown in red. Insets show zoomed-in sections of the emissions from phosphorus, magnesium, and calcium.....65

Figure 6.2: Image of filter paper after deposition of *E. coli* suspensions with and without Tween for the 1/500 dilution. The impressions from the three wells are evident.....67

Figure 6.3: Plots of total LIBS intensity as a function of spectrum number for each sample.....	68
Figure 6.4: SEM micrographs of some of the sample depositions on filter papers.....	70
Figure 6.5: Plots depicting the effect of different concentrations of Tween in a suspension of <i>E. coli</i> . (a) First three concentrations of Tween used. (b) Second three concentrations of Tween used. (c) Bar graph summarizing the results in (a) and (b). Error bars represent one standard deviation in the measurements.....	73
Figure 6.6: Average LIBS intensity of the Na 588 nm emission line in the supernatant from different washing steps for <i>E. coli</i> grown in two separate tubes with TSB.....	75
Figure 6.7: Overlapped spectra from each washing step, the broth, and a blank filter zoomed-in on two Mg emission lines to show the presence of bacteria in the supernatant. Wash #1 in red, wash #2 in green, wash #3 in blue, wash #4 in pink, broth in black, and blank filter in orange. Each spectrum is itself an average of the 45 spectra acquired across the filter.....	75
Figure 6.8: Total LIBS intensity as a function of spectrum number for <i>E. coli</i> grown in liquid culture and diluted to produce different concentrations.....	76
Figure 7.1: (a) Flocked swab used in this work. (b) Flocked swab zoomed-in on the tip.....	80
Figure 7.2: Absorbance value and average total LIBS intensity plotted as a function of vortex time for two trials.....	82
Figure 7.3: Average absorbance value plotted for samples prepared by pipetting a bacterial suspension onto a swab and vortexing it in water to release the cells and by pipetting directly into water. Error bars represent one standard deviation in the measurements.....	83
Figure 7.4: Absorbance value and average total LIBS intensity plotted for each sample for (a) <i>E. coli</i> and (b) <i>S. epidermidis</i>	85

Figure 7.5: (a) 100 μL of *E. coli* pipetted onto surface of metal plate. (b) Metal plate after heated on hot-plate for 2 minutes 20 seconds at 200 °C. Water has evaporated and film of bacteria is observed.....86

Figure 7.6: The sum of the normalized intensities of all non-carbon lines divided by the normalized intensity of the carbon line plotted as a function of spectrum number for various concentrations of *E. coli*. The black horizontal line represents the average value of this ratio for a blank filter and the horizontal dashed line represents this average plus three times the standard deviation in the measurements of this ratio for a blank filter....88

Figure 7.7: Resulting averaged spectra from 20 single-shot LIBS measurements on different samples. All samples in this figure were tested at the same spectrometer amplification.....90

List of Abbreviations

AR: anti-reflection

CCD: charge coupled device

CFU: colony forming units

CSF: cerebrospinal fluid

DFA: discriminant function analysis

DNA: deoxyribonucleic acid

FWHM: full width at half maximum

GLIER: Great Lakes Institute for Environmental Research

ICCD: intensified charge coupled device

IUPAC: International Union of Pure and Applied Chemistry

LIBS: laser-induced breakdown spectroscopy

LOD: limit of detection

LPS: lipopolysaccharide

LTE: local thermodynamic equilibrium

MALDI-TOF-MS: matrix-assisted laser desorption/ionization time-of-flight mass spectrometry

MCP: microchannel plate

MRSA: methicillin-resistant *Staphylococcus aureus*

NGS: next generation sequencing

NN: neural networks

PCA: principal component analysis

PCR: polymerase chain reaction

PFGE: pulse-field gel electrophoresis

PLS-DA: partial least squares discriminant analysis

RFLP: restriction fragment length polymorphism

SEM: scanning electron micrograph

TSA: tryptic soy agar

TSB: tryptic soy broth

UTI: urinary tract infection

Chapter 1: Introduction

1.1 Motivation

Bacteria are omnipresent microorganisms found in the environment and human body. Many types of bacteria infect humans, causing illness and mortality. Infectious diseases are the world's leading cause of premature death, according to The World Health Report 1996 by the World Health Organization (WHO).¹ The ability to rapidly identify a harmful pathogen in a clinical specimen is crucial for diseases that kill within hours of the start of symptoms so that targeted treatment can begin immediately. It is the lack of immediate targeted treatment that has led to the overuse of broad-spectrum drugs which has given rise to the crisis of antibiotic-resistant bacteria. At least 2 million people are infected with antibiotic-resistant bacteria in the United States each year and at least 23000 of them die as a result.² Rapid pathogen identification would reduce the overuse of broad-spectrum drugs that have led to this crisis of antibiotic resistance.

Some techniques, among others, used for bacterial identification include culture-based methods, polymerase chain reaction (PCR), restriction fragment length polymorphism (RFLP), pulse-field gel electrophoresis (PFGE), matrix-assisted laser desorption/ionization time-of-flight mass spectrometry (MALDI-TOF-MS), and next generation sequencing (NGS). An overview of some of the different techniques used for the classification and identification of bacteria can be found elsewhere.^{3,4,5} There are major drawbacks to the techniques used for bacterial identification. They require transferring samples to a laboratory setting, expertise in microbiology, are expensive, labor-intensive, and time-consuming (it can take hours, days, even weeks before a bacterium is identified). Some methods of identification are only useful for certain types of bacteria. For example, culture-based methods do not work for bacteria that are unable to be cultured. Identification methods may require a pure culture of the bacterial strain, meaning that the bacteria must first be cultured which takes additional time. These methods are often too slow to provide results for which bacterial identification is time-sensitive.

Identification of the bacteria causing the infection is critical in determining the proper treatment. A technique known as laser-induced breakdown spectroscopy (LIBS) has been used to identify and discriminate bacteria in research laboratory settings and has the potential to detect and identify harmful pathogens in clinical specimens within minutes, exceeding the speed at which other techniques identify bacteria. The research presented in this thesis demonstrates the efforts taken towards the development of the LIBS technique as a rapid point-of-care diagnostic tool in a clinical setting.

1.2 Laser-Induced Breakdown Spectroscopy

Laser-induced breakdown spectroscopy (LIBS) is a rapid elemental analysis technique that utilizes a pulsed laser to vaporize a small amount of a sample, creating a plasma. The plasma contains atoms, ions, and free electrons and is initially very hot – approximately 50000 K.⁶ As the plasma cools, excited electrons decay to lower energy levels, emitting photons in the process. The light that is emitted from the plasma is collected for analysis and is characteristic of the elements in the sample. The time it takes from the start of the laser pulse to the detection of elements in the sample is less than one second.

LIBS has been used for a variety of applications including analysis of metals, soils, explosives, and biological samples.⁷ It has the potential to be beneficial in the medical, environmental, and food industries, as well as in the protection against bioterrorism. LIBS has a number of advantages over other elemental analysis techniques: it can be done on solids, liquids, and gases; it requires little to no sample preparation; it uses only micrograms of sample; elemental analysis is fast; it simultaneously detects all elements in the periodic table; portable LIBS devices have been made for field measurements of samples *in situ*; the LIBS technique can be done remotely, enabling elemental analysis of samples that are hazardous or located in dangerous or difficult to reach environments. For example, the Curiosity rover, capable of performing LIBS, was sent to Mars to analyze the chemical composition of rocks and soils.

1.3 Overview of Previous Results for LIBS on Bacterial Samples

The capability of LIBS to be used as a rapid diagnostic tool for bacterial infection has been investigated since the early 2000's. Early work involved determining whether bacteria and other biotypes could be discriminated based on their elemental composition. In 2003, Samuels et al. demonstrated that different biomaterials (bacteria, molds, and pollens) could be discriminated from each other using LIBS and a chemometric technique known as principle component analysis (PCA).⁸ Also in 2003, Morel et al. performed LIBS on six different types of bacteria as well as two pollens and used ratios of the intensities of elemental emission lines to illustrate the feasibility of LIBS-based identification.⁹ In 2004, Kim et al. discriminated between different types of bacteria by plotting the LIBS intensities of certain elemental lines observed in the bacterial spectra.¹⁰ In 2010, Multari et al. also showed that it was possible to use LIBS to discriminate between bacteria.¹¹ Discrimination between different strains of a single species of bacteria was accomplished by previous members of our group.^{12,13} and Manzoor et al.¹⁴ Different strains of bacteria cause different diseases which require different treatments, making identification of different strains important so that the proper treatment can be administered for a particular strain. Manzoor et al. also showed that bacterial strains were successfully classified to their corresponding bacterial species using LIBS and neural networks (NN). The results from these preliminary experiments indicate that LIBS is capable of bacterial identification, at least in an idealized laboratory setting.

Further research included investigating the ability of LIBS to detect and identify bacteria in more realistic "real world" situations. Barnett et al. showed that *Salmonella enterica* serovar Typhimurium at various concentrations in milk could be discriminated using LIBS and a chemometric technique known as discriminant function analysis (DFA); however, it was only successful for larger concentrations ($>10^6$ CFU (colony forming units)/mL) but was expected to improve with optimization of the LIBS experimental conditions.¹⁵ Gottfried demonstrated that LIBS, along with a chemometric technique known as partial least squares discriminant analysis (PLS-DA) can be used to identify

Escherichia coli on different substrates and in the presence of interferants.¹⁶ The results from this study illustrate the robustness of the LIBS and PLS-DA techniques for identifying *E. coli*.

Our research group has extensively investigated the feasibility of the LIBS technique as a diagnostic tool. In 2007, it was shown that three non-pathogenic strains of *E. coli* were successfully discriminated from each other as well as from other biotypes such as mold and yeast,¹² and a pathogenic strain was discriminated from the three non-pathogenic strains,¹³ suggesting the possibility that a pathogenic strain could be discriminated from commonly occurring environmental strains. Two *E. coli* strains were also grown in two different culture media and the strains were successfully discriminated regardless of the growth medium.¹³ Also in 2007, Rehse et al. demonstrated that *Pseudomonas aeruginosa* grown on three different culture media were grouped together in a DFA and successfully discriminated from two different *E. coli* strains, suggesting again that growth in different culture media does not affect the LIBS-based identification of bacteria.¹⁷ In 2011, Marcos-Martinez et al. confirmed this result.¹⁸ These are promising results given that the bacteria obtained from clinical specimens could be subjected to slightly different growth conditions while in the bodies of different patients.

In 2006, Baudelet et al. performed LIBS on two different types of bacteria: *E. coli* (Gram-negative) and *Bacillus subtilis* (Gram-positive). The magnesium emission from *E. coli* was observed to be significantly larger than that for *B. subtilis*, which was thought to be due to the presence of divalent cations (Mg^{2+} and Ca^{2+}) in the outer membrane of Gram-negative bacteria.¹⁹ This suggests that the emission from Mg in a LIBS spectrum is correlated with the Gram classification of bacteria by the Gram staining procedure. In 2009, Rehse et al. confirmed that the LIBS spectra of Gram-negative bacteria are correlated with the composition of the bacterial outer membrane by intentionally altering the membrane biochemistry and observing the changes in the LIBS spectra.²⁰ It was concluded that the membrane biochemistry contributes to the LIBS-based identification. It was also shown that different genera of Gram-negative bacteria exhibit greater variation than different strains of the same species regardless of the intentional altering

of the membrane biochemistry, suggesting that identification and discrimination of different genera of bacteria is possible with LIBS regardless of the environmental conditions that the bacteria are in. Again, this is a promising result given that the environmental conditions in the body are slightly different for each person.

In 2010, Rehse et al. observed the effect on the LIBS-based identification of mixing two types of bacteria and determined that in a mixture of two species of bacteria, the majority species will be identified provided it comprises at least 70% of the mixture.²¹ In the case where a sample is contaminated, a microbiologist would need to isolate the mixed bacteria and grow them separately in order to identify them. This could take days but is almost instantaneous with LIBS. In this study, a DFA was also performed on four strains of *E. coli*, two strains of *Mycobacterium smegmatis*, two species of *Staphylococcus* and two species of *Streptococcus*. The results showed that the LIBS spectra from these bacteria were closely grouped by genus and species. For example, the two species of *Staphylococcus* were grouped together, the two species of *Streptococcus* were grouped together, all *E. coli* strains were closely grouped to each other, and the *M. smegmatis* strains were grouped together. This indicates that discrimination is not based on random differences in the LIBS spectra of these bacteria, but rather, it is based on the microbiological differences in the bacteria. Figure 1.1 (adapted from reference 21) shows a typical LIBS spectrum of *M. smegmatis* used in this study. The presence of argon

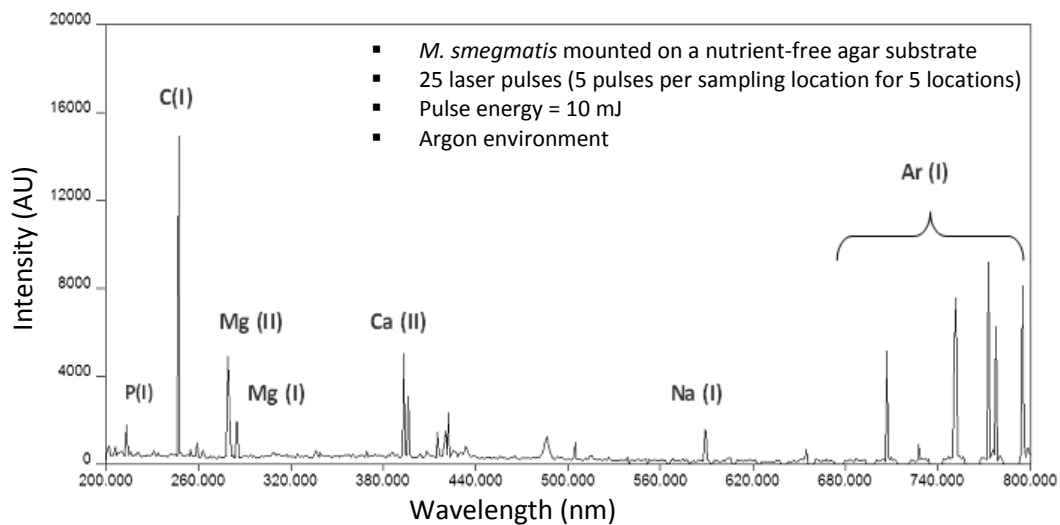


Figure 1.1: Typical LIBS spectrum of *M. smegmatis*. (Adapted from Rehse et al., reference 21).

emission lines at wavelengths greater than 680 nm is due to the laser ablation of the sample in an argon environment, and emissions from five regularly observed elements are labeled.

The feasibility of using LIBS for diagnosing urinary tract infections was also investigated by our group.²² In this study, DFA was performed on *Staphylococcus epidermidis* suspended in water, *S. epidermidis* suspended in urine, and two other species from the *Staphylococcus* genus (*S. aureus* and *S. saprophyticus*) suspended in water. It was found that the LIBS spectra of the *S. epidermidis* in urine classified as *S. epidermidis* in water, indicating that the presence of solutes in urine had no effect on the bacterial identification. DFA was also performed on thirteen different taxonomic groups (strains and species) comprising five different genera of bacteria (*Escherichia*, *Enterobacter*, *Staphylococcus*, *Streptococcus*, and *Mycobacterium*). The results are shown in Figure 1.2 (adapted from reference 22) and illustrate the ability to distinguish between different genera of bacteria. The similarity between Figure 1.2a and Figure 1.2b indicates that the LIBS spectra from the thirteen different taxonomic groups naturally group together according to genus. For example, group 9 and 10 in Figure 1.2b are both species of *Streptococcus*, and both are classified in the same region of DFA space, yet no relationship between these two groups was input into the classification algorithms. It was the intrinsic elemental similarity which caused them to be clustered together in this analysis.

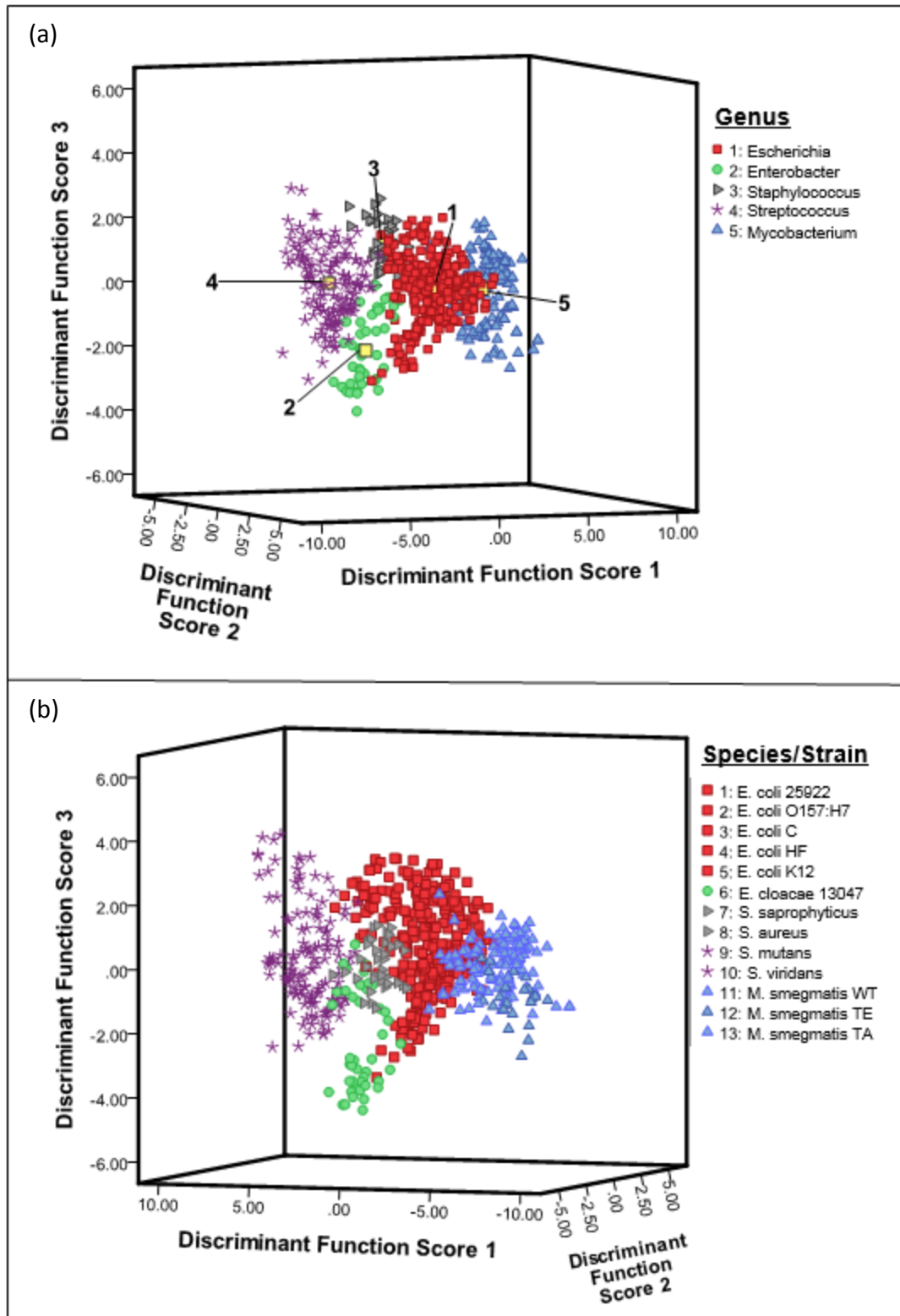


Figure 1.2: DFA of 669 LIBS spectra classified into: (a) five groups according to genus and (b) thirteen groups according to taxonomic classification. Each data point represents one spectrum. The symbols of the thirteen groups in (b) are the same as the symbols for their genus classification in (a). (Adapted from Mohaidat et al., reference 22).

The effect of the metabolic state (live, inactivated via UV exposure, and killed via autoclaving) of bacteria (*E. coli* and *Streptococcus viridans*) on the LIBS-based identification was also investigated by our group.²³ The results showed that the LIBS spectra of live, UV-inactivated, and heat-killed bacteria were indistinguishable from each other. The bacteria were correctly identified regardless of their metabolic state, suggesting that samples can be sterilized prior to LIBS testing, allowing for a safer environment for clinicians. Conversely, Sivakumar et al. and Multari et al. found that live *E. coli* was distinguishable from heat-killed *E. coli*.^{24,25}

While much research regarding LIBS on bacterial samples has been done thus far, most of the work involved “proof-of-concept” experiments for discriminating bacteria and has not yet addressed all aspects of actual biological specimens. For example, the number of cells that would be present in a clinical specimen is multiple orders of magnitude smaller than the amount of bacteria tested with LIBS in these previous studies. Many of these experiments used large concentrations of bacteria and have avoided the issue of realistic sample preparation to provide optimal results which have served to show the potential of LIBS to rapidly identify bacteria. Since LIBS has been shown to be a promising technique for rapid bacterial identification, more research into the capability of LIBS to detect and identify bacteria in samples that are clinically relevant is required.

1.4 Scope of Thesis

The goal of our research group is to develop the LIBS technology for use as a real-time medical diagnostic for rapid pathogen identification. The focus of this work was to develop quick sample preparation methods prior to LIBS testing that utilize equipment and methods that are common or easy to implement in a clinical setting by addressing the issues related to realistic clinical specimens.

In Chapter 2, I describe the theory behind LIBS and the apparatus used for all samples that were interrogated with LIBS. An overview of bacterial physiology, the method used to grow bacteria, and the procedures used to prepare samples for LIBS testing are discussed in Chapter 3. Chapter 4 addresses the issue of additional matter that could be

present in a clinical sample by presenting the results of a technique to separate unwanted material from a bacterial suspension using a novel device. In Chapter 5, I propose a new sample preparation method that utilizes a metal cone constructed in an effort to reduce the bacterial limit of detection with LIBS. In this chapter, I report on the efficacy of this sample preparation method and determine its limit of detection. In Chapter 6, I discuss the efforts taken toward the prevention of non-uniform deposition of bacterial cells on the substrate used for LIBS testing. Chapter 7 describes the investigation into performing LIBS on samples that have been collected with swabs. Since many clinical specimens are collected via swabbing an affected area, it is important to test the ability to perform LIBS on samples collected using swabs. Finally, in Chapter 8, I summarize the results of the work presented in this thesis and discuss what can be done regarding the development of the LIBS technique as a diagnostic tool going forward.

References

- ¹ The World Health Organization, *The World Health Report 1996: fighting disease, fostering development*, (Geneva, Switzerland, 1996)
- ² Centers for Disease Control and Prevention, *Antibiotic Resistance Threats in the United States*, 2013, <<https://www.cdc.gov/drugresistance/pdf/ar-threats-2013-508.pdf>> (2013)
- ³ H. Busse *et al.*, *J. Biotech.*, **47** (1), 3 (1996)
- ⁴ A. A. Salyers and D. D. Whitt, *Bacterial Pathogenesis: A Molecular Approach*, 2nd Ed. (Washington, DC, 2002)
- ⁵ R. H. Deurenberg *et al.*, *J. Biotech.*, **243**, 16 (2017)
- ⁶ J. P. Singh and S. N. Thakur, *Laser-Induced Breakdown Spectroscopy*, 1st Ed. (Amsterdam, The Netherlands, 2007)
- ⁷ S. Musazzi and U. Perini, *Laser-Induced Breakdown Spectroscopy*, 1st Ed. (Georgia, United States, 2014)
- ⁸ A. Samuels *et al.*, *Appl. Opt.*, **42** (30), 6205 (2003)
- ⁹ S. Morel *et al.*, *Appl. Opt.*, **42** (30), 6184 (2003)
- ¹⁰ T. Kim *et al.*, *J. Phys. Chem. B*, **108** (17), 5477 (2004)
- ¹¹ R. Multari *et al.*, *Appl. Spectrosc.*, **64** (7), 750 (2010)
- ¹² J. Diedrich *et al.*, *Appl. Phys. Lett.*, **90**, 163901 (2007)
- ¹³ J. Diedrich *et al.*, *J. Appl. Phys.*, **102**, 014702 (2007)
- ¹⁴ S. Manzoor *et al.*, *Talanta*, **121**, 65 (2014)
- ¹⁵ C. Barnett *et al.*, *Anal. Bioanal. Chem.*, **400**, 3323 (2011)
- ¹⁶ J. L. Gottfried, *Anal. Bioanal. Chem.*, **400**, 3289 (2011)
- ¹⁷ S. J. Rehse *et al.*, *Spectrochim. Acta Part B*, **62**, 1169 (2007)
- ¹⁸ D. Marcos-Martinez *et al.*, *Talanta*, **84**, 730 (2011)
- ¹⁹ M. Baudalet *et al.*, *J. Appl. Phys.*, **99**, 084701 (2006)
- ²⁰ S. J. Rehse *et al.*, *J. Appl. Phys.*, **105**, 102034 (2009)
- ²¹ S. J. Rehse *et al.*, *Appl. Opt.*, **49** (13), C27 (2010)
- ²² Q. I. Mohaidat *et al.*, *Appl. Opt.*, **51** (7), B99 (2012)

²³ Q. I. Mohaidat *et al.*, *Appl. Spectrosc.*, **65** (4), 386 (2011)

²⁴ P. Sivakumar *et al.*, *Astrobiol.*, **15** (2), 144 (2015)

²⁵ R. Multari *et al.*, *J. Agri. Food Chem.*, **61**, 8687 (2013)

Chapter 2: Laser-Induced Breakdown Spectroscopy and Apparatus

2.1 Laser-Induced Breakdown Spectroscopy (LIBS)

The first LIBS experiments for elemental analysis of materials were performed in the 1960's after the development of the laser in 1960. The birth of LIBS came in 1963 with the first elemental analysis of surfaces using plasmas created from a laser pulse.¹ The LIBS technique utilizes a pulsed laser to vaporize, or ablate, a small amount of a sample (which can be solid, liquid, or gas), creating a plasma. The plasma contains atoms, ions, and free electrons, and it emits light that is characteristic of the elements in the sample.² The light emitted from the plasma is collected and analyzed, revealing the sample's elemental composition. The elemental composition information gained in this way may be qualitative, indicating the absence or presence of certain elements at the 10's of part-per-million (ppm) level, or quantitative if the absolute concentrations are required. The following sections will describe the theory behind laser-induced plasmas including atomic transitions, plasma formation, plasma emissions, and important plasma parameters.

2.1.1 Atomic Transitions

Consider an atom in which electrons can occupy an upper energy level j with energy E_j and a lower energy level i with energy E_i . An electron can transition between these energy levels via three different radiative processes which involve either the emission or absorption of a photon. The processes are: spontaneous emission, stimulated emission, and absorption. Only spontaneous emission will be discussed as it is the only radiative process that plays an important role in LIBS. In spontaneous emission, an electron in an upper energy level spontaneously decays to a lower energy level, emitting a photon with energy $\Delta E = E_j - E_i = h\nu_{ji}$ which is the energy corresponding to the spacing between the two energy levels. The probability per unit time that an electron will make this transition is represented as A_{ji} which is called the Einstein A coefficient or the transition probability of spontaneous emission.

Atoms contain a number of discrete, bound energy levels, or states, that electrons can occupy. Beyond these discrete states exists a continuum where electrons are free to move. A spectral line is the result of the decay of an electron from one discrete state to another. Because the spacing between the states is different for every atom, the photons emitted during the transitions will have specific energies (and therefore wavelengths, since $E = \frac{hc}{\lambda}$) indicative of the atom in which the transition occurred. Detection and analysis of these spectral lines are crucial for LIBS measurements, otherwise determination of a sample's elemental composition with LIBS would not be possible.

Electrons can also transition between the continuum and a discrete state or they can transition within the continuum. Transition between the continuum and a discrete state is a process known as recombination (sometimes referred to as free – bound radiation). In this process, a free electron emits a photon when it is captured into a bound level of an ion. Transition within the continuum gives rise to bremsstrahlung radiation (sometimes referred to as free – free radiation). In this process, a free electron loses kinetic energy and emits a photon when it is in the presence of another charged particle. The emissions due to recombination and bremsstrahlung make up what is called the continuum emission in a plasma.^{1,2} This continuum emission is not useful in LIBS measurements as it is not wavelength-specific and it does not provide information about elemental composition. In fact, experiments are typically performed at suitably long delay times after plasma formation in order to minimize or eliminate the early-time non-specific continuum emission.

2.1.2 Plasma Formation

In LIBS, a laser pulse is focused to a small spot on the surface of a target material. The leading edge of the laser pulse rapidly heats that spot on the target, vaporizing the material. The vaporized material then absorbs the energy from the remaining part of the laser pulse, creating a plasma, and in the process shielding the sample from absorbing more laser energy. This is known as plasma shielding.³ Due to this absorption of the laser

pulse by the plasma plume, it becomes elongated towards the incident laser beam.² A schematic of the LIBS process is shown in Figure 2.1.

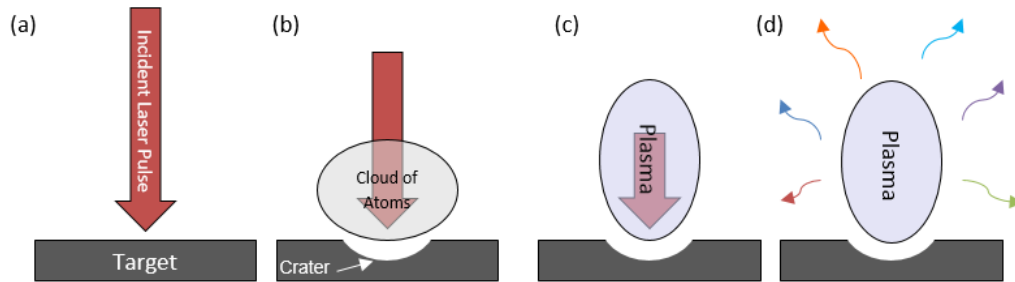


Figure 2.1: Schematic of the formation of a LIBS plasma. (a) Target is rapidly heated by absorbing the incident laser energy. (b) Target material is vaporized, leaving behind a crater in the target and generating a cloud of atoms above the target surface. (c) The cloud of atoms absorbs the remaining part of the laser pulse, ionizing the atoms and creating a plasma. (d) The plasma cools and emits photons which are characteristic of the elements vaporized in the target material.

Absorption of the laser beam by the vaporized mass occurs via multiphoton absorption and inverse bremsstrahlung. In the laser-induced breakdown of a sample, multiphoton absorption occurs, whereby an atom becomes ionized by simultaneously absorbing multiple photons. This generates a free electron. Free electrons gain energy from the laser pulse via inverse bremsstrahlung, a process in which they interact with a photon and transition to another free state. If the electron has an energy greater than the ionization potential of an atom, it can ionize it in a collision, creating another free electron. This free electron can then go on to ionize another atom, creating yet another free electron. This is known as cascade ionization.³ These absorption processes initiate the plasma.

2.1.3 Plasma Emissions

Following initiation, the plasma expands normal to the target surface. As it expands, ions and electrons recombine to form neutrals. Some neutrals recombine to form molecules.⁴ These molecules are not, in general, indicative of the sample's molecular composition. At the earliest observable time, when ionization is greatest, the ratio of electrons in a LIBS plasma to other species (atoms and ions) is less than 10%, corresponding to a weakly ionized plasma.¹ Figure 2.2 shows the total emitted optical

signal intensity as a function of time after the arrival of the laser pulse on a target and depicts the time periods in the plasma lifetime over which certain species dominate the emission spectrum. At early times, plasma emission is composed of a continuous

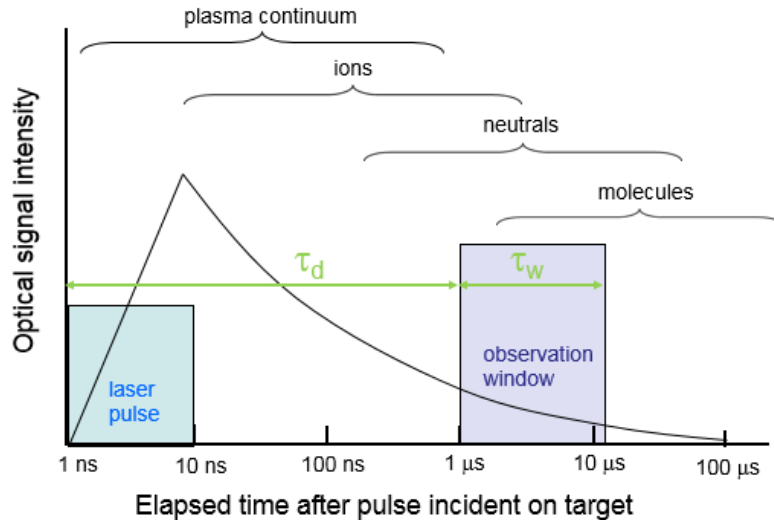


Figure 2.2: Temporal evolution of a LIBS plasma.

background known as continuum emission, which is the result of recombination and bremsstrahlung radiation.³ The continuum emission decreases over time, and by 1 μs a significant portion of it has decayed. Emissions from atomic species (ions and neutrals), known as spectral line emissions, are superimposed on the continuum emission. For elemental analysis of a sample, only the emissions from spectral lines are required as the continuum emission contributes to noise in the LIBS measurements. Thus the recording of the plasma emission is typically not done until after a certain delay time (typically 1 μs or more) from the start of the laser pulse.^{2,3,4} This avoids receiving a strong continuum emission signal, since much of it has decayed by that time, whereas the signal from ions and neutrals dominates. This gives a higher signal-to-background ratio.⁴ The delay time is represented as τ_d and defined as the time between plasma formation and the start of the recording of light emission from the plasma. The time period over which the light is recorded is known as the gate width, τ_w . The optimal choice for τ_d and τ_w will differ depending on the target and the plasma.

Emissions from different elemental lines will be stronger at different times. For example, molecules begin to form near the end of the plasma lifetime as a result of the

recombination of neutrals with each other, whereas the multiply ionized species are present at the beginning of the plasma lifetime and located in the center of the plasma, close to the target surface. As time proceeds, the plasma cools and the lower ionized species and neutrals dominate the plasma emission farther from the target.² Thus the ratio of the population of neutral species to ions in the plasma changes over time. More ion species are present initially, but as time proceeds, the plasma expands and recombination occurs, increasing the population of neutral species.² As the plasma cools, spontaneous emission of photons from electrons decaying to lower energy levels occurs and these photons are collected for analysis.

2.1.4 Plasma Parameters

There are two important parameters that are used to characterize a LIBS plasma: temperature and electron density. For the quantitative elemental analysis of a sample with LIBS, the plasma must be optically thin and in local thermodynamic equilibrium (LTE).⁵ An optically thin plasma is one in which the emitted photons are not likely to be reabsorbed,² and LTE occurs when the free electrons, ions, and neutrals in the plasma have the same temperature.⁵

The temperature of the plasma can be determined using what is called the Boltzmann plot method. The intensity of a spectral line resulting from the transition of an electron in upper energy level j to lower energy level i is

$$I_{ji} = \frac{hc}{4\pi\lambda_{ji}} A_{ji} L \frac{N}{Z} g_j e^{-\frac{E_j}{k_B T}} \quad (1)$$

where λ_{ji} and A_{ji} are, respectively, the wavelength and transition probability of the transition between the two energy levels, L is the length of the plasma, N is the total number density of species in the plasma, Z is the partition function of the species, g_j and E_j are the statistical weight and the energy of the upper level respectively, k_B is the Boltzmann constant, and T is the temperature of the plasma. After minor rearrangement and taking the natural logarithm, equation 1 becomes

$$\ln\left(\frac{I_{ji}\lambda_{ji}}{g_j A_{ji}}\right) = -\frac{1}{k_B T} E_j + \ln\left(\frac{hcLN}{4\pi Z}\right) \quad (2)$$

A plot of the left-hand side of equation 2 as a function of E_j is of the form $y = mx + b$ which is linear and is known as the Boltzmann plot. If the statistical weights and transition probabilities for the excitation states are known, measurements of a variety of line intensities of a certain species along with their upper energy levels can be used to make the Boltzmann plot. If a linear regression is performed on the plot, the slope of the line is equal to $-\frac{1}{k_B T}$, which can be easily manipulated to calculate the plasma temperature.^{1,4,5} Note that the last term in equation 2 does not need to be known to determine the temperature. Because the Boltzmann plot requires a large range of line intensities corresponding to different upper energy levels from the same species, the temperature is not determined in this work as there are not enough lines in the bacterial spectra to do this.

The electron density, n_e , in the plasma can be determined from either the Saha-Boltzmann equation or from the Stark broadening of spectral lines. In the Saha-Boltzmann method, the electron density is calculated from the ratio of the line intensities of different ionization states of an atom of the same element. The equation is given as

$$n_e = \frac{2(2\pi m_e k_B T)^{\frac{3}{2}}}{h^3} \left(\frac{I_{nm}^I A_{ji} g_j^{II} \lambda_{nm}}{I_{ji}^{II} A_{nm} g_n^I \lambda_{ji}} \right) e^{-\frac{E_{ion} + E_j^{II} - E_n^I}{k_B T}} \quad (3)$$

where the superscripts I and II correspond to the lower and higher ionization state respectively, j and n represent the two different upper energy levels in the element with energies E_j and E_n , i and m represent the two different lower energy levels, E_{ion} is the ionization potential of the atom, and m_e is the rest mass of an electron.^{2,4} Note that the plasma temperature is required to calculate the electron density, so this equation can only be used when the plasma is in LTE. Since the temperature is not determined in this work, the electron density therefore cannot be determined using this method.

Alternatively, the electron density can be calculated from the emission lines that have been broadened by the Stark effect. The broadening due to the Stark effect is the result of the interaction of emitting atoms with charged particles in the plasma, dominated by the free electron density.² The electric field from the charged particles perturbs the energy levels of the emitting atoms, resulting in a broadening of the emission lines.⁴ The concentration of electrons in the plasma affects the broadening of emission lines. For example, Figure 2.3 shows two overlaid spectra zoomed in on the singly ionized 393.366 nm calcium line. The spectrum in black represents the emission from a bacterial plasma, whereas the spectrum in red represents the emission from a fish otolith. The otolith structure is a calcium carbonate matrix, which gives rise to a high concentration of calcium ions and free electrons in the plasma which creates the Stark broadening.

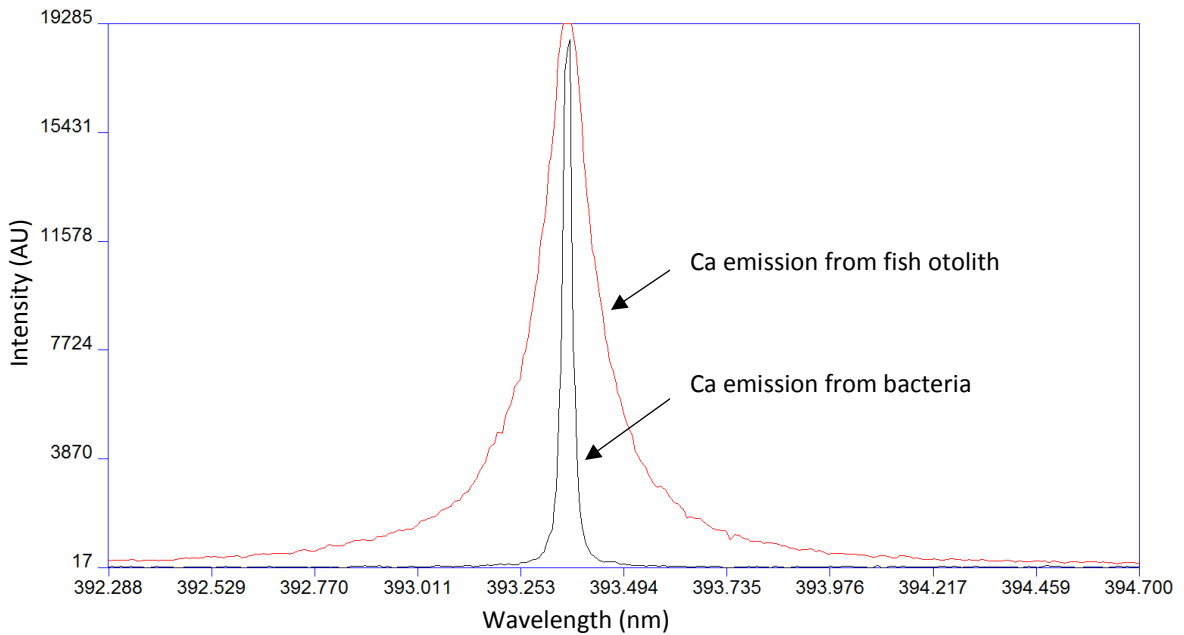


Figure 2.3: Spectrum from emission from bacterial plasma (black) overlaid with spectrum from emission from fish otolith (red) zoomed in on the Ca 393 line. Stark broadening is apparent in the emission line for the otolith spectrum.

The full width at half maximum (FWHM) of a Stark broadened emission line is

$$\Delta\lambda_{1/2} = \frac{2wn_e}{10^{16}} \left(1 + 1.75A \left(\frac{n_e}{10^{16}} \right)^{3/4} \right) \left(1 - \frac{3}{4} N_D^{-1/3} \right) \quad (4)$$

where w and A are the electron impact parameter and the ion broadening parameter respectively, and can both be found in the literature, and $N_D = 1.72 \times 10^9 \left(\frac{T_e^{3/2}}{n_e^{1/2}} \right)$ which is

the number of particles in the Debye sphere where T_e is the electron temperature.² The broadening due to ions is normally small, so that equation 4 can be reduced to^{2,4}

$$\Delta\lambda_{1/2} = \frac{2wn_e}{10^{16}} \quad (5)$$

The electron density in a LIBS plasma is most commonly determined using emission lines from hydrogen or hydrogen-like ions since they exhibit the most extreme linear Stark effect broadening.² The 393 nm emission shown in Figure 2.3 is from singly ionized calcium which is a hydrogen-like ion, and can become Stark broadened in some spectra. No broadening is observed in any of the bacterial emission lines due to the low temperature and electron density of the plasma, so electron density is not determined in this work.

2.2 LIBS Apparatus

A typical LIBS apparatus consists of a high energy pulsed laser, an optical system to direct the laser pulse and focus it onto a target, an ablation chamber to hold the target in a particular gaseous environment, a light collection system to collect the plasma emissions and direct them to a dispersion device which creates the plasma emission spectrum, a detector to record and display the spectrum, and a computer to control the laser as well as the detector and to view the resultant spectrum.³ A spectrometer is typically used for the dispersion of light from the plasma in LIBS measurements. Since LIBS is capable of detecting multiple elements simultaneously, the spectrometer must cover a large range of wavelengths in order to record all of the spectral lines. The spectrometer should also exhibit high spectral resolution in order to resolve lines that are close to each other in wavelength.⁴

2.2.1 Delivery of Laser Pulse to Target

The LIBS apparatus in this work utilizes a 1064 nm Nd: YAG laser (Spectra Physics, LAB-150-10) operating at 10 Hz with a pulse duration of 10 ns and an initial pulse energy of 650 mJ/pulse. A half-wave plate was used to reduce the pulse energy to 180 mJ/pulse, and a polarizing beam splitter then directed a portion of the beam into a beam dump,

resulting in a pulse energy of about 8 mJ/pulse incident on the target. The beam was directed to a 3x telescope beam expander with two high-reflection dielectric-coated mirrors. The 3x telescope beam expander was used to expand the beam to three times its initial diameter of 9 mm, and consisted of an antireflection (AR) coated plano-concave lens ($f=-5$ cm, $\phi=2.54$ cm) and a plano-convex lens ($f=18.5$ cm, $\phi=7.62$ cm). This was followed by a 9 mm diameter iris to revert the beam back to its initial diameter, while keeping the central, more Gaussian part of the beam. A high reflection dielectric-coated mirror then directed the beam to a beam splitter followed by a CCD camera and a high damage threshold 5x AR-coated microscope objective to focus the beam onto the target. The beam splitter and camera were used to visualize the target, with its image displayed on a TV monitor to ensure proper sampling of the target during data acquisition. An alignment He-Ne laser was directed onto the target with aluminum mirrors to visualize the location of the focused laser beam on the the target and allow for positioning of the target in the focus of the laser. A diagram of this delivery of a laser pulse to the target is shown in Figure 2.4.

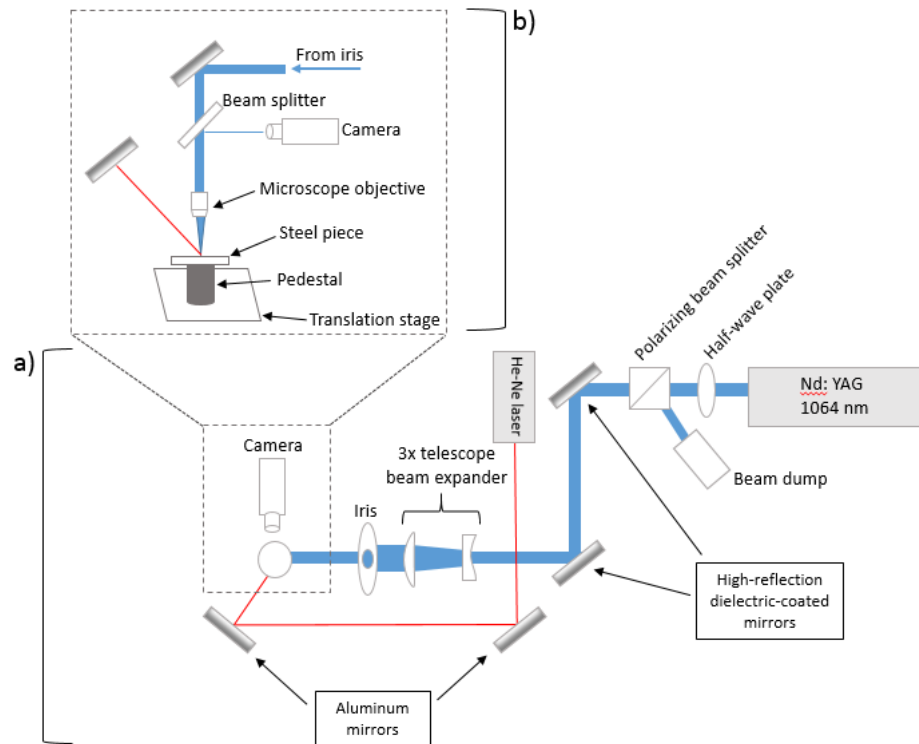


Figure 2.4: (a) Overhead schematic of the optical train used to direct laser pulses to the target. (b) Schematic side view of laser pulses emerging from the iris and directed to a target which is mounted on a steel piece.

The target was mounted on a magnetized pedestal inside a Plexiglas ablation chamber to enable ablation of the target in a controlled gas environment. The chamber was set up on a translation stage such that the chamber, and therefore the target, could be translated in the x , y , and z directions. The x and y translation allowed for movement of the laser beam across the target surface to ensure sampling of the target at different locations. The z translation allowed for proper alignment of the target in the focus of the laser beam, enabling focusing onto targets of different heights. All bacterial targets in this work were mounted on a steel piece with double-sided tape and the plasma emissions were collected at a delay time of $2 \mu\text{s}$ after the laser pulse with a gate width of $20 \mu\text{s}$ in an argon environment.

Ablation of targets in various ambient gases has been studied extensively.^{6,7,8,9} The optimal choice for which gas to use depends on the plasma temperature and electron density of the plasma in that particular gas. There is an increased population of higher energy states of the species in the plasmas with higher temperatures and electron densities, resulting in a greater number of emissions from the transitions from these higher energy states and therefore a greater emission intensity. It has been shown that the plasma temperature and electron density are greater in plasmas formed in argon compared to air, helium, neon, and nitrogen.^{7,8,9} This is because argon has the greatest mass. The species in the gas exert a force on the species in the plasma, which depends on the mass of the species in the gas. The greater the exerted force, the more collisions there are in the plasma plume which increases its temperature. Also due to the higher mass of argon, the plasma is more confined, giving a greater electron density.⁹ It was found that ablation in argon increased the signal to noise ratios of emission lines compared to air, helium, and nitrogen,^{7,9} making argon the most favourable environment for LIBS. It was also found that emission intensity was greatest at atmospheric pressure.⁹ Although our group has previously investigated the effect of using alternate gases on bacterial LIBS spectra,¹⁰ in this work, ablation of all targets was done in an argon environment at atmospheric pressure.

Emissions from the plasma were directed into a 1 m steel-encased multimode optical fiber (600 μm core diameter, N.A=0.22) using two matched off-axis aluminum parabolic mirrors ($f=5.08$ cm, $\phi=3.81$ cm) which increased the amount of light collected. The opposite end of the fiber was connected to an échelle spectrometer (ESA 3000, LLA Instruments, Inc.) coupled to an intensified charge coupled device (ICCD). Control of the spectrometer, as well as the gating of the ICCD and the operation of the laser was done with a personal computer running the software (ESAWIN v3.20) provided by the manufacturer.

2.2.2 Detection of Light from the Plasma

Dispersion and detection of the light emitted by the plasma was accomplished with an échelle spectrometer coupled to an ICCD. The spectrometer used in this work had spectral coverage from 200 – 840 nm, a range in which emission lines of most elements are found.⁴ The detection of all the emission lines emitted by a plasma from a single laser shot is essential for LIBS to have any true utility. As this essential function was accomplished by an échelle spectrometer in our experiment, a brief description of this critical piece of apparatus is provided.

An échelle spectrometer is comprised of a particular type of diffraction grating, known as an échelle grating (see Figure 2.5), and a prism which together disperse incident light in two perpendicular directions. The échelle grating is the first dispersing element of the spectrometer and it spatially disperses light by wavelength. For example, if white light

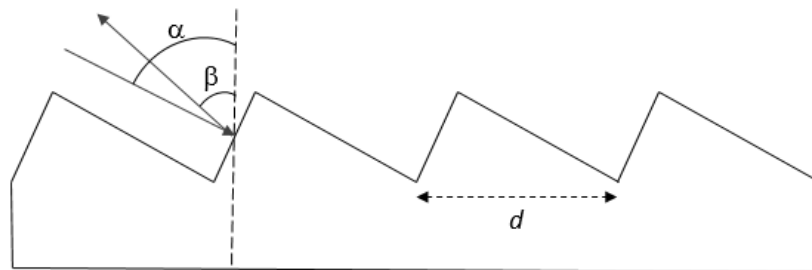


Figure 2.5: Side view of an échelle grating. The quantities α , β , and d are described below.

is incident on the grating, upon diffraction from the grating, it will be separated into its constituent wavelengths, where each wavelength is diffracted at a different angle. The grating equation is given by

$$m\lambda = d(\sin\alpha + \sin\beta) \quad (6)$$

where m is an integer known as the diffraction order, λ is the wavelength of the incident light, d is the groove spacing, and α and β are the angles of incidence and diffraction respectively. From the grating equation, it can be seen that for a given angle of incidence and groove spacing, a first order line ($m = 1$) of wavelength λ will be diffracted at the same angle as a second order line ($m = 2$) of wavelength $\lambda/2$ and so on, resulting in a series of overlapping light in different diffraction orders. In an échelle spectrometer, the grating is optimized to have high diffraction efficiency into very high orders which are all highly overlapped. In our grating, orders $m = 29$ through $m = 119$ are used. A prism set at right angles to the diffraction grating dispersion is therefore used as a cross-dispersing element to disperse the light in the highly overlapping orders, producing a two-dimensional pattern where the orders are separated vertically and wavelength is dispersed horizontally within an order. This two-dimensional pattern was imaged onto an ICCD, and is referred to as an échellogram.

Figure 2.6a shows an échellogram for the plasma emissions from a steel target piece. The échellogram is a two-dimensional plot of the spectral lines as a function of diffraction order (vertical) and wavelength (horizontal). The yellow square is the output of the 1024 x 1024 pixels of the CCD chip, the horizontal green lines each represent a diffraction order, where order 119 is located at the top of the chip and order 29 is located at the bottom, and the green circle represents the position of the image intensifier in front of the CCD chip. No light is detected in the regions beyond the green circle because it is not amplified. Each order spans a narrow range of wavelengths, representing only a part of the total spectrum. Shorter wavelengths are contained in the higher orders (top of CCD chip) and longer wavelengths are contained in the lower orders (bottom of CCD chip). For example, order 119 contains dispersed light from 201.023 – 202.615 nm and

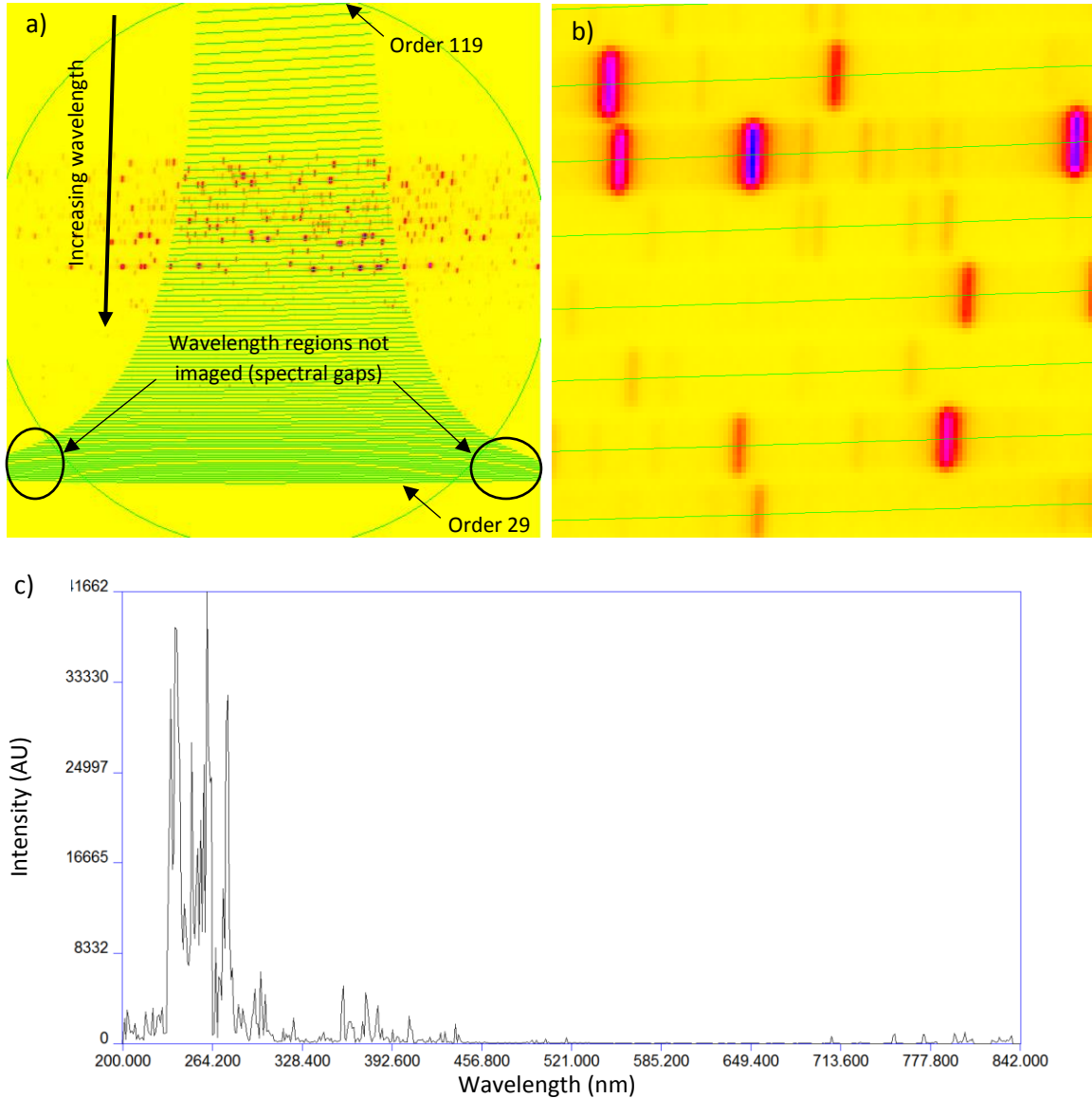


Figure 2.6: (a) Échellogram for the emissions from a steel target piece. (b) Zoomed-in section of the échellogram in (a). (c) Resultant spectrum.

order 29 contains dispersed light from 816.875 – 838.393 nm. Thus light in the UV region is mapped to the top of the chip, and the wavelength increases moving downward. The region of the chip where the orders lay outside the green circle (this occurs for the lower orders) correspond to gaps in the spectra. This was a design choice by the manufacturer to sacrifice resolution at the higher wavelengths (upper wavelengths in the visible range and wavelengths in the IR) for better resolution in the UV. This is advantageous in this work since many of the spectral lines used in this work are found in the UV region. In the false colour image shown in Figure 2.6a, the yellow colour indicates no light and the

darker spots indicate more light on the CCD. Figure 2.6b shows a zoomed-in section of the échellogram. For a spot located on a given order, that is, on a green horizontal line, there are another two spots corresponding to the same wavelength located beyond the green lines (this can be seen in Figure 2.6a). These spots beyond the green lines are not used in analysis as they are not as intense as the spot located on the green line. This has to do with the intensity of the diffracted light. The ESAWIN software (ESAWIN v3.20) transforms the échellogram into a spectrum by stitching the orders together. The corresponding spectrum is shown in Figure 2.6c.

A schematic of the échelle spectrometer taken from the owner's manual of our ESA 3000 is shown in Figure 2.7.¹¹ Light from the plasma enters the slit, is collimated with a mirror, directed through a prism to the échelle grating where it is dispersed by wavelength, then cross-dispersed by the prism to separate the light in the overlapping orders, and finally imaged onto the CCD. The resolution of the spectrometer is maximized

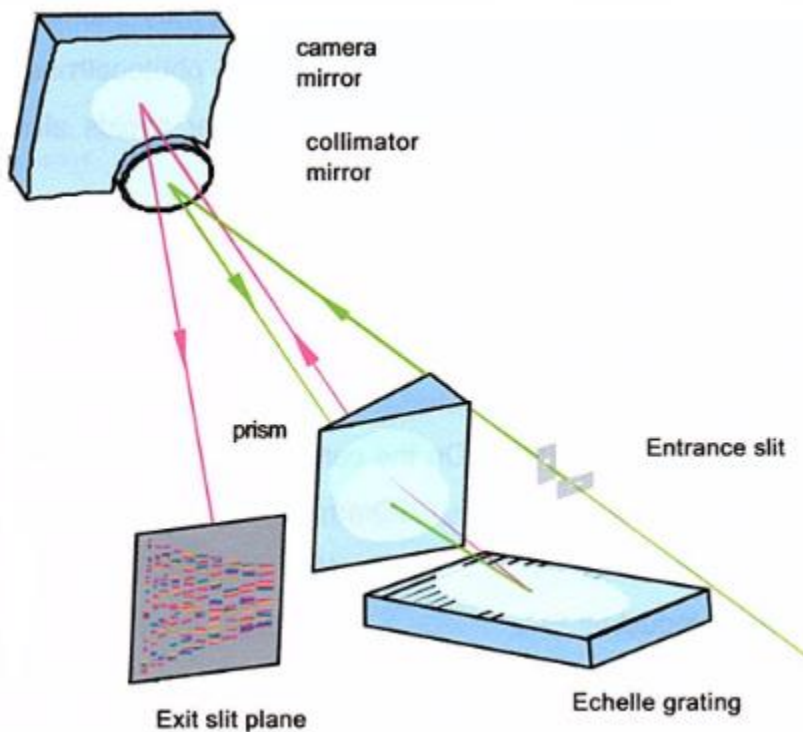


Figure 2.7: Schematic of the Echelle spectrometer.¹¹

in the UV and changes with wavelength. Our spectrometer has a stated resolution of 0.005 nm at 200 nm and 0.019 nm at 780 nm.¹¹

A 1024 x 1024 pixel (24 μm x 24 μm pixel size) ICCD camera (Kodak KAF 1001) was used as the detection device which is an image intensifier coupled to a charge coupled device (CCD). The image intensifier consists of a photocathode to convert incoming photons to electrons, a microchannel plate (MCP) to multiply the number of electrons, and a phosphor screen to convert the electrons to photons which are then transferred to the CCD for detection. A CCD contains an array of light-sensitive elements, called pixels, arranged on a semiconductor material. Incident photons generate free electrons when they strike the CCD, leaving electron-hole pairs in each pixel in the array which is exposed to light for the same amount of time. Each pixel then “fills up” with a varying amount of electrons which is linearly proportional to the number of incident photons. The charge in each pixel is measured and read out as an intensity value which is digitized, and an image is displayed on a computer monitor nearly simultaneously. The ICCD is advantageous because it multiplies the number of incoming photons on the CCD and it allows for gating of the device such that incoming light is only detected at certain times for certain durations. The gating is done by applying a voltage between the photocathode and MCP. For example, electrons are accelerated from the photocathode into the MCP when a 200 V pulse is applied.¹¹ In this case, the intensifier is said to be gated on.

2.2.3 Steel Calibration

Spectra from a steel target piece were collected each day prior to the collection of spectra for experiments to ensure the proper functioning of the system. A steel piece was used for calibration since it does not change over time and it is elementally uniform. All steel spectra were collected at a gate delay of 1 μs and gate width of 10 μs in an argon environment. Three laser pulses were fired at a single location and the plasma emissions were only collected/recorded after the third laser pulse. The first two pulses, referred to as “clean pulses,” served only to clean the surface of any debris. The pulses were done far enough apart in time that none of the corresponding plasmas overlapped. After the

first set of three laser pulses, the steel piece was moved to a new location and three laser pulses were again fired. This was done a total of five times, resulting in a single spectrum representing an average of the spectra from the five locations. Since the steel piece is uniform in composition and time, its spectra should always be the same (within some statistical fluctuation). Thus, any change in the regularly observed steel spectra served as an indicator of the presence of an issue in the system.

A total of 65 spectral lines from iron (40 neutral lines and 25 singly ionized lines) were used in the analysis of the steel piece to assess the reproducibility of the system. The intensities of these iron lines were determined by the ESAWIN software (ESAWIN v3.20). To determine the intensity, a region of interest (ROI) about the spectral line peak is first defined, which consists of 60 pixels about the peak wavelength, with 30 pixels on either side of the peak wavelength. If there is no peak within 3 pixels of the expected wavelength after a peak search using the NIST atomic database is done, it is flagged as an error. If a peak is found within 3 pixels of the expected wavelength, the full width at half maximum (FWHM) is calculated and the peak area is determined by integrating the peak over the FWHM.¹² Figure 2.8 shows the ROI view for a spectral line. In a Microsoft Excel

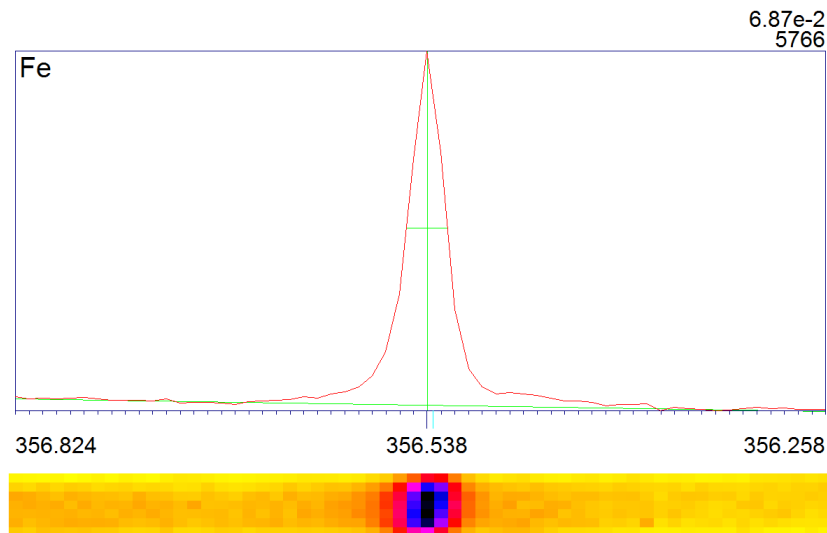


Figure 2.8: ROI view from ESAWIN software. The line plot in red is the intensity as a function of the X-pixel coordinates for 60 pixels. The vertical green line depicts the center of the peak according to ESAWIN, and the blue line below and to the right of the vertical green line shows the expected location of an emission line according to the NIST atomic database. The horizontal green lines designate the background and the FWHM. The text in the upper left corner denotes the element. The numbers in the upper right, from top to bottom, denote the ratio of the peak area to some reference line (not used in this work) and the peak area. Numbers below the window are wavelengths in nm. Below the window shows the portion of the échellogram corresponding to that ROI.

sheet, the area-under-the-curve intensities for these 65 iron lines were summed to give a value referred to as the total LIBS intensity. The intensity of each line was then divided by the total LIBS intensity, giving a value referred to as the normalized intensity. This was done to account for the shot-to-shot fluctuations in the plasma emissions as a result of the amount of material ablated.

Steel spectra from May 2013 to July 2018 were collected and analyzed. The fractional standard deviation was determined for each of the 65 normalized iron lines, where fractional standard deviation was calculated as the standard deviation divided by the average of the normalized intensities for a single emission line. For the lines with the highest intensity, the fractional standard deviation was ~ 5%, and for the less intense lines, the fractional standard deviation was ~ 15-20%. The higher fractional standard deviation for less intense lines was to be expected since the average normalized intensity was smaller while the standard deviation remained similar for all lines. Thus from 5 years of collected data, emission lines with the highest intensities are expected to vary by ~ 5% and less intense emission lines are expected to vary by ~ 15-20%. This was used to indicate whether the system was functioning properly before any bacterial LIBS experiments were performed.

References

- ¹ D. A. Cremers and L. J. Radziemski, *Handbook of Laser-Induced Breakdown Spectroscopy*, 1st Ed. (West Sussex, England, 2006)
- ² J. P. Singh and S. N. Thakur, *Laser-Induced Breakdown Spectroscopy*, 1st Ed. (Amsterdam, The Netherlands, 2007)
- ³ S. Musazzi and U. Perini, *Laser-Induced Breakdown Spectroscopy*, 1st Ed. (Georgia, United States, 2014)
- ⁴ A. Miziolek *et al.*, *Laser-Induced Breakdown Spectroscopy*, 1st Ed. (New York, United States, 2006)
- ⁵ V. K. Unnikrishnan *et al.*, *Pramana*, **74** (6), 983 (2010)
- ⁶ M. Adamson *et al.*, *Spectrochim. Acta Part B*, **62**, 1348 (2007)
- ⁷ J. G. Son *et al.*, *Appl. Spectrosc.*, **64** (11), 1289 (2010)
- ⁸ W. Sdorra and K. Niemax, *Mikrochim. Acta* **107**, 319 (1992)
- ⁹ M. Dawood, *Space and Time Characterization of Laser-Induced Plasmas for Applications in Chemical Analysis and Thin Film Deposition*, Ph.D. thesis, Université de Montréal (2015)
- ¹⁰ S. J. Rehse and Q. I. Mohaidat, *Spectrochim. Acta Part B*, **64**, 1020 (2009)
- ¹¹ *Installation Guidelines Echelle Spectra Analyzer ESA 3000*, LLA Instruments GmbH, Berlin, Germany, 2005
- ¹² *ESAWIN Software Manual Version 3.20*, LLA Instruments GmbH, Berlin, Germany, 2005

Chapter 3: Bacterial Physiology and Sample Preparation

3.1 Bacterial Physiology

Bacteria are small microorganisms that are ubiquitous in the environment and human body. Thousands of species of bacteria are in the human body and many of them are harmless to humans. Out of all the bacteria currently known, only a small amount cause disease. There are a number of public health issues due to harmful bacteria, such as food-borne infections, water-borne infections, hospital-acquired (nosocomial) infections, bioterrorism, and antibiotic resistance.¹ It is therefore important to study bacteria, to understand their structure and how they operate so that preventative and combative measures can be taken against harmful bacteria. With regards to LIBS, the idea that the outer membrane of bacteria may play an important role in LIBS-based identification was first put forward and tested by Rehse et al.² It has been shown that the membrane biochemistry of bacteria, specifically the presence of calcium and magnesium in the outer membrane, contributes to the emissions from bacterial plasmas and thus to LIBS-based identification of bacteria.^{2,3} A list of 19 regularly observed emission lines in bacteria in this work from 5 different elements (C, P, Mg, Ca, and Na) is shown in Table 3.1. Our LIBS analysis does not detect genetic differences among bacteria since most of the elements that comprise DNA are not observed in the LIBS bacterial spectra. Instead, LIBS detects the differences in the chemical composition of the bacterial cell wall, membrane, and the cytoplasm which varies between species according to their genetic differences. This section will therefore provide a necessary overview of bacterial physiology.

Table 3.1: Regularly observed spectral lines in bacterial LIBS spectra in this work

Element	Wavelength (nm)	Ionization State
C	247.856	I
P	213.618	I
P	214.914	I
P	253.398	I
P	253.560	I
P	255.326	I
P	255.491	I
Mg	279.079	II
Mg	279.553	II
Mg	279.806	II
Mg	280.271	II
Mg	277.983	I
Mg	285.213	I
Ca	317.933	II
Ca	393.366	II
Ca	396.847	II
Ca	422.673	I
Na	588.995	I
Na	589.593	I

Bacteria have three main shapes: spheres (also known as cocci), rods (also known as bacilli), and spirals. They are all single-celled organisms known as prokaryotes. Prokaryotes lack a nucleus and their DNA and organelles are not bound in membranes, rather, they are in contact with the cytoplasm. Among other structures, bacteria in general contain a cytoplasmic membrane surrounding their cytoplasm, and a cell wall outside the membrane. The structures surrounding the cytoplasm comprise what is called

the cell envelope. In general, there are two major groups that many bacteria can be divided into based on their cell envelope: Gram-positive or Gram-negative. These groups represent different ways in which bacteria protect their cytoplasmic membrane from different stresses.⁴ Distinguishing between Gram-positive and Gram-negative bacteria is done with a staining procedure known as the Gram stain which stains bacteria a certain colour depending on its cell wall structure. The cell wall is largely responsible for giving bacteria their shape due to its rigidity.⁵

Gram-positive bacteria are surrounded by a thick cell wall that protects their cytoplasmic membrane. The cell wall is made mostly of a polymer of sugars and amino acids known as murein or peptidoglycan. Due to charged amino acids, the peptidoglycan layer is highly polar, preventing hazardous hydrophobic compounds from passing through.⁴

Gram-negative bacteria also contain a peptidoglycan layer, but it is much thinner than the one in Gram-positive bacteria. The cell envelope of Gram-negative bacteria consists of the cytoplasmic membrane, the peptidoglycan layer, and an outer membrane.⁵ The presence of an outer membrane beyond the peptidoglycan layer is unique to Gram-negative bacteria and it is this feature that serves as a protective barrier, protecting their cytoplasmic membrane from hazardous compounds. The outer membrane is a lipid bilayer structure, with phospholipids on the inner face and lipopolysaccharide (LPS) molecules on the outer face. Because of the lipid nature of the outer membrane, it is expected to prevent hydrophilic compounds from passing through, but a way to transport nutrients is needed. To do this, the outer membrane has special channels made from proteins called porins that have holes which allow for the entry of small hydrophilic molecules. Hydrophobic compounds cannot enter because the channels are small enough that the compound must also come in contact with the polar region of the bilayer. Hydrophilic compounds that are too large to pass through the channels but are necessary for survival are passed through the outer membrane by specific transport mechanisms.⁴ The divalent cations Ca^{2+} and Mg^{2+} are present in the outer membrane and act to stabilize it. Rehse et al. showed that the calcium and magnesium seen in bacterial LPS plasmas are

at least partly due to the presence of calcium and magnesium in the outer membrane.³ This was accomplished by intentionally altering the membrane biochemistry via growth in extreme nutrient environments and observing the changes in the LIBS spectra.

A bacterium is distinguished as Gram-positive or Gram-negative depending on which colour it appears after the Gram staining procedure. In the Gram stain procedure, a bacterium is first stained with a purple dye known as crystal violet, then treated with potassium iodide and washed with alcohol. Due to the thick peptidoglycan structure of the cell wall of Gram-positive bacteria, the purple dye is retained in the staining procedure and therefore Gram-positive bacteria appear purple. Safranin is used as a counter stain which does not alter the purple colour of Gram-positive bacteria but causes Gram-negative bacteria to appear pink.⁴ Interestingly, there has not yet been any observed or suggested correlation between the Gram stain and LIBS-based identification of bacteria although many representative species of both phenotypes have been tested with LIBS. The Gram-positive and Gram-negative species that have been used in LIBS experiments are shown in Table 3.2 which has been adapted from reference 6.

3.2 Bacterial Species used in this work for LIBS Testing

Bacteria are named by their genus and species. For example, consider the bacterium *Escherichia coli*. *Escherichia* refers to the genus and *coli* refers to the species. Typically, the genus name is shortened to its first letter. Variety can exist within a species, leading to multiple strains of a bacterium. For example, some strains of *E. coli* include: *E. coli* O157:H7, *E. coli* C, and *E. coli* K-12. In 2012 our group was the first in the world to show a very strong LIBS spectral correlation between species of a given genus.⁷ It was proven in a five-genus test that strains of *Escherichia coli* were highly similar to each other as were strains of *Mycobacterium smegmatis* while two species of *Staphylococcus* (*S. aureus* and *S. saprophyticus*) and two species of *Streptococcus* (*S. mutans* and *S. viridans*) showed high similarities relative to the other bacteria. In fact, a genus level test showed very good discrimination ability (sensitivities of approximately 85% and specificities above 95%). This lends support to the idea that even if previously encountered bacteria are

tested with LIBS, an unknown spectrum should classify with its corresponding genus. Three types of bacteria from different genera were used in this work: *Escherichia coli*, *Staphylococcus epidermidis*, and *Pseudomonas aeruginosa*. They are discussed below.

E. coli is a well-studied bacterium that has many non-pathogenic strains and is easy to grow, making it ideal for use in this work. Early work on the identification of bacteria by our group using LIBS focused on *E. coli*.^{8,9} It is a motile Gram-negative rod found in the intestines of humans and animals. *E. coli* is often found on meat because it is contaminated with intestinal contents during slaughter.¹ Among other things, pathogenic *E. coli* is responsible for causing diarrhea, kidney failure, bladder infections, septicemia, pneumonia, meningitis, and urinary tract infections (UTI's).^{1,4} Pathogenic *E. coli* is the most common cause of community-acquired UTI's. The feasibility of using LIBS as a diagnostic for UTI's was investigated by our group.⁷ By mixing a small amount of *Enterobacter cloacae* with *E. coli*, both bacterial specimens that are relevant to UTI's, it was shown that *E. coli* could still be correctly identified in the presence of low concentrations of *E. cloacae*. It was also shown that the effect of solutes in urine on LIBS-based identification is negligible by suspending *S. epidermidis* in separate tubes of deionized water and sterile urine and analyzing the classification of the suspension in urine relative to the suspension in water and two other bacterial species from the *Staphylococcus* genus.

P. aeruginosa is also a motile Gram-negative rod and it is ubiquitous in the environment. It is found in water (and therefore on wet surfaces such as taps, drains, etc.), soil, and on plants.^{1,4} It can be found almost anywhere in a hospital, and it temporarily colonizes the skin and intestinal tract of humans and animals. It can cause infections by invading the body through breaches in the defense system, making it an opportunistic bacterium.^{1,4} It is responsible for nosocomial infections, eye infections in people that wear contact lenses due to the contact lens scratching the cornea, septic shock from burn and wound infections, and lung infections in patients with cystic fibrosis due to their impaired lung defenses.¹ *P. aeruginosa* is also resistant to many antibiotics.^{1,4}

S. epidermidis is a Gram-positive cocci found on the skin. It is responsible for catheter-associated infections, endocarditis, and can cause life-threatening septicemia.^{1,4} It can enter the bloodstream through breaches in the skin and also adheres to plastic surfaces, forming a biofilm, which can lead to bloodstream infections in patients with intravenous plastic catheters. *S. epidermidis* and *S. aureus* are the leading causes of nosocomial bacteremia and sepsis and have become resistant to many antibiotics.¹

A fourth type of bacteria, *Mycobacterium smegmatis*, which belongs to the acid-fast group, has been previously tested by our group with LIBS due to its different structure to observe its classification relative to the Gram-positive and Gram-negative bacteria using chemometric techniques.^{10,11} Acid-fast bacteria have the ability to withstand harsh chemicals and acids due to the presence of waxes in their cell wall and are not affected by the Gram stain.⁴ *M. smegmatis* was added to the list of bacteria regularly tested by our group for the purpose of investigating the ability of LIBS to identify and distinguish bacterial species representative of the different groups (Gram-positive, Gram-negative, and acid-fast).

3.3 Bacterial Sample Preparation

Bacterial samples were first provided by Ms. Ingrid Churchill of the Biology department at the University of Windsor. These initial samples were provided in the form of colonies on an agar plate which were then removed and suspended in deionized water and stored in microcentrifuge tubes in a fridge. This section will describe the procedure used to grow more bacteria from the colonies initially provided as well as the procedures used in preparing bacterial targets for LIBS testing.

3.3.1 Preparation of Growth Media and Harvesting of Bacteria

The bacterial samples used in this work were grown on plates containing tryptic soy agar (TSA) nutrient media. Nutrient media contain nutrients that bacteria require to grow and divide. TSA is used as a general purpose culture medium and is made from pancreatic digest of casein, papaic digest of soybean, NaCl, and agar. The TSA plates were

prepared by first dissolving 4 g of TSA powder in 100 mL of deionized water in a flask, then autoclaving the solution for 20 minutes at 121°C as per the instructions on the TSA container. After autoclaving, which sterilizes the culture media, the solution was left to cool until the flask could be safely handled. Once it could be safely handled, the solution was poured into petri dishes and left to set. The solution solidifies at room temperature into a substance with gelatinous consistency.

To culture more bacteria, 50 – 100 μ L of a bacterial suspension was pipetted onto a TSA plate and spread across the plate using an L-shaped spreader bar. The plate was then incubated for 24 hours at 37 °C to allow the bacteria to grow. An image of the plate before and after growth is shown in Figure 3.1. Following incubation, bacteria were harvested using a sterile toothpick and transferred to a microcentrifuge tube containing 1.5 mL of deionized water. The bacterial suspensions were stored in a fridge until an experiment was ready to be performed.

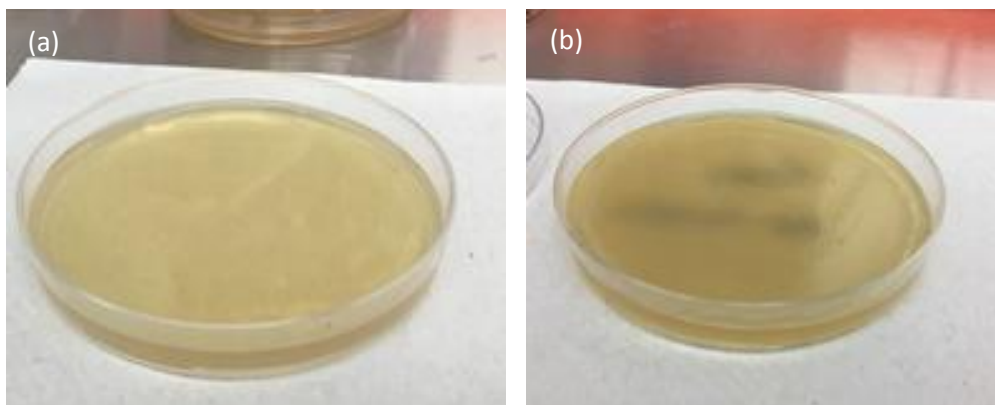


Figure 3.1: TSA plate: (a) before addition of bacteria (*E. coli*) and (b) after incubation with bacteria. Bacteria grow in an even layer across the surface of the TSA medium. The black markings in (b) are from the labeling of the bottom of the petri dish.

3.3.2 Target Preparation

Bacterial samples were deposited on standard Millipore nitrocellulose filter papers with a pore size of 0.45 μ m via two different devices: a well-plate or a centrifuge tube insert. Deposition with both devices utilize materials, equipment, and methods that are either common, or would be easy to implement in a clinical setting. The following sections will describe how bacterial targets are prepared using the two devices.

3.3.2.1 Well-plate

Bacterial samples were deposited on a nitrocellulose filter paper 13 mm in diameter (HAWP01300, Millipore Corporation) using a metal well-plate. The well-plate was placed on top of the filter and contains three 4.7 mm diameter wells. A cylindrical metal piece was then pressed into each of the wells, forming an impression in the filter paper to aid in the collection of bacteria inside the wells only. When a bacterial sample was ready to be tested with LIBS, it was first vortexed to distribute the cells evenly throughout the suspension, then 30 μL of the suspension was pipetted into each of the three wells. The well-plate was left on the filter for approximately 15 minutes to allow the water to pass through and bacterial cells to settle on the filter. Once this occurred the well-plate was removed, leaving three bacterial lawns on the filter which was left to further dry for approximately 5 minutes. This is depicted in Figure 3.2. Once dry, the filter was mounted on a steel piece using double-sided tape and tested with LIBS.

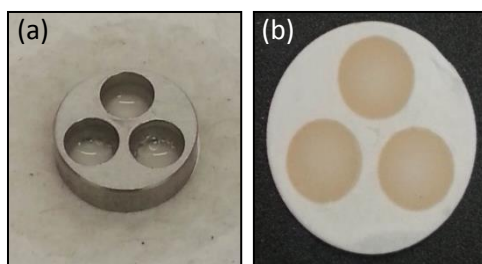


Figure 3.2: (a) Well-plate sitting on top of a filter paper with bacterial suspension in each of the three wells. (b) Filter paper after well-plate is removed. Three bacterial lawns are evident.

A spectrum of a filter paper with nothing on it (also referred to as a blank filter) and a spectrum of a filter paper with bacteria on it are shown in Figure 3.3. These spectra represent the resultant averaged spectrum from three laser shots in three different locations on the filter. Observation of these two spectra show that a blank filter can be easily distinguished from a filter with bacteria on it. A blank filter contains mainly C, and the presence of the CN molecule in both spectra is due to the carbon and nitrogen in the nitrocellulose filter recombining in the plasma. Bacterial spectra, however, contain 19 regularly observed spectral lines that were listed in Table 3.1. The area-under-the-curve intensities of these lines were determined by the ESAWIN software (as discussed in

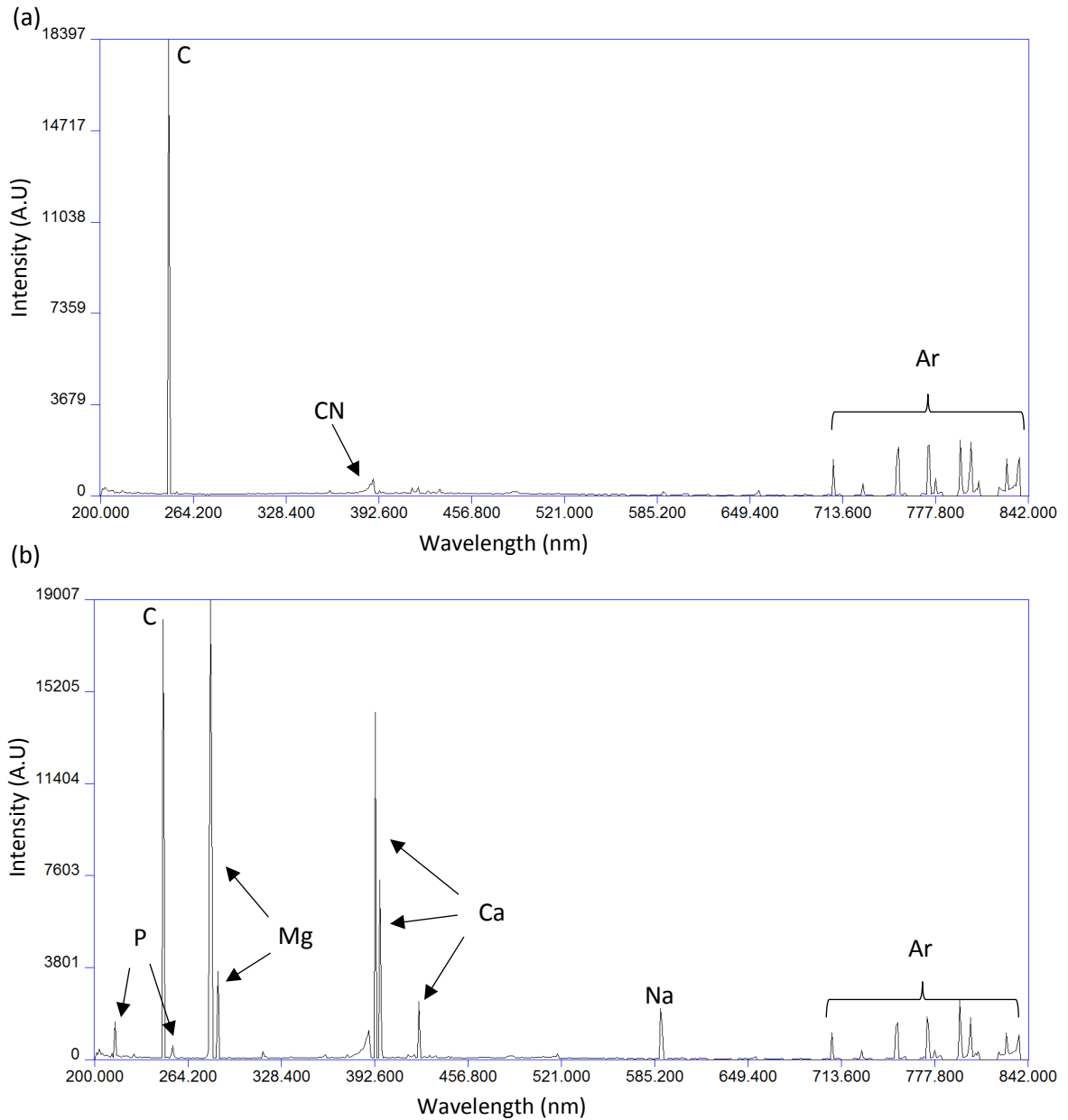


Figure 3.3: (a) Typical LIBS spectrum acquired from a blank filter. (b) Typical LIBS spectrum acquired from a filter with *E. coli* on it.

Chapter 2 section 2.2.3) and used for analysis of samples. It should be obvious from an inspection of Figure 3.3 that the carbon line at 247 nm (C247) seen in the bacterial spectrum (Figure 3.3b) must result at least in part from the ablation of the nitrocellulose filter (Figure 3.3a). Unfortunately, it is not possible to deconvolve these two contributions, therefore the measured intensity of the carbon line is not totally due to purely bacterial carbon. Fortunately, when the bacteria are deposited on the filter, not

much of the filter is ablated, but this becomes a problem at very low bacterial concentrations/coverages. In these situations, our spectrum is dominated by the filter contribution, which prevents us from increasing the gain of our detection system to make more sensitive measurements. This is an ongoing area of research. To date, the presence of carbon in the filter has not affected our ability to discriminate between bacteria, as the majority of the variance comes from bacterial phosphorus and metal ions.

3.3.2.2 Insert

A 3-D printed centrifuge tube insert (designed and constructed by a previous student in our group⁶) was used to deposit bacterial samples on a nitrocellulose filter paper. This insert has a design similar to the inserts that are commercially available. For example, this insert and those that are available on the market are the same shape, hold a filter paper at their base which contains a hole in the center, and fit inside a centrifuge tube. They are then filled with a solution and centrifuged. The solution is drawn through the filter, where anything larger than the filter's pore size is caught on the filter, and anything smaller passes through it and settles at the bottom of the centrifuge tube. What settles at the bottom of the tube is referred to as the filtrate. The inserts available on the market are designed for experiments that require only the filtrate, leaving the filter paper inaccessible. In this work, it is the filter paper that is required, so the 3-D printed insert was designed in such a way to allow for removal of the filter paper from the insert. A filter paper sits on top of the base of the insert, which is threaded at the top so it can screw into the main body. There is a hole in the center of the base to allow fluid to drain into the centrifuge tube. The insert is depicted in Figure 3.4. The bottom of the base is also threaded to allow a second base piece to screw into it. This feature of the insert will be described in more detail in Chapter 4. To properly fit on the base of the insert, the 13 mm diameter filter papers were cut with a punch and die set, resulting in a 9.5 mm diameter filter.



Figure 3.4: 3-D printed insert. (a) Main body and base of insert. (b) Filter paper sitting on top of the base. (c) The base screwed into the bottom of the main body. (d) The insert sitting inside a centrifuge tube.

Table 3.2: A list of bacterial species investigated in LIBS experiments to date^a

Species	Gram Classification	Author	Year of Publication
<i>Acinetobacter baumannii</i>	negative	Multari	2013
<i>Acinetobacter baylyi</i>	negative	Baudelet	2006
<i>Acinetobacter calcoaceticus</i>	negative	Lewis	2011
<i>Bacillus anthracis</i>	positive	Kiel	2003
		Multari	2012
<i>Bacillus atrophaeus</i>	positive	Morel	2003
		Hybl	2003
		Samuels	2003
		Leone	2004
		Hahn	2005
		De Lucia	2005
		Gottfried	2007
		Miziolek	2008
		Gottfried	2011
		Cisewski	2012
<i>Bacillus aureus</i>	positive	Saari	2016
<i>Bacillus cereus</i>	positive	Samuels	2003
		De Lucia	2005
		Cisewski	2012
<i>Bacillus megaterium</i>	positive	Kim	2004
<i>Bacillus pumilus</i>	positive	Hahn	2005
<i>Bacillus subtilis</i>	positive	Kim	2004
		Baudelet	2006
		Guyon	2006
		Merdes	2007
<i>Bacillus thuringiensis</i>	positive	Morel	2003
		Kiel	2003
		Samuels	2003
		Leone	2004
		Kim	2004
		De Lucia	2005
		Cisewski	2012
<i>Enterobacter cloacae</i>	negative	Lewis	2011
		Mohaidat ^b	2012
		Putnam ^b	2013

Species	Gram Classification	Author	Year of Publication
<i>Erwinia chrysanthemi</i>	negative	Baudelet	2006
<i>Escherichia coli</i>	negative	Morel	2003
		Leone	2004
		Kim	2004
		Baudelet	2006
		Guyon	2006
		Rehse ^b	2007
		Rehse ^b	2007
		Rehse ^b	2009
		Rehse ^b	2010
		Multari	2010
		Barnett	2011
		Gottfried	2011
		Marcos-Martinez	2011
		Mohaidat ^b	2011
		Mohaidat ^b	2012
		Multari	2013
		Putnam ^b	2013
		Manzoor	2014
		Sivakumar	2015
		Malenfant ^b	2016
Prochazka	2017		
Sauz	2017		
Farid	2018		
Liao	2018		
<i>Geobacillus stearothermophilus</i>	positive	Hahn	2005
		Cisewski	2012
<i>Klebsiella pneumoniae</i>	negative	Multari	2013
		Manzoor	2014
<i>Listeria innocua</i>	positive	Gamble	2016
<i>Methylophilus methylotrophus</i>	negative	Lewis	2011
<i>Mycobacterium smegmatis</i>		Rehse ^b	2010
		Mohaidat ^b	2011
		Mohaidat ^b	2012
		Putnam ^b	2013
		Malenfant ^b	2016
<i>Pantoea agglomerans</i>	negative	Lewis	2011
<i>Proteus mirabilis</i>	negative	Morel	2003
		Leone	2004

Species	Gram Classification	Author	Year of Publication
<i>Pseudomonas aeruginosa</i>	negative	Rehse ^b	2007
		Lewis	2011
		Marcos-Martinez	2011
		Multari	2013
		Manzoor	2014
		Malenfant ^b	2016
<i>Pseudomonas putida</i>	negative	Gamble	2016
<i>Salmoella enterica</i>	negative	Barnett	2011
<i>Salmonella pullorum</i>	negative	Manzoor	2014
<i>Salmonella salamae</i>	negative	Manzoor	2014
<i>Salmonella typhymurium</i>	negative	Marcos-Martinez	2011
		Manzoor	2014
		Gamble	2016
		Liao	2018
<i>Shewanella oneidensis</i>	negative	Baudelet	2006
<i>Staphylococcus aureus</i>	positive	Morel	2003
		Leone	2004
		Rehse ^b	2010
		Multari	2010
		Barnett	2011
		Mohaidat ^b	2012
		Multari	2013
		Putnam ^b	2013
		Gamble	2016
		Sauz	2017
		Prochazka	2017
		Farid	2018
		Liao	2018
<i>Staphylococcus epidermidis</i>	positive	Malenfant ^b	2016
<i>Staphylococcus pseudintermedius</i>	positive	Prochazka	2017
<i>Staphylococcus saprophyticus</i>	positive	Rehse ^b	2010
		Mohaidat ^b	2012
		Putnam ^b	2013
<i>Staphylococcus sciuri</i>	positive	Prochazka	2017

Species	Gram Classification	Author	Year of Publication
<i>Streptococcus mutans</i>	positive	Rehse ^b	2009
		Rehse ^b	2010
		Mohaidat ^b	2012
		Putnam ^b	2013
<i>Streptococcus viridans</i>	positive	Rehse ^b	2010
		Mohaidat ^b	2011
		Mohaidat ^b	2012
		Putnam ^b	2013

^a Specific strains utilized for experiments are not noted

^b These studies were performed by the Rehse research group

References

- ¹ A. A. Salyers and D. D. Whitt, *Bacterial Pathogenesis: A Molecular Approach*, 2nd Ed. (Washington, DC, 2002)
- ² S. J. Rehse *et al.*, *Spectrochim. Acta Part B*, **62**, 1169 (2007)
- ³ S. J. Rehse *et al.*, *J. Appl. Phys.*, **105**, 102034 (2009)
- ⁴ M. Schaechter *et al.*, *Mechanisms of Microbial Disease*, 3rd Ed. (Baltimore, USA, 1999)
- ⁵ T. Silhavy *et al.*, *Cold Spring Harb. Perspect. Biol.*, **2** (5), a000414 (2010)
- ⁶ D. J. Malenfant, *Influences on the Emissions of Bacterial Plasmas Generated through Nanosecond Laser-Induced Breakdown Spectroscopy*, Master's thesis, University of Windsor (2016)
- ⁷ Q. Mohaidat *et al.*, *Appl. Opt.*, **51** (7), B99 (2012)
- ⁸ J. Diedrich *et al.*, *Appl. Phys. Lett.*, **90**, 163901 (2007)
- ⁹ J. Diedrich *et al.*, *J. Appl. Phys.*, **102**, 014702 (2007)
- ¹⁰ S. J. Rehse *et al.*, *Appl. Opt.*, **49** (13), C27 (2010)
- ¹¹ D. J. Malenfant *et al.*, *Appl. Spectrosc.*, **70** (3), 485 (2016)

Chapter 4: Technique to Separate a Contaminant from a Bacterial Suspension

4.1 Introduction

In the context of bacterial identification, there are many different types of clinical samples (swab, blood, urine, etc.) that can be taken from a patient depending on the nature of the bacterial infection. For example, urine samples are taken when a UTI is suspected and blood samples are taken when septicemia (a bloodstream infection) is suspected. Some clinical samples such as blood and cerebrospinal fluid (CSF) are sterile, meaning that if there is an infection, the bacteria causing it are the only bacteria present in the sample. However, in all clinical samples, sterile or not, the sample also contains other unwanted matter mixed in. For example, in an infected patient, in addition to the bacteria present, a blood sample contains blood cells and a urine sample contains solutes. The presence of this unwanted matter in the clinical sample may affect the LIBS-based identification of bacteria. It is therefore necessary to quickly and easily separate the bacteria from the other unwanted matter prior to testing with LIBS.

Some clinical samples such as sputum and stool are not sterile, meaning that they contain a mixture of different species of bacteria. Our group has shown that in the case of samples with two species of bacteria mixed together, the majority species, which would likely be the one causing the infection, was correctly identified.^{1,2} This chapter will only address the separation of bacteria from other unwanted material. Separation of different species of bacteria mixed together was not investigated. In this chapter, a novel method for separating bacteria from a contaminant using a centrifuge tube insert device and nitrocellulose filter papers with different pore sizes is described.

4.2 Method

Fortunately bacteria are small, about 1 μm in size, compared to red blood cells which are one of the smallest human cells and are $\sim 6 - 8 \mu\text{m}$, and typical eukaryotic cells

which are about 10 – 100 μm .^{3,4} This difference in size can be taken advantage of by isolating bacteria based on their smaller size. To accomplish this, the centrifuge tube insert device described in Chapter 3 was used. This insert device consists of a main body and two base pieces and is shown in Figure 4.1. The bottom of the main body and top of

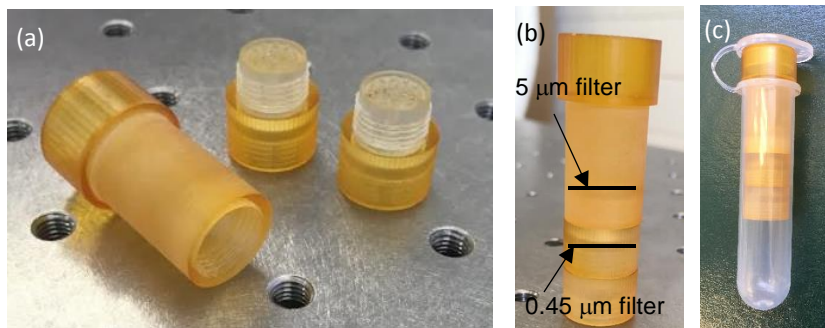


Figure 4.1: Centrifuge tube insert device with the main body of the insert alongside two base pieces in (a), all pieces screwed together in (b), and sitting inside a centrifuge tube in (c). Black lines in (b) show approximate location of where filter papers sit inside the insert.

the base pieces are threaded to allow a base piece to screw into the main body. The bottoms of the base pieces are also threaded, enabling them to screw into each other. This allows for the strategic placement of filter papers of different pore sizes in the insert. When everything is screwed together, as in Figure 4.1b, the filter papers sit on top of the base pieces and a suspension is pipetted into the top of the device and centrifuged. There is a hole in the center of each base piece to allow liquid to drain through into a centrifuge tube. Utilizing the two base pieces enables two filter papers to be used at once, where each filter paper has a different pore size to allow for the separation of bacteria from unwanted material based on their size difference. The pore sizes of the two filter papers used were 5 μm and 0.45 μm , and are, respectively, referred to as the 5 μm filter and 0.45 μm filter in this chapter. When a suspension is deposited through the top of the insert, it first encounters the 5 μm filter, then the 0.45 μm filter. This is done so that anything larger than 5 μm should get caught on the first filter while anything smaller should pass through it and get caught on the second filter provided it is larger than 0.45 μm . To test the efficacy of this device for the purpose of separating unwanted material from a bacterial suspension, tungsten powder (10401, Alfa Aesar) with an average particle size of 12 μm was used to simulate a contaminant. Tungsten powder was chosen simply

due to its biologically relevant size as well as for the presence of tungsten in the LIBS spectra which is not observed in bacterial spectra, allowing for the easy identification of the presence or absence of tungsten powder on a filter paper.

4.3 Experiments and Results

Tungsten powder was added to a suspension of *E. coli*, vortexed, and ~ 0.1 mL was pipetted into the top of the insert device with the $5\ \mu\text{m}$ filter sitting on the top base piece and the $0.45\ \mu\text{m}$ filter sitting on the bottom base piece as depicted in Figure 4.1b. The entire insert device sat inside a centrifuge tube and was centrifuged at 5000 rpm with 2500 g's of force for 3 minutes. After centrifugation, the filter papers were removed and images of them were acquired prior to LIBS testing, as shown in Figure 4.2a. Tungsten

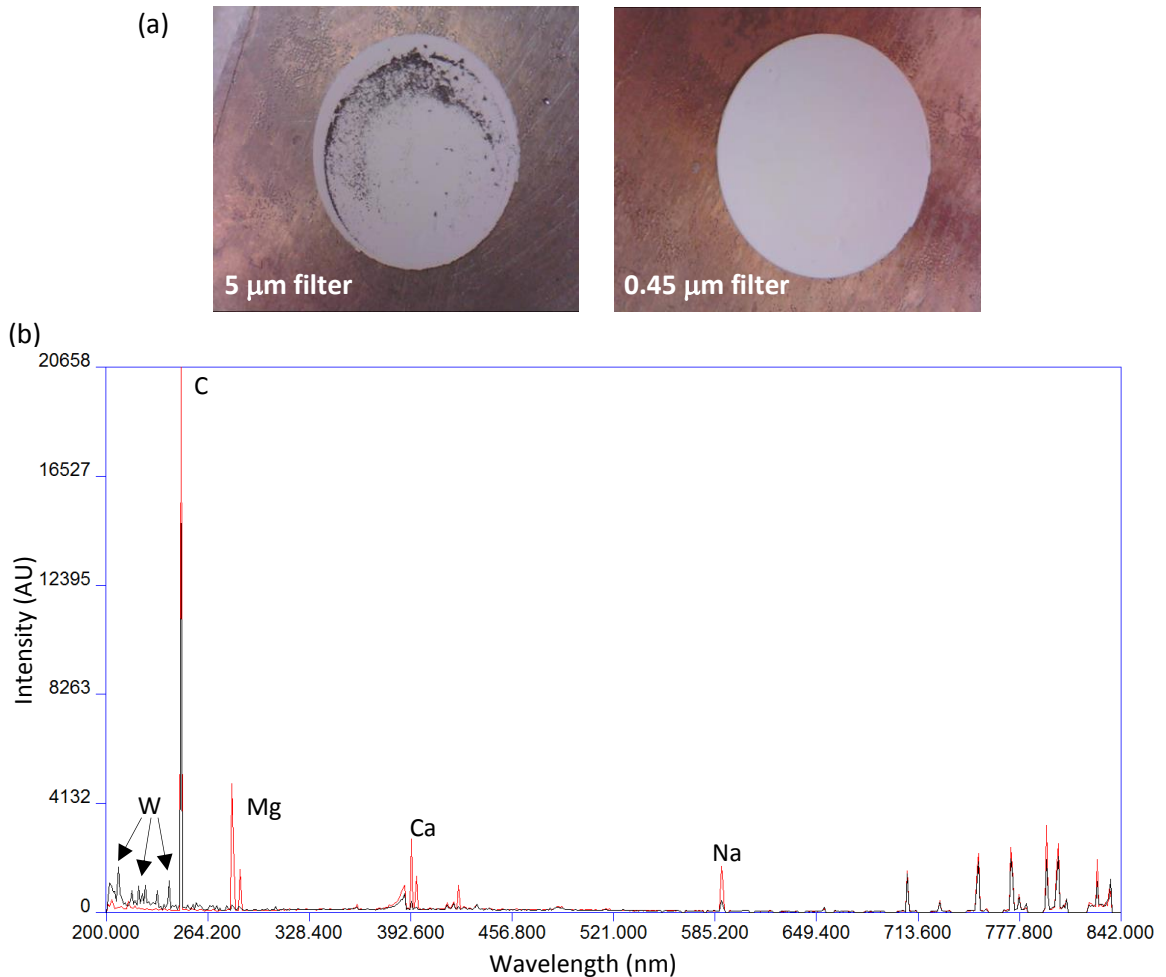


Figure 4.2: (a) Images of the filter papers after centrifugation through the insert device. Black spots on $5\ \mu\text{m}$ filter are tungsten powder. (b) Spectrum from $5\ \mu\text{m}$ filter (black) overlaid with spectrum from $0.45\ \mu\text{m}$ filter (red). Tungsten emission lines in $5\ \mu\text{m}$ filter are evident and bacterial emission lines in $0.45\ \mu\text{m}$ filter are evident.

powder was clearly observed on the 5 μm filter, while none of it was observed on the 0.45 μm filter, nor in the filtrate after centrifugation. Each filter paper was then tested with LIBS, where 45 spectra were acquired across each filter paper. Each of the 45 spectra was an average of the spectra from 3 single-shot spectra acquired at different locations. This averaging was done to minimize noise in the measurements. Figure 4.2b shows a representative spectrum from the 0.45 μm filter (red) overlaid with a representative spectrum from the 5 μm filter (black). Unfortunately, only one truly representative spectrum from the 5 μm filter was acquired because the tungsten powder was blown away after the first laser shot. Nonetheless, emission lines from tungsten were observed in the spectrum of the 5 μm filter and not in the spectrum of the 0.45 μm filter. Also of note is the presence of bacterial emission lines in the spectrum of the 0.45 μm filter and the lack of bacterial emission lines in the 5 μm filter, although bacterial emission lines were observed in some other spectra from the 5 μm filter. These results indicate that the tungsten powder was caught by the first filter while the majority of the bacteria passed through it and got caught on the second filter.

To determine approximately how much of the bacterial suspension is caught on the 5 μm filter, the average total LIBS intensity from the 45 spectra acquired on the filter papers was used. The total LIBS intensity used here was calculated as the sum of the intensities of all bacterial emission lines (shown in Table 3.1 of Chapter 3) except for the emission line from C since the 5 μm filter and 0.45 μm filter contain different amounts of C. This experiment was performed three times: once with the suspension of *E. coli* mixed with tungsten powder (referred to as *E. coli* + W) discussed above, and twice with a suspension of just *E. coli* (referred to as *E. coli* trial 1 and *E. coli* trial 2). The results are shown in Figure 4.3. In all three cases, the LIBS bacterial signal was greater on the 0.45 μm filter compared to the 5 μm filter, indicating that the majority of the bacteria bypass the first filter and get caught on the second one. With the exception of *E. coli* trial 2, the LIBS bacterial signal on the 5 μm filters are not the same within error of the 5 μm blank filter, indicating that some bacteria are caught on the 5 μm filter. An approximation of how much of the bacterial suspension gets caught on the first filter was done by

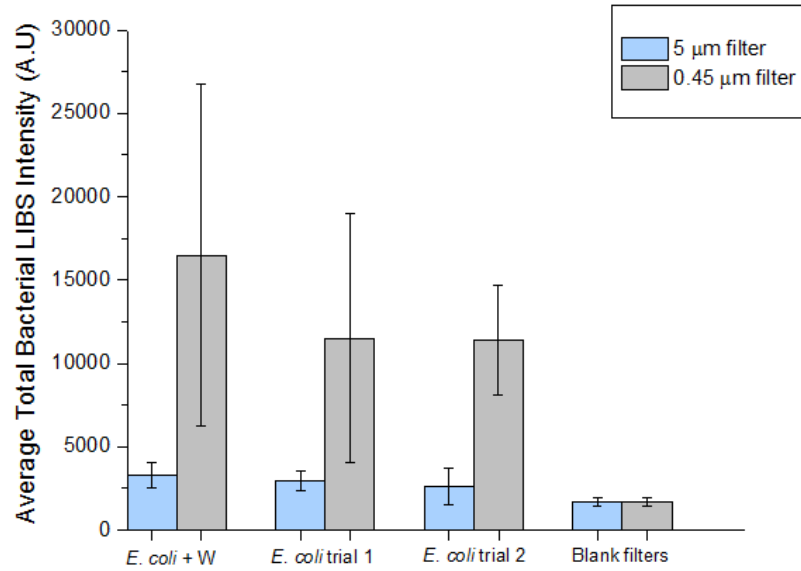


Figure 4.3: Average total LIBS intensity of the 5 μm and 0.45 μm filters for three bacterial suspensions. Error bars represent one standard deviation in the measurements.

subtracting the average total LIBS intensity of the blank 5 μm filter from that of the non-blank 5 μm filter and dividing that by the sum of the average total LIBS intensities of the 5 μm filter and 0.45 μm filter minus the average total LIBS intensities of the blank 5 μm and 0.45 μm filters. This is represented mathematically as

$$\% \text{ caught on } 5\mu\text{m filter} = \frac{(I_{5\mu\text{m}} - I_{5\mu\text{m}}^{\text{blank}})}{[(I_{5\mu\text{m}} - I_{5\mu\text{m}}^{\text{blank}}) + (I_{0.45\mu\text{m}} - I_{0.45\mu\text{m}}^{\text{blank}})]} * 100\% \quad (1)$$

where I represents the average total LIBS intensity. For the three suspensions (*E. coli* + W, *E. coli* trial 1, *E. coli* trial 2) it was determined, respectively, that approximately 10%, 12%, and 9% of the bacteria in the suspension are caught on the first filter. It is important to note that these values are based on the assumption that all of the bacterial cells in the suspension settle on the two filter papers and none of them settle anywhere else. This is likely not the case, as some bacteria may also bypass the 0.45 μm filter. In fact, it was determined previously that a small fraction of the bacteria do somehow bypass the 0.45 μm filter, and the amount of bacteria that bypass it depend on the concentration of bacteria in the suspension.⁵ If some bacteria are bypassing the 0.45 μm filter here, its total LIBS intensity would be smaller than if none of the bacteria bypassed the filter,

meaning that a smaller percentage of bacteria are caught on the 5 μm filter than initially calculated. Although these values may not be entirely accurate, they provide an approximation for the amount of bacteria that are lost on the first filter paper in this sample preparation process.

In conclusion, the preliminary experiments to test the efficacy of the insert device indicated that it offers a promising technique for separating bacteria in a suspension mixed with some contaminant, provided the contaminant is appropriately larger than the bacteria. A possible drawback of the technique is that some bacteria in the suspension are lost on the first filter paper, reducing the number of bacteria that make it through to proceed to LIBS-based identification. For LIBS-based identification, a loss of bacteria in sample preparation processes is not ideal, as a lower number of bacteria lead to a smaller bacterial signal, hindering the identification. Bacteria tend to clump together, and if they form a clump that is larger than 5 μm , it would be caught by the first filter paper. If the clumping could be prevented, then in theory all of the bacterial cells should pass through the first filter. This would eliminate the drawback that some bacteria are lost on the first filter in this preparation process. Prevention of bacterial cell clumping was investigated and more details can be found in Chapter 6. Another drawback of this technique is that it is not capable of separating mixtures of different species of bacteria since they are similar in size. This technique is meant for size-based separation. In addition, to assess the true utility of this technique, experiments need to be performed using actual clinical samples. The work done in this chapter simply illustrates the success of the proof-of-concept preliminary experiments. This preparation process offers a quick and easy way to separate unwanted matter from bacterial suspensions using materials and equipment that are either already found in a clinical laboratory or would be easy to introduce into a clinical setting, and require no expertise in microbiology.

References

- ¹ S. J. Rehse *et al.*, *Appl. Opt.*, **49** (13), C27 (2010)
- ² Q. Mohaidat *et al.*, *Appl. Opt.*, **51** (7), B99 (2012)
- ³ M. L. Turgeon, *Clinical Hematology: Theory and Procedures*, 4th Ed. (Baltimore, USA, 2005)
- ⁴ *Size Scales of Cell Biology*, Moosmosis. <<https://moosmosis.org/2015/09/17/size-scales-of-cell-biology/>> (2015)
- ⁵ D. J. Malenfant, *Influences on the Emissions of Bacterial Plasmas Generated through Nanosecond Laser-Induced Breakdown Spectroscopy*, Master's thesis, University of Windsor (2016)

Chapter 5: Effect of Metal Cone in Target Preparation

5.1 Motivation

Detection and identification of bacteria with LIBS are possible with large quantities of bacterial cells, but to be clinically relevant they must be possible with the amount of bacterial cells that would be present in a clinical sample. For example, the concentration of microbes in a typical blood sample from a bacteremic patient is 1-100 CFU/mL,¹ and 0-200 CFU of methicillin-resistant *S. aureus* (MRSA) are recovered from a typical nasal swab.² The limit of detection of bacterial cells with LIBS was determined by a previous student in our research group to be ~50000 CFU per laser ablation event when the bacteria were deposited on filter media via the well-plate, and ~90000 CFU per laser ablation event when deposited via the centrifuge tube insert.³ These limits of detection are much too high and not realistic for bacterial detection and identification in a clinical setting. It is therefore important to lower the limit of detection.

The bacterial limit of detection with LIBS can be improved by maximizing the number of bacterial cells that are ablated in a single laser shot. This can be accomplished by depositing bacterial cells onto a very small area of the filter paper. As a result, this would concentrate the cells in a smaller region rather than spreading them out across a larger area, allowing for ablation of more cells in a laser shot and thus increasing the LIBS bacterial signal. To achieve this, a hollow metal cone was designed to fit inside the centrifuge tube insert, allowing bacterial suspensions to pass through it while forcing the bacteria to settle onto a smaller area of the filter paper compared to both the well-plate and the centrifuge tube insert methods of deposition where the bacterial cells are spread out across larger regions. The design of this metal cone, as well as its ability to concentrate bacterial cells and lower the limit of detection will be discussed in this chapter.

5.2 Design

The metal cone was constructed out of aluminum and made by the machine shop at the University of Windsor. It was designed to fit inside the insert for the centrifuge tube which was described in detail in Chapter 3. The height of the cone was chosen such that when it is inside the insert which is inside the centrifuge tube, the cap of the centrifuge tube presses the metal cone onto a filter paper that is placed on top of the base of the insert. This is depicted in Figure 5.1. The end of the cone that presses into the filter paper has a hole approximately 1 mm in diameter, so that the bacterial cells deposited on the filter paper should occupy an area of roughly the same size as the hole in the cone. This can be compared with the 4.7 mm diameter of the bacterial lawns formed with the well-plate, and the 9.5 mm diameter of the bacterial lawn formed with the insert alone.



Figure 5.1: (a) Metal cone. (b) Insert with filter paper placed on the base. (c) Metal cone inside the insert which is inside a centrifuge tube. (d) Cap of centrifuge tube presses metal cone into filter paper sitting on the base of the insert.

5.3 Bacterial Concentration

To qualitatively test the ability of the metal cone to concentrate bacterial cells onto a small region at the center of a filter paper, a suspension of *P. aeruginosa* was centrifuged through the metal cone and deposited onto a filter paper. Figure 5.2 shows the resulting deposition. The lawn of bacteria is evident in the center of the filter and four trapezoidal indentations around the circular lawn are visible from where the apex of the cone pressed the filter into the underlying insert. This could assist in locating the bacterial lawn in less visible depositions (i.e. low concentrations of bacteria in suspension). The metal cone clearly accomplished its goal of forcing the bacterial cells to settle onto a smaller area of the filter paper.



Figure 5.2: After centrifugation with the metal cone, a bacterial lawn is observed near the center of the filter.

To quantitatively test the effectiveness of the metal cone, 50 μL of an *E. coli* suspension with a concentration of 9.2×10^7 CFU/mL was centrifuged through the metal cone at 5000 rpm with 2500 g's of force for 5 minutes. Single-shot LIBS data were acquired across the filter. A colour map depicting total LIBS intensity as a function of position on the filter paper is shown in Figure 5.3a, where the total LIBS intensity was calculated as the sum of the intensities of the elemental emission lines stated in Table 3.1 of Chapter 3. The colour indicates the intensity of the LIBS bacterial signal, with purple corresponding to no bacterial signal and red corresponding to strong bacterial signal (in arbitrary units). The black circle on the colour map is 1 mm in diameter and serves to show the approximate location of where the cone presses into the filter paper. As can be seen in the figure, most of the region with the strongest bacterial signal is found within the black circle. Some LIBS bacterial signal is observed beyond the black circle (blue and green regions), indicating that there is not a perfect seal between the cone and the filter paper, allowing some bacterial cells to settle on regions of the filter outside of the cone hole. Figure 5.3b shows an image taken of the filter paper after it was tested with LIBS. The laser shots are clearly identifiable in the image, as well as the region with bacteria which exhibits some discolouration in comparison to the rest of the filter paper. This experiment demonstrated quantitatively that the metal cone was effective at forcing bacterial cells to settle onto a smaller area of a filter paper.

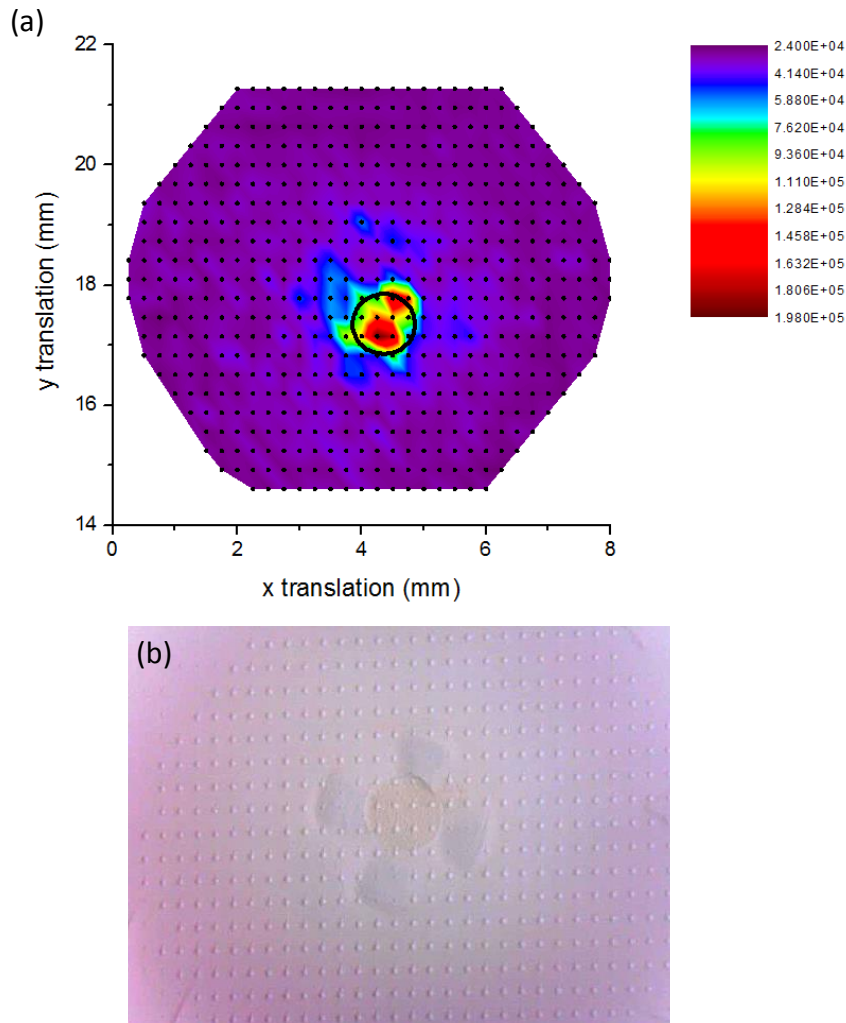


Figure 5.3: (a) Colour map depicting total LIBS intensity as a function of position on the filter. Each black dot represents a data point corresponding to a single laser shot. The black circle indicates the approximate location of the cone hole on the filter. (b) Image of the filter after data acquisition. The four trapezoidal indentations are again evident.

5.4 Comparison of LIBS Signal from Targets Prepared with Metal Cone, Well-Plate, and Insert

30 μL of an *E. coli* suspension with a concentration of 8.8×10^7 CFU/mL was deposited on filter papers via three different deposition methods to determine whether deposition with the metal cone results in an increased LIBS bacterial signal. Single-shot LIBS data were acquired across each filter. Two targets were prepared with the metal cone, and 20 LIBS spectra were acquired from each, resulting in a total of 40 LIBS spectra acquired from deposition with the metal cone. The average total LIBS intensity for deposition with the metal cone was calculated by averaging the total LIBS intensities of

the 40 LIBS spectra. One target was prepared with the well-plate, where 30 μL of the bacterial suspension was deposited in each well, and 20 LIBS spectra were acquired from the bacterial lawns formed from each of the three wells, resulting in a total of 60 LIBS spectra. These 60 LIBS spectra were used to compute the average total LIBS intensity for deposition with the well-plate. Four targets were prepared with the insert, and 30 LIBS spectra were acquired on each, resulting in a total of 120 LIBS spectra used to compute the average total LIBS intensity for deposition with the insert. A filter with no bacteria, referred to as a blank filter, was centrifuged with the metal cone and 20 single-shot LIBS spectra were acquired. The average total LIBS intensity for the blank filter was determined.

A plot of the average total LIBS intensities for the three bacterial deposition methods is shown in Figure 5.4. It can be seen that the LIBS bacterial signals from the *E. coli* suspension deposited with both the well-plate and the insert are comparable to the signal of a blank filter, but this was to be expected. The reason for this is that the amount of bacteria deposited was lower than the known limits of detection for bacteria deposited with the well-plate and with the insert. The LIBS signal from the target prepared with the metal cone, however, is larger and outside the error of the LIBS signal from the other

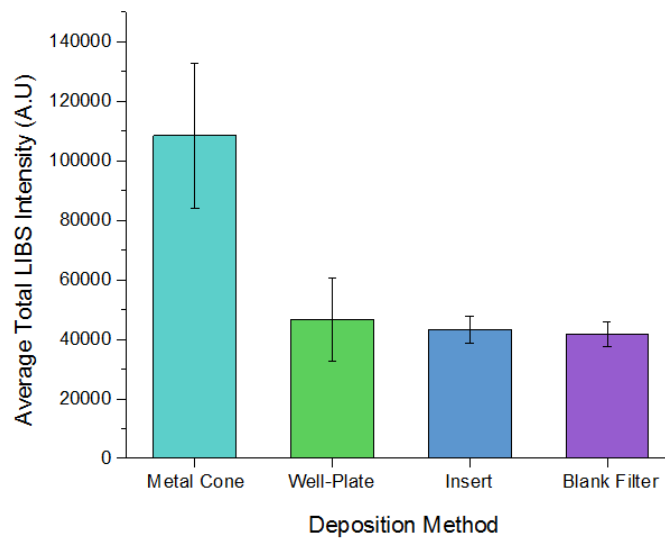


Figure 5.4: Average total LIBS intensity of bacteria deposited using three different methods. Error bars represent one standard deviation in the measurements.

deposition methods. Since the same amount of bacteria is deposited on filter papers with the metal cone, well-plate, and insert, the LIBS signal from deposition with the metal cone is expected to be the greatest due to its smallest deposition area. Based on area, the LIBS signal from bacteria deposited with the metal cone should be approximately 20 times greater and approximately 90 times greater than bacteria deposited with the well-plate and insert, respectively. Since the amount of bacteria deposited was outside of the limits of detection for both the well-plate and the insert, their average total LIBS intensities cannot be used to verify this.

In conclusion, deposition of bacteria with the metal cone provides an increased LIBS signal compared to the other two procedures used for deposition. Where the signal from the well-plate and insert methods are comparable to a blank filter due to the use of too little bacteria for detection, the metal cone method provides a signal great enough to be distinguished from a blank filter, suggesting that there is a lower limit of detection of bacteria when the metal cone is used to prepare targets.

5.5 Limit of Detection

5.5.1 Introduction

As seen from the previous two sections, the metal cone was effective at concentrating bacterial suspensions onto a smaller region of a filter paper and increasing the LIBS bacterial signal compared to the other two methods of bacterial deposition. This indicates that more bacteria are ablated per laser shot when deposited with the metal cone, which should result in an improvement of the bacterial limit of detection with LIBS.

A calibration curve of measured analytic signal plotted as a function of the amount of analyte present in a sample is used to determine limit of detection, where the amount of analyte will be represented as a bacterial concentration in this chapter. It is important, however, to define what is meant by “bacterial concentration.” First, the bacteria are not dissolved in a solution, rather all bacterial suspensions are characterized by the number of cells (in CFU) suspended in a volume of water (in mL). Therefore a quantity such as

1×10^7 CFU/mL is an appropriate concentration. However, due to the way the suspension is tested in this work (i.e. centrifuged and passed through a filter) the volume of water is actually immaterial. 1×10^7 CFU suspended in 1 mL or in 2 mL would yield identical LIBS measured signals after being passed through the filter. It is therefore our standard practice to report the “concentration” merely as the quantity of bacteria, in CFU. This standard will be used in this chapter.

Calibration curves in LIBS typically contain a region at lower concentrations where the signals from the elemental lines present in the sample are linearly related to the amount of analyte ablated in a laser pulse. This is called the linear dynamic range.⁴ At higher concentrations, however, the relationship is no longer linear. The LIBS signal begins to plateau, such that a large increase in the concentration no longer results in a correspondingly large increase in LIBS signal. This is often due to self-absorption in the LIBS plasma, a plateauing of the amount of analyte ablated into the plasma due to laser-substrate interactions, or other plasma effects. Self-absorption is a process where the photons emitted by the excited atoms in the middle of the plasma are reabsorbed by the cooler atoms in the outer layer of the plasma. The number of cooler atoms in the outer layer of the plasma increases as the concentration of analyte in the sample increases, resulting in the reabsorption of more photons before they reach the detector, reducing the signal from the emission lines.⁴

The limit of detection in terms of bacterial detection with LIBS is defined as the smallest concentration of bacteria required for distinction from a sample with no bacteria (referred to as a “blank”).⁵ More specifically, it is the minimum number of bacterial cells needed to provide a LIBS signal that is discernable from a blank filter with reasonable confidence that it is not a random fluctuation of the blank.⁶ A plot of LIBS intensity as a function of bacterial concentration can be constructed, and a linear fit to the data in the linear dynamic range of the plot can be performed. Once this is accomplished, the slope and the error in the y-intercept can be obtained to calculate the limit of detection which is defined mathematically as

$$c_L = \frac{k s_B}{m}$$

where c_L is the limit of detection, s_B is the standard deviation of the blank measurements (error in y-intercept), m is the slope of the line, and k is a numerical factor representing the desired level of confidence that the minimum discernable signal is not a random fluctuation of the blank sample.⁶ The choice of $k = 3$ is recommended by IUPAC,^{5,6} which gives a limit of detection corresponding to 99.7% confidence that a measured signal is not a random fluctuation of the signal from a blank sample. In other words, there is a 0.3% chance that a measurement of a sample with a concentration equal to or greater than the limit of detection results in a measured signal that corresponds to a random fluctuation in the signal of the blank sample rather than a signal corresponding to bacteria.

5.5.2 Experiment and Results

E. coli was cultured on an agar plate and suspended in deionized water. Nine different dilutions in deionized water were prepared, and their concentrations in CFU/mL were determined from optical densitometry measurements. Each dilution was deposited onto two filter papers with the metal cone, where 30 μ L of each suspension was centrifuged through the cone at 5000 rpm with 2500 g's of force for 5 minutes. The amount of bacteria deposited in CFU for each dilution was calculated by multiplying the concentration in CFU/mL by the 30 μ L that was deposited through the metal cone. Twenty single-shot LIBS spectra were taken on each filter in the region where the cone presses into the filter, resulting in a total of 40 spectra acquired for each dilution. The average total LIBS intensity for each dilution was then calculated by averaging the total LIBS intensities of each of the 40 spectra.

A plot of the average total LIBS intensity as a function of the amount of bacteria in CFU for each of the dilutions is shown in Figure 5.5a. One can note that the linear dynamic range exists for concentrations below 1×10^7 CFU, and above this value the curve plateaus. A linear fit to the seven data points in the linear dynamic range is shown in Figure 5.5b, where the errors in the measurements are included in the fit. The resulting

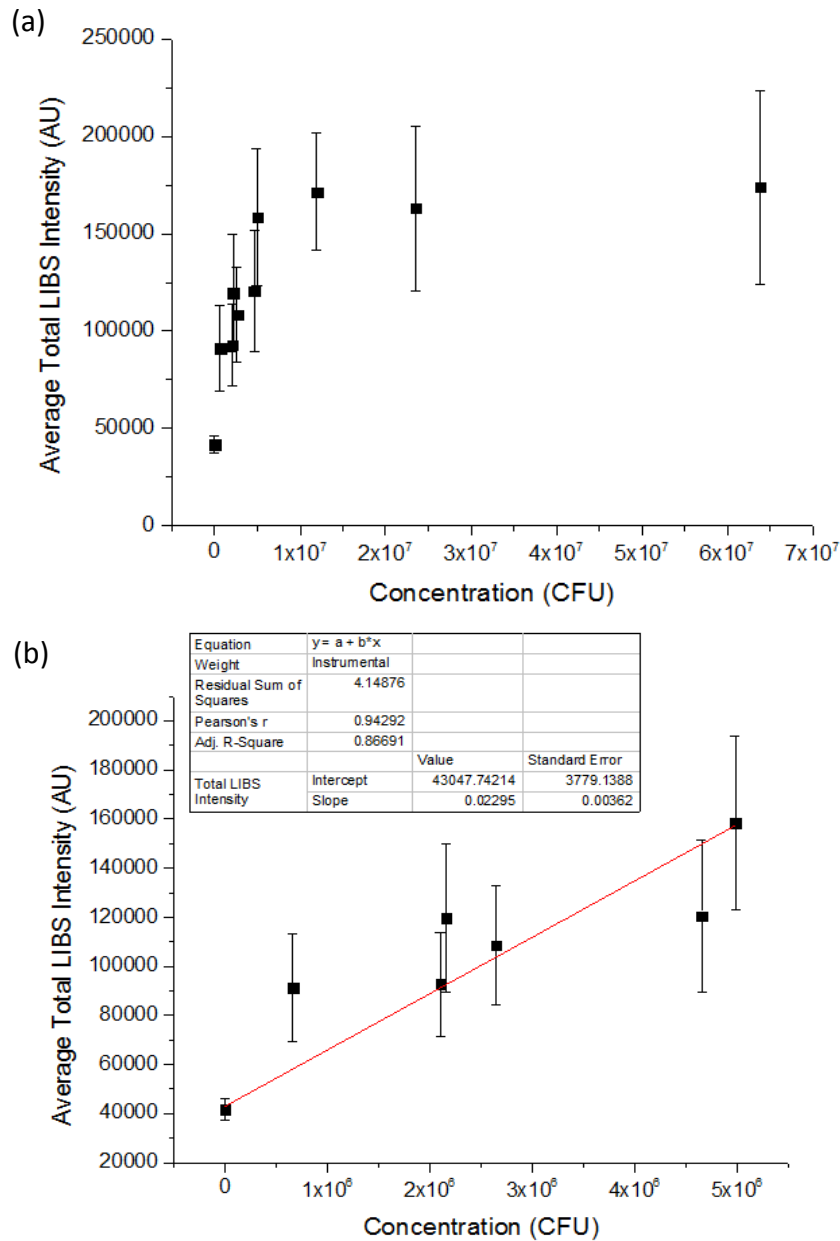


Figure 5.5: (a) Plot of average total LIBS intensity as a function of CFU. Error bars represent one standard deviation in the measurements. (b) Linear fit to the linear dynamic range in (a).

LIBS bacterial limit of detection is 5530 ± 872 CFU per laser ablation event. This is a substantial improvement in the limit of detection given that ~ 50000 CFU per laser ablation event are required for detection when deposited with the well-plate, and ~ 90000 CFU per laser ablation event are required for detection when deposited with the insert.

Based on the area of bacterial deposition on the filter paper, the limit of detection for bacteria deposited with the metal cone should be approximately 20 times greater than

that for bacteria deposited with the well-plate, and approximately 90 times greater than that for bacteria deposited with the insert. Unfortunately, the metal cone only improved the limit of detection by factors of approximately 9 and 16 compared to the limits of detection for bacteria deposited with the well-plate and insert respectively. One reason for this smaller than expected limit of detection with the metal cone is that not all of the bacteria escape from the cone and land on the filter paper. When suspensions of higher bacterial concentration were deposited, some bacteria were clearly seen remaining in the cone after centrifugation. It is suspected that, although it cannot be seen by eye, at lower concentrations some bacteria remain in the cone as well. Another reason is due to the fact that there is not a perfect seal between the cone and the filter paper, resulting in some bacterial cells settling on the filter outside of the circular region where the cone deposits the majority of the cells. If not all of the cells are making their way out of the cone and onto the filter paper, and if not all of the cells on the filter are settled in the circular region at the center, the resulting LIBS bacterial signal would be lower, giving rise to a higher limit of detection than expected. Despite this, when bacteria are deposited with the metal cone, the limit of detection is lowered by an order of magnitude, which is a significant improvement compared to deposition with the well-plate and insert.

References

- ¹ A. Boardman *et al.*, PLoS ONE, **10** (2), e0116837 (2015)
- ² P. Warnke *et al.*, PLoS ONE, **9** (10), e111627 (2014)
- ³ D. J. Malenfant, *Influences on the Emissions of Bacterial Plasmas Generated through Nanosecond Laser-Induced Breakdown Spectroscopy*, Master's thesis, University of Windsor (2016)
- ⁴ D. A. Cremers and L. J. Radziemski, *Handbook of Laser-Induced Breakdown Spectroscopy*, 1st Ed. (West Sussex, England, 2006)
- ⁵ Analytical Methods Committee, *Analyst*, **112** (2), 199 (1987)
- ⁶ G. L. Long and J. D. Winefordner, *Anal. Chem.*, **55** (7), 712 (1983)

Chapter 6: Effects of Tween 20 and Growth in Liquid Culture on the LIBS Analysis of *E. coli* Cells

6.1 Introduction

6.1.1 Motivation

Bacterial cells aggregate, forming clusters or clumps. This reduces their surface area, making them less exposed to their surroundings which may be a strategy to protect them from an environment that may be harmful to them. As discussed in Chapter 4, this clumping is an issue when it comes to separating bacteria from a contaminant using the insert device and filter papers of certain pore sizes. Some bacteria are filtered out with the contaminant due to this clumping, reducing the number of bacterial cells that make it through to be identified with LIBS.

Evidence of shot-to-shot variation was observed in the LIBS spectra of low concentrations ($< 1 \times 10^9$ CFU/mL) of bacteria deposited on filter papers using the well-plate method of deposition (method described in Chapter 3). While testing a filter with LIBS, it was observed that some spectra obtained from sampling locations adjacent to each other on the filter (0.25 mm apart) were highly inconsistent. One location yielded high bacterial signal and the one next to it yielded little to no bacterial signal. This evidence is shown in Figure 6.1 where two spectra of *E. coli* from the same filter paper are overlapped. The spectrum in black shows high bacterial signal and the spectrum in blue shows little to no bacterial signal, comparable to the signal of a blank filter which is shown in red and does not exhibit such shot-to-shot variation. We interpret this behaviour as clumping or non-uniform deposition of bacterial cells. This is an issue when it comes to determining a limit of detection because it results in non-uniform laser ablation. Thus it is important to prevent such shot-to-shot variations in bacterial signal by controlling how the bacterial cells cluster and are deposited on the filter. The effectiveness of a detergent known as Tween 20 as well as the effectiveness of growing bacteria in a liquid medium rather than on a solid medium to improve the repeatability

of the LIBS signal and provide more uniform laser ablation were investigated and are discussed in this chapter.

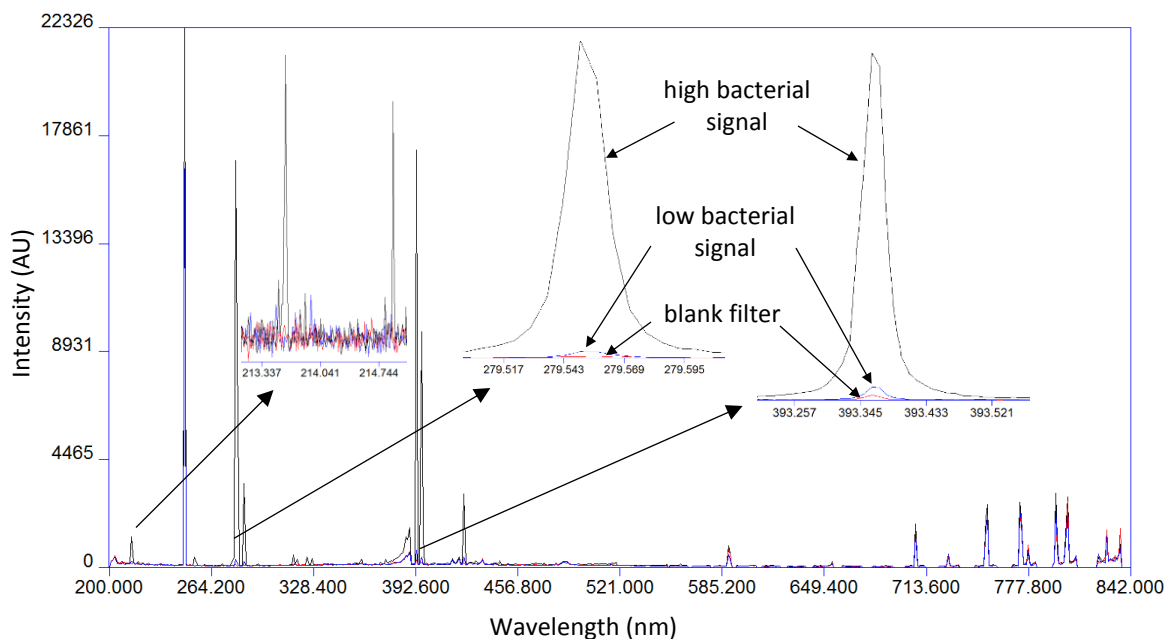


Figure 6.1: Two overlapped *E. coli* spectra taken side-by-side on the same filter paper, showing evidence of non-uniform laser ablation. Black spectrum exhibits high bacterial signal and blue spectrum exhibits signal comparable to a blank filter which is shown in red. Insets show zoomed-in sections of the emissions from phosphorus, magnesium, and calcium.

6.1.2 Tween 20

Detergents disrupt the cell membranes of bacteria and the intracellular components are released as a result. This is known as lysis. Detergents are amphipathic organic compounds with a hydrophilic head group and hydrophobic hydrocarbon tail. Depending on the head group, a detergent can be anionic, cationic, zwitterionic, or non-ionic.^{1,2} A detergent makes hydrophobic compounds that are insoluble in water miscible in aqueous media.² Tween 20 ($C_{58}H_{114}O_{26}$) is a non-ionic detergent that is used to solubilize cells.^{1,3} It acts as an emulsifier,¹ which is a substance that helps to combine liquids that are normally immiscible. Non-ionic detergents are non-denaturing, so they do not disrupt the structure of water-soluble proteins, maintaining protein function.² It was thought that treatment of bacteria with Tween 20 prior to deposition on a filter paper would aid in distributing the cells more evenly throughout the suspension, preventing

bacterial cells from forming clumps and giving rise to a more consistent LIBS bacterial signal.

6.1.3 Liquid Culture

Growth of bacteria in a nutrient broth rather than on solid media like agar plates was thought to aid in the prevention of bacterial cell clumping. Nutrient broth is a liquid growth medium for bacteria that consists of a variety of nutrients in powder-form dissolved in water. Growth in liquid media can be used to assess the oxygen requirements of bacteria. Aerobic bacteria (bacteria that require oxygen) grow near the surface of the broth, and anaerobic bacteria (oxygen is toxic to this type of bacteria) grow near the bottom of the tube of broth.⁴ Some bacteria, such as *E. coli* and the *Staphylococcus* species, have the ability to grow in both the presence and absence of oxygen.⁵ Bacteria grow dispersed in liquid media, often forming colloidal suspensions where bacteria are suspended throughout the broth. Growth in this way more closely resembles the growth of bacteria in the body compared to growth on agar plates, and is therefore more representative of clinical specimens. Although, typically, bacterial cultures grown in liquid media are constantly agitated or shaken during culturing to avoid conglomeration, we did not have access to this type of incubator, so our samples were not shaken during growth.

6.2 Experiments and Results

6.2.1 Investigation of the Effect on the LIBS Bacterial Signal of *E. coli* Cells Treated with Tween 20

To evaluate the effectiveness of Tween 20 to prevent clumping of *E. coli* cells and provide more uniform laser ablation, two sets of dilutions were prepared from the same initial suspension of *E. coli*. The dilutions were prepared in the same manner to enable testing of one set with Tween and the other set without Tween to act as a control. The concentration of each dilution before the addition of Tween was determined through optical densitometry to ensure that the concentration of each diluted sample in one set was similar to the corresponding diluted sample in the other set. The dilutions used for

this experiment were represented as a fraction of the initial concentration and are as follows: 1/10, 1/50, 1/500, and 1/1000. All dilutions in one set were treated with a 0.1% concentration of Tween which was only added to the bacterial suspension and vortexed immediately prior to deposition on a filter paper. The original concentration of each of the diluted samples was very minimally altered (<2% difference in concentration) as a result of the addition of a small amount of Tween, but, nevertheless, water was added to each of the “no Tween” diluted samples in the same amount that Tween was added to the “with Tween” diluted samples to ensure that the minor change in bacterial concentration of the samples in each set was the same. The samples were deposited on nitrocellulose filter papers using the well-plate. Each dilution was deposited on a different filter paper, with the “no Tween” and “with Tween” samples for the same dilution factor in each set deposited side-by-side in the wells on the same filter paper. A total of 30 spectra were acquired in each well, where each spectrum was the average of the spectra from 3 laser shots in different locations. For clarity, this is shown in Figure 6.2.

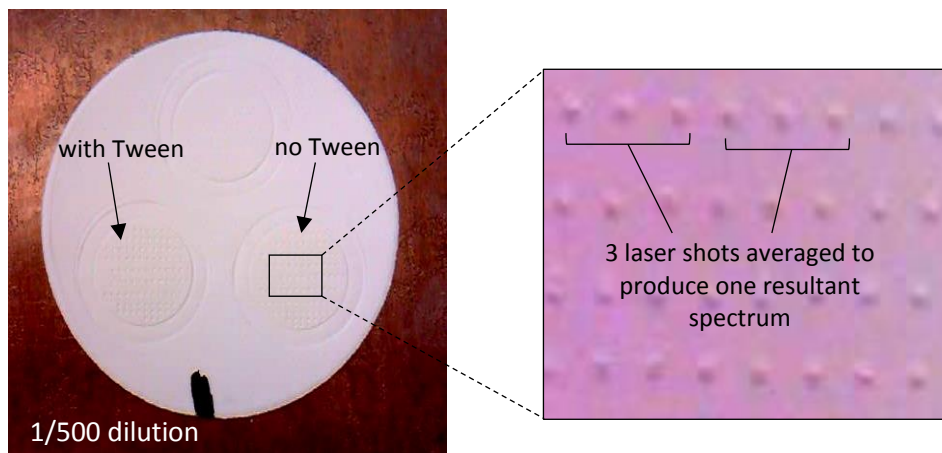


Figure 6.2: Image of filter paper after deposition of *E. coli* suspensions with and without Tween for the 1/500 dilution. The impressions from the three wells are evident.

For each dilution factor, a plot of the total LIBS intensity as a function of spectrum number was constructed. These plots are shown in Figure 6.3, where the total LIBS intensity was calculated as the sum of the intensities of all bacterial emission lines (stated in Table 3.1 of Chapter 3) excluding carbon due to its presence in Tween, and each spectrum number represents the resultant averaged spectrum from 3 laser shots in different locations within the impression of the well on the filter paper. It can be seen

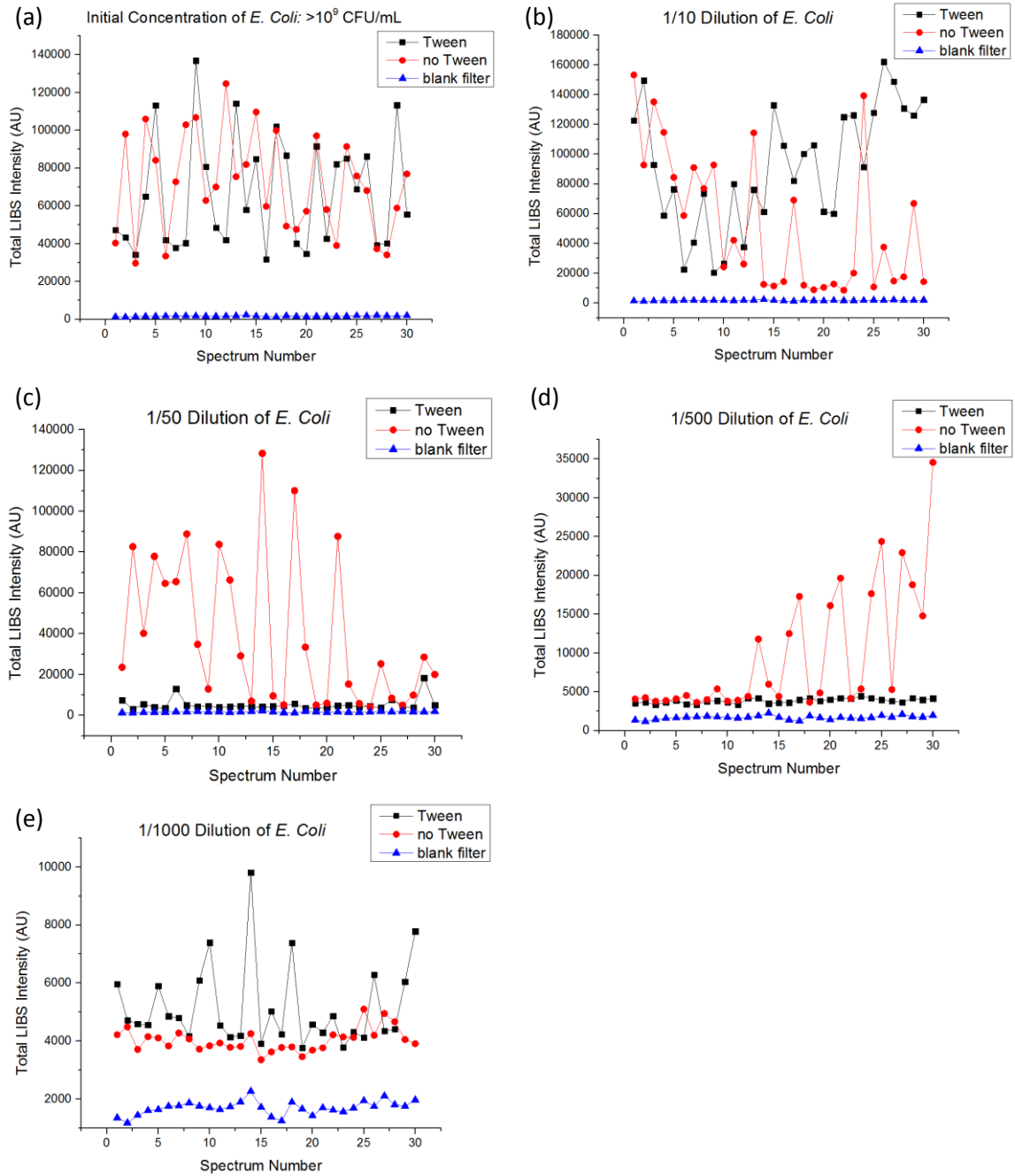


Figure 6.3: Plots of total LIBS intensity as a function of spectrum number for each sample.

from Figure 6.3a that there is no difference between the sample with Tween and the sample without Tween, indicating that Tween had no effect on the initial concentration of *E. coli*. This was not surprising since bacterial clumping is not an issue during LIBS testing at higher concentrations (although it certainly should occur) due to the presence of a large number of cells with no gaps between cells on the filter medium. No significant difference

between the sample with Tween and the sample without Tween is observed for the 1/10 dilution shown in Figure 6.3b. The reason for this may be that there were still too many cells present that clumping was also not an issue at this concentration. Figures 6.3c and 6.3d show the plots for the 1/50 and 1/500 dilutions, and in both cases, the sample with no Tween exhibits evidence of clumping (some locations have high LIBS bacterial signal and others have low bacterial signal, some of which are comparable to that of a blank filter). The LIBS signal of the samples with Tween are similar to that of a blank filter, and much more consistent than the samples without Tween. If Tween is preventing clumping, it would allow the bacteria to spread out in a thin, even layer on the filter paper, resulting in a lower bacterial LIBS signal compared to the LIBS signal resulting from a clump of bacteria. Ideally, the sample with Tween would have a relatively constant LIBS signal with a value around the average of that of the sample without Tween. This was not the case here. Perhaps the Tween was effective at causing the bacterial cells to spread out so much that they settled in regions beyond the impression of the well on filter paper. Figure 6.3e shows the plot for the 1/1000 dilution which exhibited a different result compared to the 1/50 and 1/500 dilutions. The signal for the sample without Tween was more constant than the signal for the sample with Tween, which was not expected if Tween was assumed to prevent clumping. It was thought that perhaps the Tween prevents the sticking of bacterial cells to the tube they are stored in and to the pipette when they are transferred to the filter paper. At such a low concentration, a significant amount may be lost due to sticking. If Tween prevents sticking, it would allow more bacteria to make it to the filter paper without being lost in the transfer process. This could explain why the bacterial signal is higher for the sample with Tween.

Scanning electron micrographs of representative regions within some of the samples on the filter papers were acquired at two magnifications after testing with LIBS and can be seen in Figure 6.4. Laser ablation craters can be seen in Figure 6.4c, e, i, and m. There are four things to note. First, the micrographs of a section of the filter paper that was not expected to have bacteria on it (Figure 6.4a, b) actually appeared different than all other micrographs of sections that were expected to have bacteria (Figure 6.4c-n). This

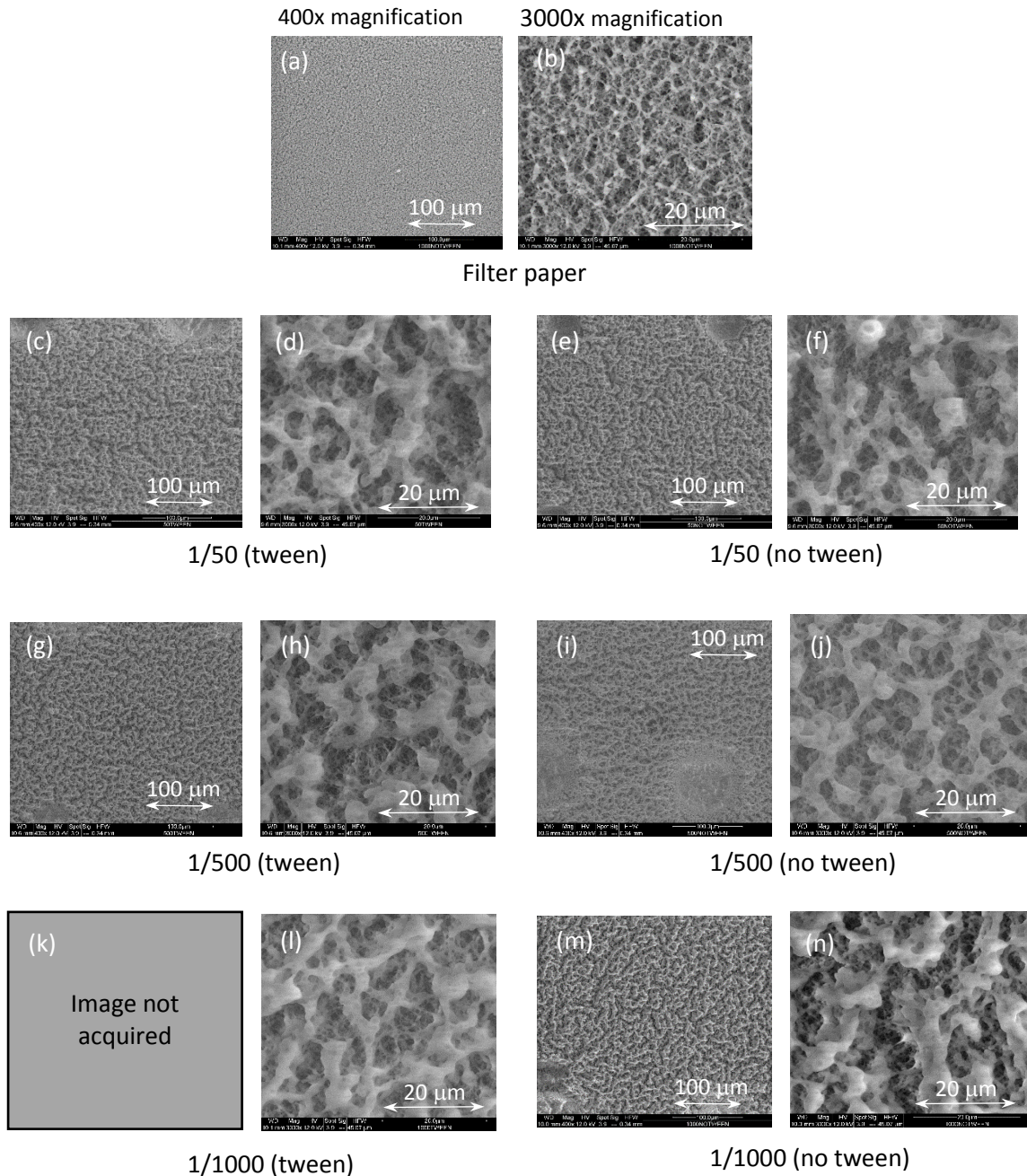


Figure 6.4: SEM micrographs of some of the sample depositions on filter papers.

allowed us to definitively identify sections of filter that did have bacteria deposited on it, even though they do look casually similar. Second, no qualitative differences were observed between the “Tween” and “no Tween” micrographs taken at each dilution. For example, the 1/50 sample with Tween did not appear different from the 1/50 sample without Tween (Figure 6.4 c compared to e, and d compared to f), and so on for the other

dilutions. This was not expected when compared to the plots in Figure 6.3c (1/50 dilution) and Figure 6.3d (1/500 dilution), which both show a difference in the LIBS signal for the “Tween” and “no Tween” samples. Third, there was no significant difference between the amount of bacteria observed in each of the micrographs at each dilution, which does not agree with the plots in Figure 6.3. For example, it can be seen from Figure 6.3c and Figure 6.3e that the total LIBS intensity of the 1/50 dilution without Tween is approximately 15 times greater than that of the 1/1000 dilution without Tween, yet the corresponding SEM micrographs in Figure 6.4e,f and Figure 6.4m,n do not appear to have any significant difference in the amount of bacteria present. The same can be said for the depositions with and without Tween for the 1/50 dilution. Unfortunately, the reason for these disagreements between the plots in Figure 6.3 and the SEM micrographs in Figure 6.4 is not known. Fourth, note that two LIBS craters (the laser samples a region of approximately 100 μm in diameter) are visible at the bottom of Figure 6.4i. There does not appear to be any more or less bacteria under or near these craters, and in addition, there does not appear to be any more or less bacteria in any regions in each of the micrographs in Figure 6.4c, e, g, and m, indicating that the bacteria do not form clumps on this scale. However, clumping is apparent in Figure 6.4d, f, h, j, l, and n, where each of these micrographs represent a region smaller than a LIBS crater. It is the clumping on this scale that gives rise to non-uniform laser ablation. The bacteria in these micrographs appear stringy, resembling a mucous-like substance where there are some gaps that expose the blank filter paper underneath. Because ablation is fundamentally a thermal process, requiring the uniform absorption and flow of heat underneath the laser spot, this sort of structure does not ablate consistently every time like a blank filter paper or a solid steel piece does. Our results spanning multiple years of ablating a test piece of stainless steel shows this consistency. Conversely, the laser ablation of the mucous-like bacteria is inconsistent; sometimes removing a large amount of mass, yielding a high bacterial signal, and other times removing a smaller amount of mass, yielding a low bacterial signal. Aside from the sample with the 1/1000 dilution, Tween was not observed to have beneficial

effects on the ablation of the bacteria. This may be due to the concentration of Tween used.

To determine whether Tween is effective at only a certain concentration given the initial concentration of a bacterial suspension, seven suspensions of *E. coli* were prepared, where each suspension was prepared to have the same concentration of bacteria ($\sim 5 \times 10^8$ CFU/mL). Optical densitometry measurements were taken to ensure this was the case. One of the seven suspensions was tested without Tween as a control, and the other six were each combined with different concentrations of Tween. The suspensions were each deposited on a separate filter paper using the well-plate, and 60 LIBS spectra were acquired across the filter in the regions where the suspension was deposited. Each of the 60 spectra was an average of 3 laser shots performed at different locations. The total LIBS intensity was calculated in the same way as stated above and plotted as a function of spectrum number which is shown in Figure 6.5. Figure 6.5a shows the plot for the first three concentrations of Tween used along with the suspension without Tween and Figure 6.5b shows the plot for the second three concentrations of Tween used along with the same suspension without Tween. Figure 6.5c shows a bar graph of the average total LIBS intensity of each suspension. The inconsistency of the LIBS intensity as a function of spectrum number (which corresponds to a specific location on the filter) in Figure 6.5a and b as well as the large errors on the bar graph in Figure 6.5c show that unfortunately none of the concentrations of Tween used helped with the issue of shot-to-shot variations in the bacterial LIBS intensity.

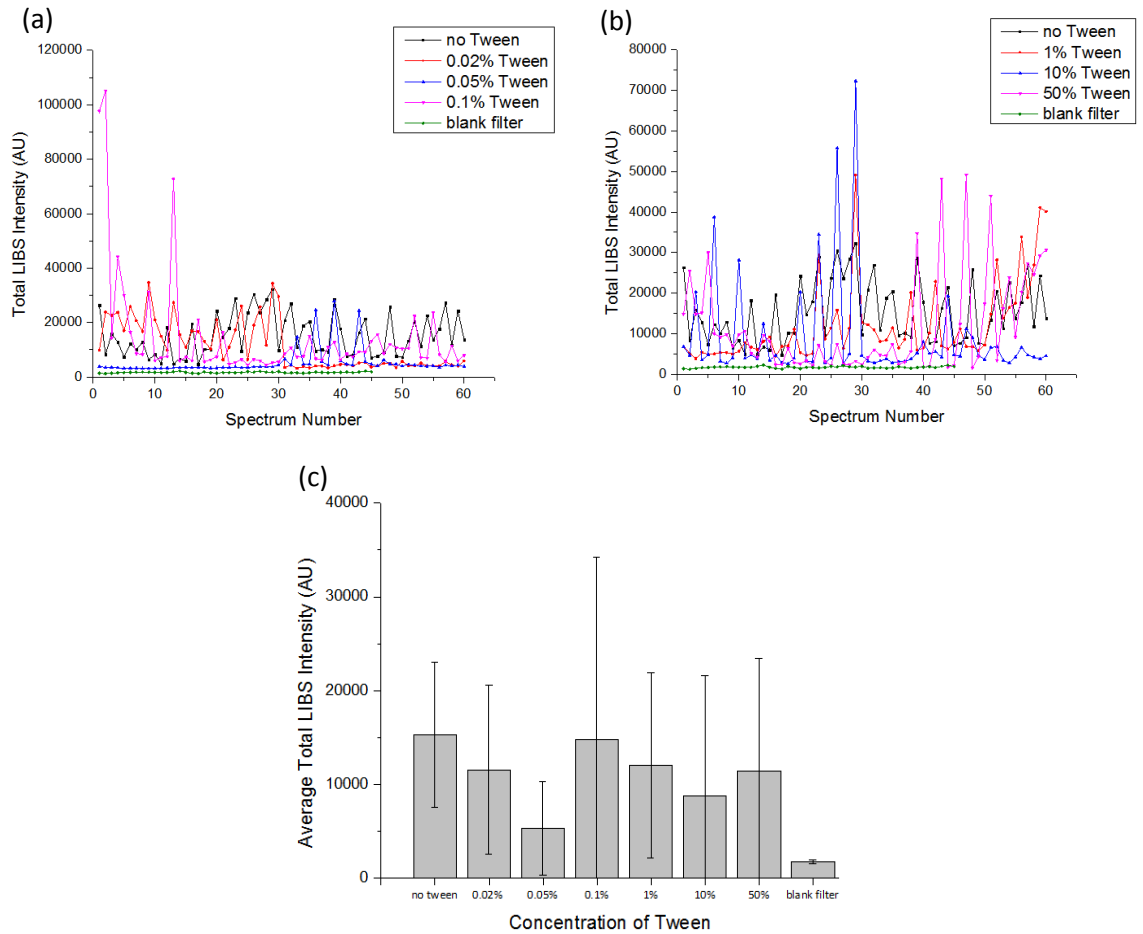


Figure 6.5: Plots depicting the effect of different concentrations of Tween in a suspension of *E. coli*. (a) First three concentrations of Tween used. (b) Second three concentrations of Tween used. (c) Bar graph summarizing the results in (a) and (b). Error bars represent one standard deviation in the measurements.

6.2.2 Effect of Growing *E. coli* in Liquid Medium to Reduce Inconsistencies in the LIBS Bacterial Signal

E. coli that had previously been grown on TSA plates (see Chapter 3) was grown in a liquid medium known as trypticase soy broth (TSB) to evaluate whether growth in a liquid medium would yield better behavior with regards to shot-to-shot repeatability. TSB is used as a general purpose culture medium and is made from pancreatic digest of casein, papaic digest of soybean, NaCl, dipotassium phosphate, and dextrose. The TSB was prepared by first dissolving 3 g of TSB powder in 100 mL of deionized water, then pouring the solution into centrifuge tubes, covering them with aluminum foil and autoclaving for

20 minutes at 121°C as per the instructions on the TSB container. After autoclaving, which sterilized the culture media and the centrifuge tubes, the broth was left to cool until the centrifuge tubes could be safely handled. Once they could be safely handled, 50 – 100 µL of an *E. coli* suspension that was previously grown on TSA plates was pipetted into the centrifuge tubes containing the broth. The centrifuge tubes were then lightly vortexed to incorporate the bacteria into the broth, and incubated for 24 hours at 37°C. After removal from the incubator, *E. coli* was separated from the broth by first centrifuging the mixture for 3 minutes at 5000 rpm with 2500 g's of force to pelletize the bacteria. The supernatant was removed, 1 mL of deionized water was added, vortexed with the bacteria, and centrifuged again. After centrifugation, the supernatant was removed and deionized water was added again. This process of centrifugation with water was done a total of four times. To ensure that four washing steps was sufficient for removing the broth from the bacteria, the supernatant from each washing step for two tubes of *E. coli* were deposited on filter papers using the well-plate and tested with LIBS to observe the sodium content since culture media contain significantly more sodium than bacteria. A total of 45 LIBS spectra were acquired across each filter in the regions where the suspension was deposited. Each of the 45 spectra was an average of 3 laser shots in different locations. The presence of a significant amount of sodium in the supernatant would serve to indicate that the broth had not been fully removed from the bacteria. Figure 6.6 shows a plot of the average LIBS intensity of the Na 588 nm emission line for each washing step from the two tubes of *E. coli* as well as for the broth and a blank filter. The average LIBS intensity of an emission line was calculated by averaging the area-under-the-curve intensity of that emission line for all 45 spectra. From the figure, the sodium content in the washing steps appear similar to each other and are more comparable to the sodium content of a blank filter than the broth, indicating that any number of washing steps will suffice. Some bacteria were removed with the supernatant, which could be the reason that the sodium content in the washing steps was greater than the sodium content in the blank filter. Evidence of the presence of bacteria in the wash water is shown in Figure 6.7, where an

averaged spectrum from all 45 spectra for each washing step as well as the broth and blank filter were overlapped and zoomed-in on two emission lines from magnesium.

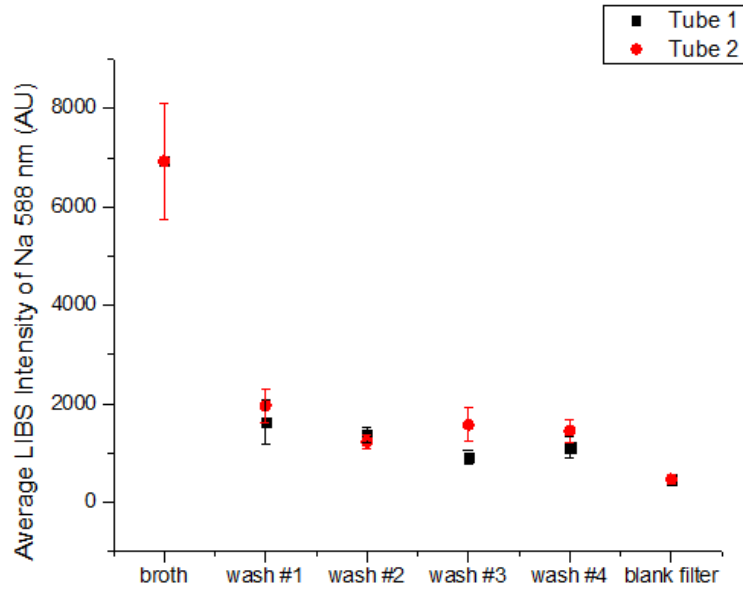


Figure 6.6: Average LIBS intensity of the Na 588 nm emission line in the supernatant from different washing steps for *E. coli* grown in two separate tubes with TSB.

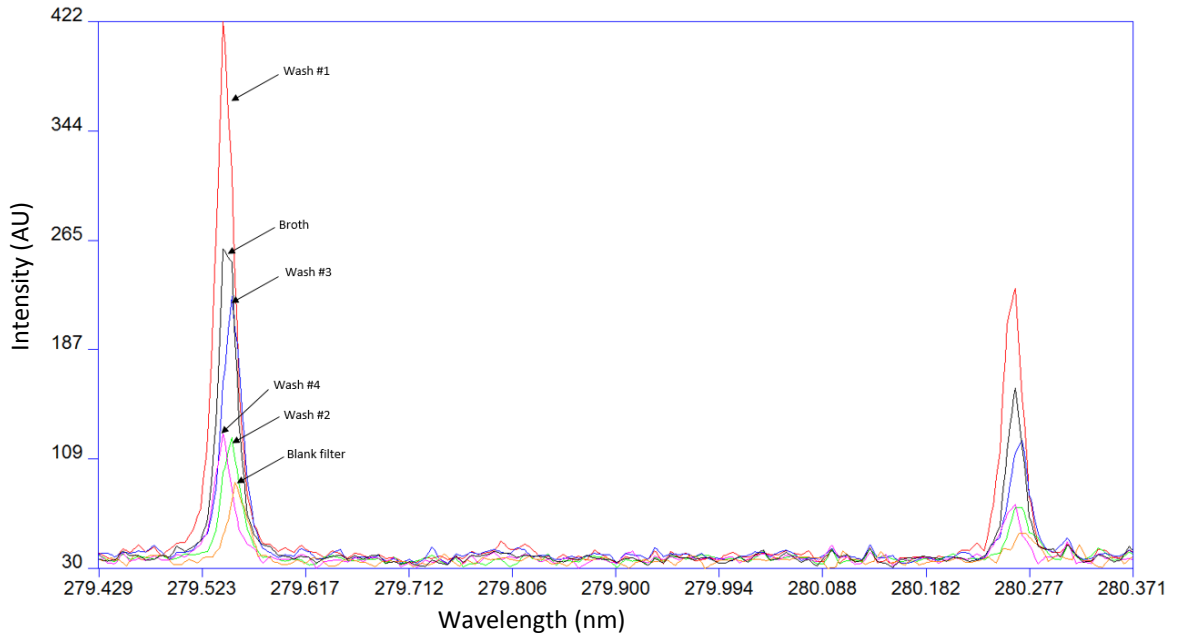


Figure 6.7: Overlapped spectra from each washing step, the broth, and a blank filter zoomed-in on two Mg emission lines to show the presence of bacteria in the supernatant. Wash #1 in red, wash #2 in green, wash #3 in blue, wash #4 in pink, broth in black, and blank filter in orange. Each spectrum is itself an average of the 45 spectra acquired across the filter.

Various concentrations of the *E. coli* that was grown in one of the two tubes were prepared and deposited on filter papers using the well-plate to investigate the effect on the signal repeatability of growing *E. coli* in a liquid medium. Again, 45 LIBS spectra were acquired where each spectrum was the average of 3 laser shots performed at different locations on the filter paper. A plot of the total LIBS intensity for each of the 45 spectra for the various concentrations of *E. coli* is shown in Figure 6.8. The total LIBS intensity was calculated as the sum of all the intensities of the emission lines stated in Table 3.1 of Chapter 3. Although the average total LIBS intensity does decrease as the concentration decreases, as expected, there does not appear to be a reduction in the variability of the LIBS signal except for the sample with 4.4×10^6 CFU (shown in pink), which is comparable to a blank filter anyway and therefore not useful.

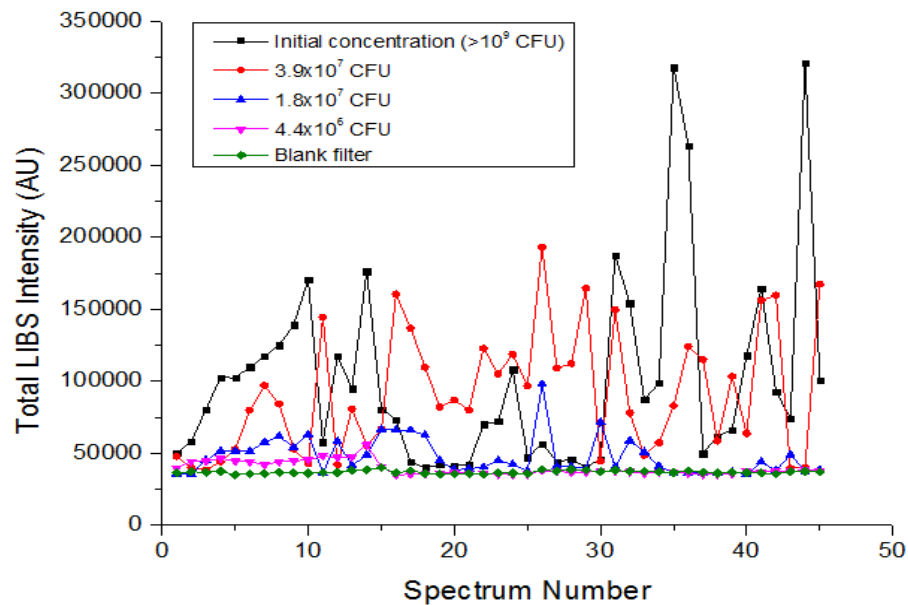


Figure 6.8: Total LIBS intensity as a function of spectrum number for *E. coli* grown in liquid culture and diluted to produce different concentrations.

6.3 Conclusion

The use of Tween 20 did not seem to improve the bacterial clumping problem, nor did it provide any advantageous effects in regards to LIBS signal repeatability. No amount of Tween added to an *E. coli* suspension appeared to reduce the shot-to-shot variations. It was observed, however, that the Tween may be effective at preventing bacteria from

sticking to the walls of the tube and pipette as suggested from Figure 6.3e. Tween may be more effective on a different species of bacteria – one that has a different Gram classification and/or shape than *E. coli*. SEM images of every sample used in a variety of experiments would enable us to better understand how the bacteria are arranging themselves on the filter paper under certain conditions, but this type of imaging would be impractical. The SEM micrographs in this work were taken on the instrument located at the Great Lakes Institute for Environmental Research (GLIER) which is a pay-for-use instrument. Its use for regular imaging of a large number of our samples would be impractical, prohibitively expensive, and time-consuming.

Growth of *E. coli* in a liquid medium also appeared to be ineffective at improving the repeatability of the LIBS signal. This may be due to the incubation procedure used. As stated in the introduction, when bacteria are grown in liquid media, they are typically placed in a shaking incubator which helps to distribute the nutrients throughout the culture media and to incorporate oxygen into the mixture. In this work, no shaking was done in the incubation process since we did not have a device to do so. There may be other advantages to using bacterial cells cultured in a liquid medium, but no evidence of improvements in the shot-to-shot repeatability of the depositions was observed.

References

- ¹ M. Johnson, *Detergents: Triton X-100, Tween-20, and More*, Synatom Research, Princeton, New Jersey, United States, <<https://www.labome.com/method/Detergents-Triton-X-100-Tween-20-and-More.html>> (2016)
- ² *Detergents for Cell Lysis and Protein Extraction*, ThermoFisher Scientific, <<https://www.thermofisher.com/ca/en/home/life-science/protein-biology/protein-biology-learning-center/protein-biology-resource-library/pierce-protein-methods/detergents-cell-lysis-protein-extraction.html>> (n.d.)
- ³ *Polysorbate 20*, National Center for Biotechnology Information, PubChem Compound Database, <https://pubchem.ncbi.nlm.nih.gov/compound/Tween_20#section=Top> (2018)
- ⁴ *Microbiology Introduction: Physical/Environmental Factors*, Sigma-Aldrich, <<https://www.sigmaaldrich.com/technical-documents/articles/microbiology/microbiology-introduction.html>> (2018)
- ⁵ G. Raho and B. Abouni, *The Battle Against Microbial Pathogens: Basic Science, Technological Advances and Educational Programs*, Microbiology Series N° 5, 2nd Vol., (Badajoz, Spain, 2015)

Chapter 7: LIBS Analysis of Bacteria Collected with Swabs

7.1 Introduction

7.1.1 Motivation

Swabs are often used to collect clinical specimens. Swab samples of the nose, throat, ears, eyes, etc. are taken to diagnose certain bacterial infections. For example, screening for methicillin-resistant *Staphylococcus aureus* (MRSA) is often done by swabbing the nose or throat,^{1,2} a throat swab is taken to diagnose streptococcal pharyngitis (strep throat) which is caused by the presence of *Streptococcus pyogenes* in the throat,³ and swabs are taken of infected wound sites on the body to diagnose which type of bacteria is causing the infection (often it is *Pseudomonas aeruginosa*).⁴ Diagnoses of many other bacterial infections are done with specimens that have been acquired with swabs. For LIBS to be a realistic diagnostic tool in a clinical setting, and since many clinical specimens are collected with swabs, it is important to ensure that samples collected in this way can be appropriately tested with LIBS. Our preliminary work with swabs, including LIBS analysis of bacteria that have been collected with swabs will be discussed in this chapter.

7.1.2 Flocked Swabs

In this work, sample collection was done with flocked swabs (Puritan PurFlock Ultra) which are often used in clinical settings for specimen collection, and more efficiently collect and release the sample.⁵ An image of a flocked swab used in this work is shown in Figure 7.1. Flocked swabs keep the sample close to the surface and release it easily when placed on a solid growth medium or in a liquid medium. Flocked swabs contain short nylon fiber strands and a sample is drawn into the swab by capillary action.⁶ Sometimes swabs are vortexed in a liquid to maximize the release of the sample.



Figure 7.1: (a) Flocked swab used in this work. (b) Flocked swab zoomed-in on the tip.

7.2 Determination of Vortex Time Required for Maximum Release of a Sample from a Swab

Of course, LIBS testing directly on the swab would be most convenient, but the swab is not a good substrate for laser ablation. The surface of the swab is too irregular (see Figure 7.1b) and the bacterial cells are not concentrated enough in one region. Another issue is that in a clinical specimen, the swab, although sterile prior to use, may not only contain bacteria, but other unwanted biological material that could affect the LIBS-based identification of bacteria and must be separated out prior to testing with LIBS. A sample preparation method involving this sort of separation was described in Chapter 4.

Nevertheless, preliminary experiments were conducted to attempt to perform LIBS directly upon the nylon strands of a flocked swab. One previous demonstration of LIBS performed on the surface of a cotton-tipped swab has been reported, but the data shown in this demonstration are far too scarce to be convincing.⁷ For completeness, cotton-tipped swabs (Puritan Medical Products Company LLC, Guilford, ME) were also initially investigated by us, but the superior performance of the flocked swabs led us to pursue their use in subsequent studies. Performing LIBS directly upon a swab was difficult, as the laser spot used for alignment could not be observed on the swab, and the swab itself does not have an even surface, making adjustment of the swab in the focus of the laser beam impossible. This convinced us that such a sampling methodology was unfeasible.

Instead of LIBS testing directly on the swab, the swab was vortexed in deionized water to shake off the cells, with the aim of using the metal cone (described in Chapter 5) to deposit the vortexed suspension on a filter paper. Since the swab was to be vortexed in water, determination of an optimal vortex time was required, where the optimal time was chosen as the one which provided maximum release of the sample from the swab.

To determine the required vortex time, 50 μL of an *E. coli* suspension was pipetted directly onto a flocked swab and vortexed in a centrifuge tube with 1 mL of deionized water for 1, 5, 15, and 30 seconds. The swab was discarded and the resulting water/cell suspension was either tested with LIBS or transferred to an optical quality cuvette for optical densitometry (absorbance) concentration measurements. An absorbance measurement was obtained for each of the vortex times using a spectrophotometer, where the measured absorbance value can be converted to a concentration since an absorbance value of 0.1 A.U. is approximately 10^8 CFU/mL. Higher measured absorbance values correspond to higher concentrations of bacteria. The amount of bacteria is represented as an absorbance value throughout this chapter, since for most of our studies it is the relative concentrations that we are concerned with, not absolute concentrations. Figure 7.2 shows a plot of the measured absorbance values for the different vortex times. Two trials of this experiment were performed. Figure 7.2 also shows the corresponding average total LIBS intensity for the different vortex times of Trial 1 (which were deposited on filter papers using the metal cone and 20 single-shot LIBS spectra were acquired). Higher absorbance values indicate that a greater amount of bacteria are released from the swab.

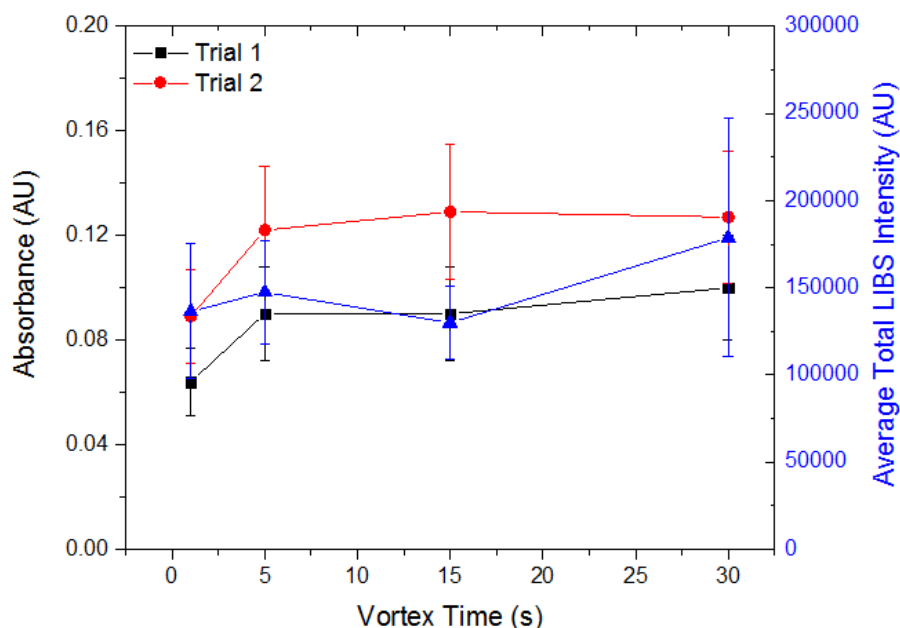


Figure 7.2: Absorbance value and average total LIBS intensity plotted as a function of vortex time for two trials.

The error bars in the absorbance measurements in Figure 7.2 were calculated by utilizing the average fractional standard deviation obtained from two different trials of pipetting the same amount of the same *E. coli* suspension onto swabs five times and then vortexing them for 15 seconds. We did not perform this reproducibility measurement for all vortex times, but utilized the fractional standard deviation we obtained for the 15 second experiment for all the times, as we believe this reproducibility measurement should be similar for all times. The average total LIBS intensity was calculated as the average of the sums of the intensities of all bacterial emission lines stated in Table 3.1 of Chapter 3 for the 20 LIBS spectra acquired. As seen from the figure, all but the 1 second vortex time released a similar amount of bacteria into the water as determined by spectrophotometric absorbance, and all vortex times exhibited the same average total LIBS intensity within error. Thus, a vortex time of 15 seconds was deemed to be sufficient for maximum release of the cells.

7.3 Determination of Amount of Cells Released from Swab

It was important to quantify the fraction of bacteria that were released from the swab as a result of being vortexed in water. A large amount remaining on the swab post-

vortexing is not ideal since one of the main goals of this work has been to lower the limit of identification of the LIBS test. To determine what percentage of bacteria was released by vortexing the swab in water, 50 μL of an *E. coli* suspension with known concentration was pipetted onto a flocced swab and vortexed in 1 mL of deionized water for 15 seconds, and 50 μL of the same suspension was pipetted directly into a tube with 1 mL of deionized water. This was done a total of five times on the swab and five times directly into water. This experiment was then repeated for a different suspension of *E. coli*. Absorbance measurements were taken for the twenty total samples and the average and standard deviation of the absorbance values for each set of five samples were calculated and are shown in Figure 7.3. Absorbance values from pipetting directly into water represent the

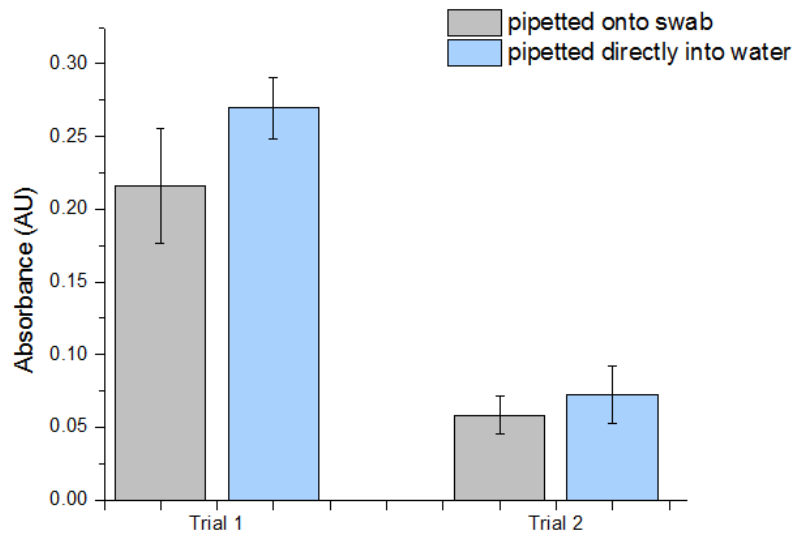


Figure 7.3: Average absorbance value plotted for samples prepared by pipetting a bacterial suspension onto a swab and vortexing it in water to release the cells and by pipetting directly into water. Error bars represent one standard deviation in the measurements.

amount of bacteria that should be present if pipetted onto a swab and all cells were shaken off the swab and into the water. From the figure, it is observed that absorbance measurements on cell suspensions pipetted directly into water and suspensions pipetted onto a swab which was then vortexed in water were the same within statistical uncertainty, although the absolute values were always lower for the vortexed swab suspensions, as expected. Determination of the percentage shaken off the swab was done by dividing the average absorbance value obtained from the water vortexed with the

swab by the average absorbance value obtained from the water with bacteria pipetted directly into it. It was found that $80.1 \pm 15.9\%$ and $80.2 \pm 29\%$ of the bacteria picked up by the swab were released after vortexing in water for Trials 1 and 2 respectively. About 20% of the bacteria deposited on the swab initially were either not released from the swab or were lost in some other process, and were thus not available for LIBS testing. Ideally, 100% of the bacteria should be released from the swab to proceed to LIBS-based identification. As mentioned in Chapter 6, treatment with Tween 20 (or some other substance) may prevent bacterial cells from sticking to surfaces, so it is thought that perhaps it could be used in the future to improve the bacterial cell shake-off efficiency. Such a treatment is typically not performed on clinically obtained swabs, however.

7.4 Absorbance Values and LIBS Intensity

Swabs were used to collect *E. coli* and *S. epidermidis* for the purpose of observing the relation between the absorbance value obtained after the swab was vortexed in water and the resulting LIBS intensity. 50 μL of an *E. coli* suspension was pipetted onto a flocked swab, then vortexed for 15 seconds in 1 mL of deionized water. The swab was removed and a measurement of its absorbance value was made. This was repeated four more times for a total of 5 samples of *E. coli* pipetted onto swabs. The same process was repeated for *S. epidermidis*, which yielded a total of 6 samples. The entire 1 mL from each sample was deposited on a filter paper using the metal cone and 20 single-shot LIBS spectra were acquired. Figure 7.4 shows plots of the absorbance value and the average total LIBS intensity for each sample of *E. coli* and *S. epidermidis*. The error bars on the absorbance values represent the standard deviation in the measurements. The average total LIBS intensity was calculated in the same way as stated in section 7.2, and the error bars represent one standard deviation in the measurements. The absorbance values in each plot are similar within error and the average total LIBS intensities from all five samples of *E. coli* and all six samples of *S. epidermidis* are the same within error. This result was to be expected since each sample was prepared in the same way from the same suspension of bacteria.

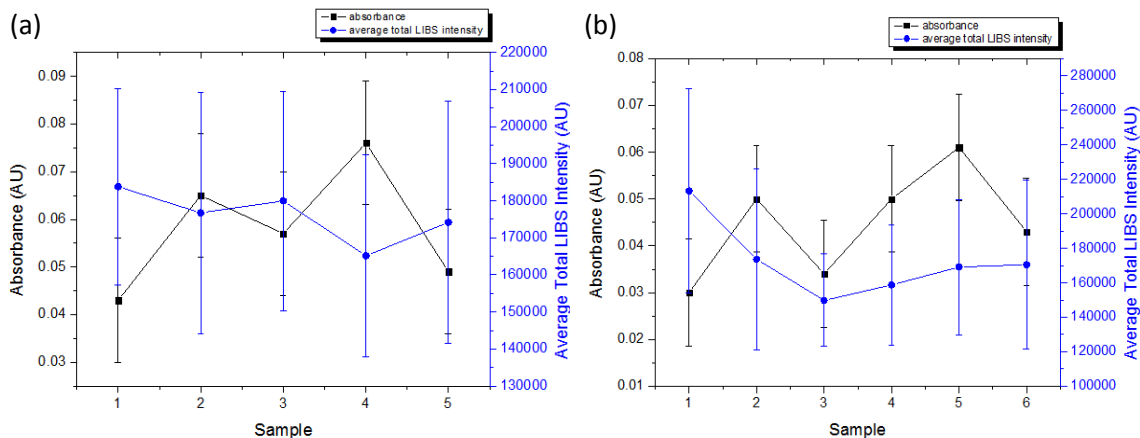


Figure 7.4: Absorbance value and average total LIBS intensity plotted for each sample for (a) *E. coli* and (b) *S. epidermidis*.

7.5 LIBS Analysis of Samples Collected from Swabbing Bacteria off a Metal Plate

In the previous sections, all samples were obtained by pipetting known quantities of bacteria-containing suspensions directly onto a flocked swab tip. In this section, samples were prepared by pipetting a bacterial suspension of known concentration onto a sterile metal plate and swabbing the surface of the metal plate to pick up the bacteria. Samples collected by swabbing a surface more closely resemble specimen collection with swabs in a clinical setting. An overview of the sample preparation process used in this work for swabbing off a metal plate is described below.

The metal plate used was a 2.6 x 2.1 cm stainless-steel piece and was cleaned after each use by first submerging in a 10% bleach solution, drying with a paper towel, submerging in deionized water, and drying again with a paper towel. A bacterial suspension was deposited on the metal plate by pipetting 100 μ L onto it, and a hot-plate was used to heat the steel piece to draw off the water in the suspension. The hot-plate was set at 200°C and the bacterial suspension on the steel piece was heated for 2 minutes and 20 seconds, by which time the water had evaporated and a dry film of bacteria was observed on the metal plate. This is depicted in Figure 7.5. The metal plate was then swabbed using a flocked swab that was pre-wet with 10 μ L of deionized water that was pipetted onto it. The plate was swabbed in such a way to collect as much bacteria as possible. The swab was then placed in 1 mL of deionized water and vortexed for 15

seconds, as per the procedure developed earlier in this chapter. After this, the swab was removed, a measurement of the absorbance value of the suspension was taken, the entire 1 mL was deposited on a filter paper using the metal cone, and 20 single-shot LIBS spectra were acquired.

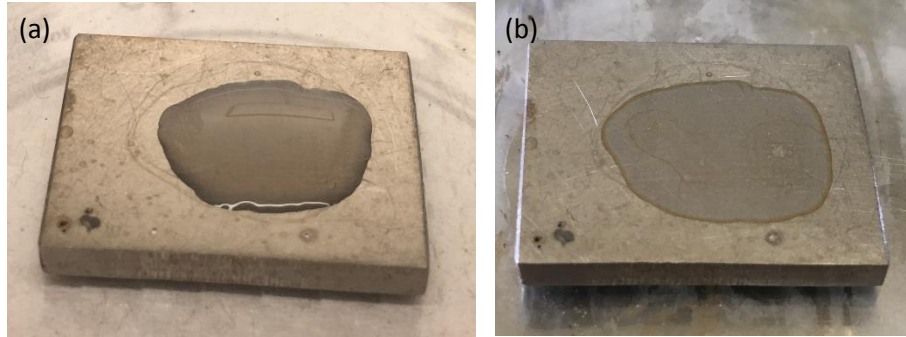


Figure 7.5: (a) 100 μL of *E. coli* pipetted onto surface of metal plate. (b) Metal plate after heated on hot-plate for 2 minutes 20 seconds at 200 $^{\circ}\text{C}$. Water has evaporated and film of bacteria is observed.

A suspension of *E. coli* was diluted to make five different concentrations, where the dilutions used were represented as a fraction of the initial concentration and were as follows: 1/5, 1/10, 1/50, 1/100, and 1/500. Each of the different dilutions was pipetted onto the metal plate four separate times, swabbed, and tested with LIBS as per the method described above. The absorbance values of the different dilutions before deposition on the metal plate as well as after collection with the swab and vortex release into 1 mL of water are shown in Table 7.1. The initial absorbance is the absorbance value

Table 7.1: Absorbance values for the different dilutions of *E. coli*

Dilution	Initial absorbance (AU)	Final absorbance (AU)			
		1	2	3	4
1/5	2.486	0.224	0.131	0.267	0.254
1/10	2.056	0.137	0.159	0.178	0.177
1/50	0.459	0.015	-0.007	-0.008	-0.004
1/100	0.269	-0.015	-0.015	-0.012	-0.006
1/500	0.023	-0.027	0.006	-0.022	-0.015

of the suspension before deposition on the metal plate and final absorbance is the

absorbance value of the suspension resulting from vortexing the swab in 1 mL of water. The negative absorbance values of some samples indicate that the concentrations of the samples are not within the limit of detection of the spectrophotometer. The absorbance values for the 1/5 and 1/10 dilutions can be used to determine the percentage of bacteria that are collected off the plate and released in water by dividing the average concentration of bacteria released in water from the four trials by the concentration of bacteria deposited on the metal plate. It was found that for the 1/5 dilution, approximately 88% of the bacteria that were deposited on the metal plate were picked up by the swab and released in water, and for the 1/10 dilution, approximately 79% were picked up and released in water. These results indicate that the amount of bacteria collected off the plate and released in water may have had some dependence on the initial concentration of bacteria deposited on the plate, but the uncertainties of the absorbance measurements make this difficult to quantify.

Despite the negative absorbance values of some samples, they were all tested with LIBS. The intensities of the measured LIBS spectra were compared to spectra from a blank filter as well as spectra from concentrated *E. coli* suspensions deposited on filter papers using the well-plate method of deposition described in Chapter 3 and the *E. coli* spectra from section 7.4 that were obtained by vortexing swabs and deposited using the metal cone. Because several of these experiments were performed at different spectrometer amplifications, the sum of the absolute intensities of the observed LIBS emission lines, referred to as the total LIBS intensity, could not be used (as was done, for example, in Figure 7.4). Instead, the normalized intensities of the bacterial emission lines were used for the comparison, where the normalized intensity of a particular emission line is the area-under-the-curve intensity of that particular emission line divided by the total LIBS intensity of its corresponding spectrum.

Because the sum of the normalized intensities for all lines must, by definition, sum to 1, this value cannot be used to compare concentrations. However, we make use of the fact that in the blank filter spectra, the carbon line dominates the spectrum, but this intensity is due to the carbon in the nitrocellulose filter. It is possible to utilize this by

summing the normalized intensities of all lines except for the carbon line. This sum will not be 1, and will in fact change as the coverage of the bacteria on the filter changes and the relative weight of the carbon emission line decreases. Additionally, since the normalized intensity of the carbon line will be high in the blank filter spectra and much lower in the bacterial spectra, the sum of the non-carbon lines was then divided by the normalized intensity of the carbon line. This ratio is plotted in Figure 7.6 for various bacterial suspension concentrations. Simply put, the blank filter spectra possess a small numerator and a large denominator, while the high-concentration bacterial spectra possess a larger numerator and a smaller denominator, making this ratio sensitive to the concentration of bacteria, as can be seen in the figure. Other schemes for analyzing the normalized data were investigated, including using only the phosphorus lines, using the

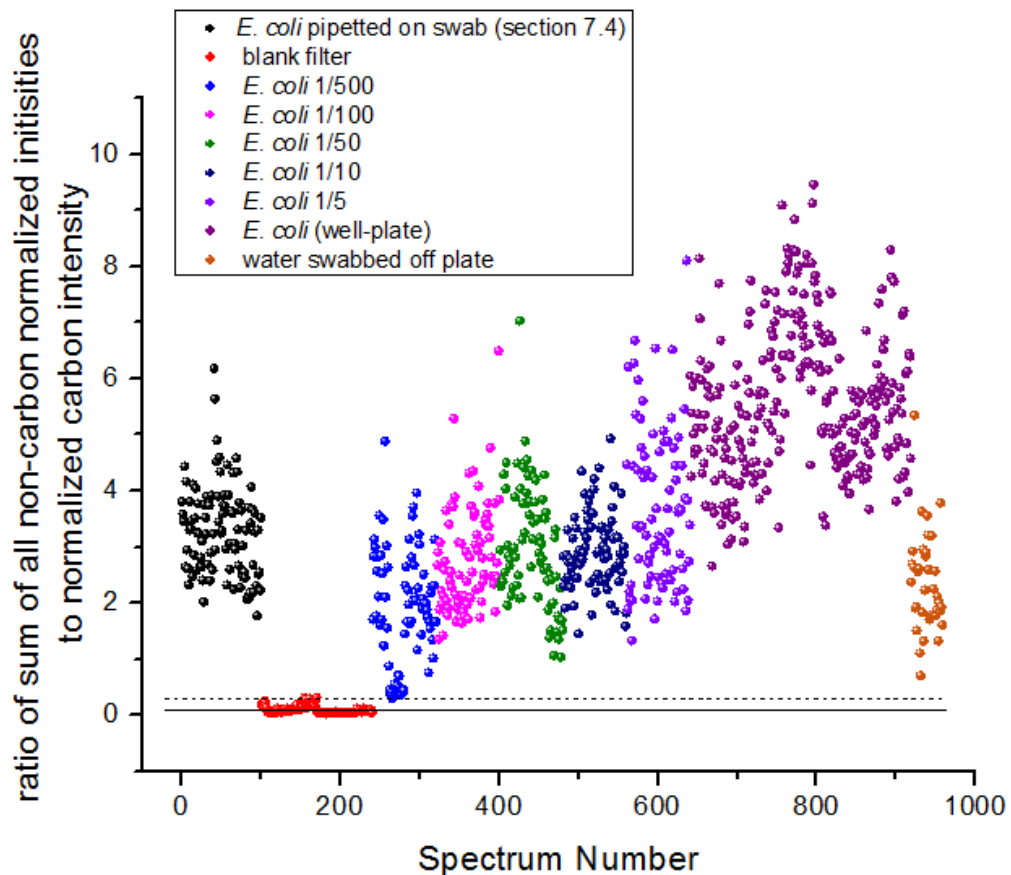


Figure 7.6: The sum of the normalized intensities of all non-carbon lines divided by the normalized intensity of the carbon line plotted as a function of spectrum number for various concentrations of *E. coli*. The black horizontal line represents the average value of this ratio for a blank filter and the horizontal dashed line represents this average plus three times the standard deviation in the measurements of this ratio for a blank filter.

phosphorus lines divided by the carbon line, etc. The results shown in Figure 7.6 provided the greatest discrimination between a blank filter and spectra containing bacteria.

As a control, water with no bacteria was pipetted onto the metal plate and swabbed off in the same manner used for the different dilutions of *E. coli*. Ideally, LIBS testing of this control sample should yield spectra comparable to a blank filter, but unfortunately, spectra consistent with a blank filter were not observed, as can be seen by the orange data points (located at the far right) in Figure 7.6. It was initially theorized that such contamination in this control sample was either due to the swab itself or due to ineffective cleaning of the metal plate. To test whether this contamination was due to the swab, a swab was vortexed in water and deposited on a filter paper using the metal cone. LIBS testing revealed similar contamination. It was then theorized that the contamination was coming from the water, the metal cone, the swab, or a combination of these. This was investigated further by depositing water on filter papers using just the centrifuge tube insert and using the metal cone. Water deposited using just the centrifuge tube insert was tested with LIBS and yielded spectra comparable to a blank filter, indicating that contamination was not due to the water. Water deposited using the metal cone was tested with LIBS and yielded spectra containing a fraction of such contamination, indicating that the metal cone may be partially responsible for the contamination. A summary of these results is shown in Figure 7.7, where each spectrum is an average of all the spectra acquired from 20 single-shot LIBS spectra. The metal plate may also be largely responsible for the contamination, however, experiments to investigate the role of the metal plate in the contamination have yet to be performed. Future experiments investigating an adequate cleaning technique for the metal plate and cone remain to be performed.

Although the control sample did not yield spectra comparable to a blank filter, Figure 7.6 shows the spectra still had low ratios compared to the ratios of the other samples of *E. coli* with the exception of the least concentrated bacteria (the 1/500 dilution). After the investigation and implementation of a sufficient cleaning method for the metal plate and cone, it is believed that the contamination will be significantly

reduced and the spectra resulting from the laser ablation of the control sample will be consistent with a blank filter. Experiments to determine identification accuracy and to calculate a limit of detection for bacteria collected with a swab can then be performed to determine the feasibility of the LIBS technique to detect bacteria that have been collected in this way.

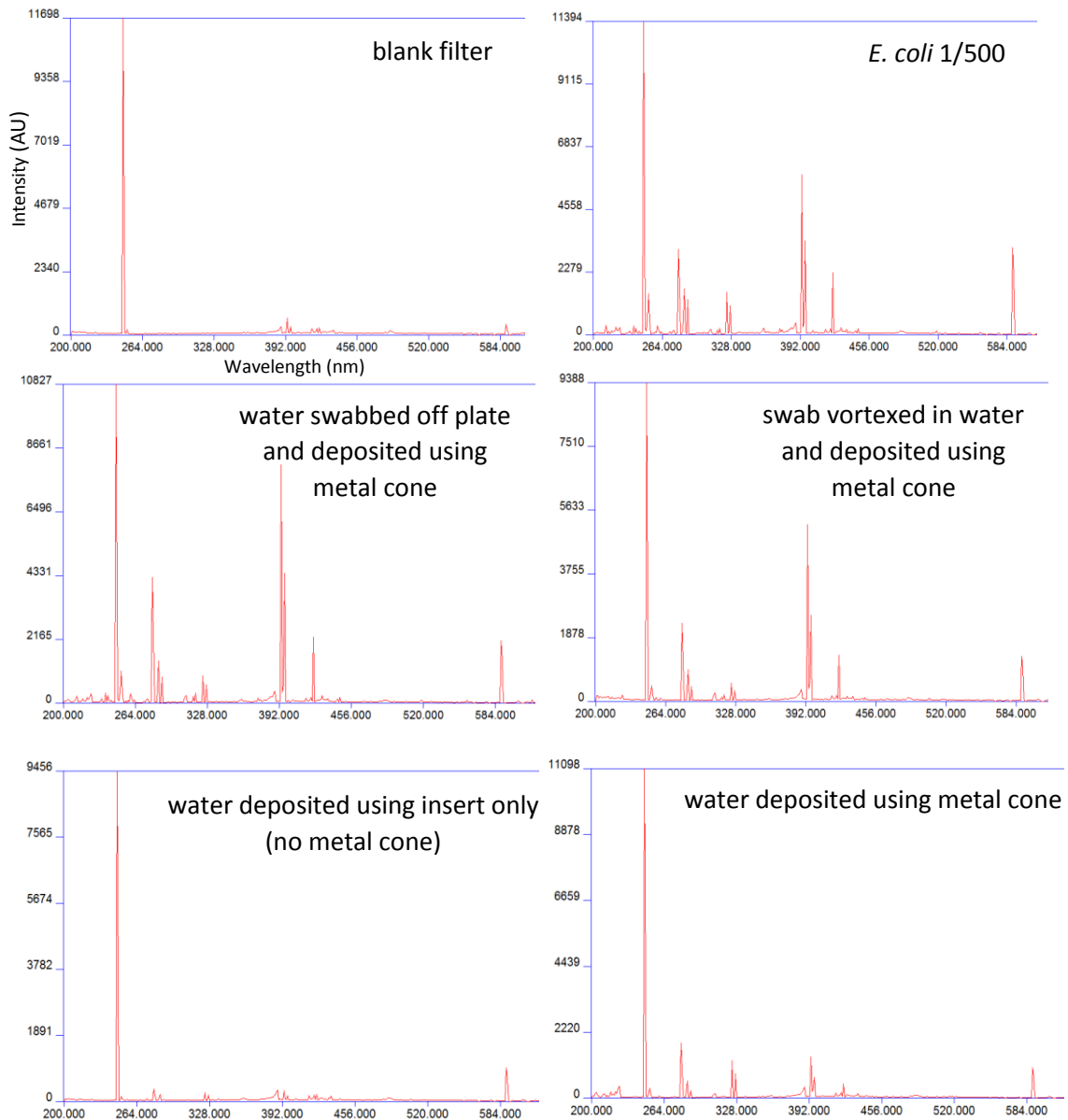


Figure 7.7: Resulting averaged spectra from 20 single-shot LIBS measurements on different samples. All samples in this figure were tested at the same spectrometer amplification.

References

- ¹ G. L. French, *Clin. Microbiol. & Infec*, **15** (7), 10 (2009)
- ² B. Brekle and J. Hartley, *Specimen collection – microbiology and virology*, Great Ormond Street Hospital for Children, <<https://www.gosh.nhs.uk/health-professionals/clinical-guidelines/specimen-collection-microbiology-and-virology>> (2017)
- ³ *Pharyngitis (Strep Throat)*, Centers for Disease Control and Prevention, <<https://www.cdc.gov/groupastrep/diseases-hcp/strep-throat.html>> (2016)
- ⁴ K. Pondei *et al.*, *Trop. Med. Health*, **41** (2), 49 (2013)
- ⁵ E. Baron *et al.*, *Clin. Infect. Dis.*, **57** (4), e22 (2013)
- ⁶ D. M. Goldfarb *et al.*, *J. Clin. Microbiol.*, **47** (9), 3029 (2009)
- ⁷ R. A. Multari *et al.*, *J. Agric. Food Chem.*, **61** (36), 8687 (2013)

Chapter 8: Conclusions and Future Work

8.1 Conclusions

The aim of this work was to address some of the issues related to the LIBS testing of actual clinical specimens that could be collected from a patient and to evaluate the effectiveness of the LIBS technique on samples that were clinically relevant. The conditions which were considered in realistic samples included the presence of other contents in addition to bacteria in a clinical specimen (i.e. the presence of red and white blood cells, plasma, and platelets in a blood sample), the low numbers of bacterial cells that would be present in a clinical specimen, and the nature of the sample collection procedure (i.e. many samples are collected using swabs).

A technique for separating unwanted material from a bacterial suspension was developed to address the issue of the presence of other contents in addition to bacteria in a clinical specimen. This technique involved the use of a centrifuge tube insert device that was specially constructed by a previous student in our research group. Separation was achieved based only on the size difference between bacteria ($\sim 1 \mu\text{m}$) and the “unwanted material” (unwanted material in a clinical specimen will be $\sim 10 - 100 \mu\text{m}$). Preliminary experiments were performed using tungsten powder ($\sim 12 \mu\text{m}$) to simulate the unwanted material and served to demonstrate the initial success of this separation technique. All of the tungsten powder was removed from the suspension but it was determined that $\sim 10\%$ of the bacteria were also removed and lost in this separation process. Efforts must be taken to lower the amount of bacteria that are lost when using this technique. It was thought that this loss of bacteria was due to the clustering of bacterial cells. Since the separation is based on size, a large cluster of bacteria would be separated out from the suspension. Treatment of the bacteria with something such as a detergent prior to performing this separation procedure might split up the cells, allowing them all to be separated from the unwanted material. This separation technique was also only tested using tungsten powder to simulate the unwanted material. The next step would be to test this technique using something that more closely resembles biological

material such as yeast or even beginning testing on actual clinical specimens such as cerebrospinal fluid (CSF) or blood.

The previous bacterial mounting procedures (well-plate and centrifuge tube insert device) used by our group utilized materials and equipment that are inexpensive and easy for clinicians to use; however, the minimum number of bacteria required for detection with LIBS using these procedures was unrealistically high to be clinically relevant. For example, the bacterial limit of detection (LOD) for the well-plate method of deposition is ~50000 CFU per laser ablation event and the LOD for the insert device is ~90000 CFU per laser ablation event, whereas typical clinical specimens may contain bacteria on the order of hundreds of CFU or less. In an effort to reduce the LOD with LIBS, a metal cone was designed and constructed to be used in conjunction with the insert device for bacterial deposition on a filter paper. The LOD for this new mounting procedure was determined to be ~5000 CFU per laser ablation event which reduced our LOD by an order of magnitude compared to the previous two procedures. Although the LOD was significantly reduced, it is still too high to be clinically relevant. Further efforts to reduce the LOD must be taken if the LIBS technique is ever to be used as a medical diagnostic. Suggestions for improvement of the LOD are discussed later in this chapter.

To improve the repeatability of the LIBS signal and provide more uniform laser ablation, treatment of *E. coli* cells with a detergent known as Tween 20 was investigated as well as growing the cells in a liquid culture medium. Unfortunately, neither of these efforts appeared to improve the repeatability of the LIBS signal. It is thought that the Tween may be more effective on a different type of bacteria. Bacteria have different shapes and structures which can affect the way that they aggregate. A detergent to prevent such aggregation may only be effective on bacteria that exhibit a certain shape or structure, and as demonstrated in this work, *E. coli* was not one of them. In regards to growth in liquid culture, typically the culture medium and bacterial suspension are shaken regularly throughout the incubation period. This was not done in this work as we did not have a device to do so. Treatment of different types of bacteria with Tween as well as growing bacteria in a liquid culture medium with a device to regularly shake the

suspension remains to be explored. Other methods (besides Tween 20 and liquid culture) to improve the repeatability of the LIBS signal must also be explored and it must be understood why there is such shot-to-shot variation in the LIBS signal of bacterial targets.

Bacteria collected using swabs were analyzed with LIBS. It was determined that LIBS could not be performed directly on the swab, but rather, the swab required vortexing in water to shake off the bacterial cells. To test with LIBS, the water with the shaken-off cells was then deposited on a filter paper. Preliminary experiments included determining the optimal vortex time for maximum shake-off of the cells (15 seconds) and calculation of the number of cells that are released from the swab by vortexing (~80% released). The ability of LIBS to detect bacteria that were collected by swabbing them off a surface to more closely simulate the way many clinical specimens are collected was investigated. Unfortunately, contamination was observed in the control sample. Tests were performed to determine the sources of the contamination, but further testing is required since not all of the possible sources were tested. Once all sources of contamination are identified, proper techniques for prevention of such contamination must be determined. When this is achieved, a limit for the minimum number of bacterial cells required on a surface for collection with a swab and subsequent detection with LIBS must be determined. The results will indicate whether the LIBS technique is a successful diagnostic tool for clinical specimens that are collected using swabs.

8.2 Future Work

For LIBS to be a realistic point-of-care medical diagnostic tool, it should be performed using inexpensive disposable substrates for mounting the samples, simple sample preparation procedures, and it must have a clinically relevant bacterial LOD while adhering to the previous two points. Our group has demonstrated that LIBS-based identification is possible using inexpensive substrates (nitrocellulose filter papers) and sample preparation methods that are fast and require no expertise; however, the bacterial LOD associated with these is not realistic to clinical specimens. Efforts must be taken to reduce our LOD. The emission from carbon (247.856 nm) is an inherent limitation

in our nitrocellulose filter-based mounting procedure. In theory, at low bacterial concentrations, we could increase the amplification on the spectrometer which would increase the bacterial LIBS signal, but the presence of carbon in the filter paper itself prevents this. Increasing the amplification would also result in an increase in the intensity of the carbon line so much so that it would damage the ICCD in the spectrometer. Further reduction of the LOD must involve finding a way around the carbon line. One way to do this is by mounting the bacteria on a different substrate – one without such strong emission from carbon – but certain obstacles must be overcome for this. For example, the substrate should contribute very little (ideally, it should contribute nothing) to the LIBS signal. In addition, it must be easy to use by a clinician and inexpensive if the LIBS technology is to be used for rapid diagnoses of pathogens. We have yet to find such a substrate. Another suggestion for dealing with the carbon line is to eliminate its detection. This can be done either by using an optical filter known as a notch filter to block emission from carbon before light from the plasma is directed into the spectrometer, or by using a spectrometer system in which no carbon emission can be detected. Notch filters are designed to attenuate light within a narrow wavelength range, but would need to be custom-made for the wavelength of the carbon line and is an expensive solution. A spectrometer system in which no carbon emission is detected can be achieved using multiple spectrometers that have a smaller wavelength coverage. For example, one spectrometer that covers wavelengths below 247.856 nm and one that covers wavelengths above 247.856 nm can be used. Emissions from carbon will be completely undetected, however, this is an extremely costly solution and it eliminates the ability to detect carbon in any other non-bacterial samples we wish to analyze with LIBS.

All of the previous work involving testing bacteria using LIBS has involved the use of chemometric algorithms to identify the similarities and differences in the LIBS spectra of various bacteria. Bacteria can be classified into certain groups using chemometric techniques including, but not limited to, principal component analysis (PCA), partial least squares discriminant analysis (PLS-DA), and discriminant function analysis (DFA). None of the work presented in this thesis made use of chemometric techniques to discriminate

between bacteria since this work was focused more on the preliminary experiments testing the feasibility of the use of the LIBS technique in a clinical setting. These preliminary experiments offered promising results as well as results that we believe could be improved upon with some further work mentioned in section 8.1. In regards to chemometric techniques, work remains to be done in observing the ability to correctly classify bacteria that have been prepared using the methods developed in this work. For example, it needs to be determined whether bacteria can be correctly classified when they are mounted on filter papers using the metal cone, and when they are collected with a swab. If the results are promising, these methods must be tested using actual clinical specimens from healthy individuals in which the specimen is doped with a known amount of a certain type of bacteria. If bacteria in these specimens are correctly classified, this would bring the LIBS technique a significant step closer to being a realistic diagnostic tool. The sensitivity and specificity of this technique for classifying and identifying bacteria must be determined and a limit of detection for identifying bacteria (referred to as a “limit of identification”) using this technique must then be determined. If these results are promising, LIBS spectra from a variety of medically relevant pathogens can be collected to create a library with the goal being that when a sample is taken from a patient, it can be tested with LIBS and the pathogen can be identified by comparing it to the library using a chemometric technique provided that pathogen is in the library.

The sensitivity and specificity of identifying bacteria from different locations in a patient must also be determined. For example, the ability to correctly identify bacteria in urine, blood, cerebrospinal fluid, a throat swab, pus from an infected site, etc. may not all be the same. This could indicate that the LIBS technique may only be useful for specimens collected from certain regions of the body. In addition, further work remains to be done in determining the sensitivity and specificity of the LIBS-based identification technique regarding the metabolic state (live, inactivated, or dead) of bacteria when it is tested using the preparation methods developed in this work. As stated in Chapter 1, there are contradictory results between our group and two other groups. The effect of the metabolic state on bacterial identification using LIBS must be accurately determined, then

it will be known whether a sample with a different metabolic state can still be correctly identified. It will also be known whether sterilization of a sample prior to LIBS testing is possible, and if possible, testing of samples would be a much safer task for clinicians.

Continued efforts must be taken to develop better techniques for isolating bacteria from other unwanted material that may be present in a clinical specimen. Even if the bacterial LOD with LIBS is reduced to as little as a single cell, detection and identification of the bacterial cell will not be possible if it is mixed with many other types of cells. The technique developed and described in Chapter 4, although the preliminary results were promising, is only capable of isolating bacteria based on size. It does not address the issue of isolating bacteria that is in a mixture with multiple different species of bacteria or other material that is similar in size to bacteria. Once a particular species or strain of bacteria is isolated, correct identification with LIBS should be possible.

LIBS may also be capable of detecting antibiotic resistance in bacteria since the LIBS signal is linearly dependent on the number of cells (provided the number of cells are in the linear dynamic range). If a bacterium is resistant to antibiotics, it will continue to reproduce in the presence of the antibiotics. If a bacterium is susceptible to antibiotics, its reproduction in the presence of such antibiotics will be halted. The time it takes for bacteria to double in number is known as the doubling time or generation time. The generation time for most known bacteria ranges from 15 minutes to 1 hour. To test for antibiotic resistance using LIBS, the LIBS signal of bacterial cells before and after treatment with antibiotics can be acquired. If the LIBS signal is lower than expected when factoring in the generation time of the bacteria, it indicates that the bacterium is susceptible to that kind of antibiotic. Conversely, if the LIBS signal is proportional to the number of cells expected after factoring in the generation time, it indicates that the bacterium is resistant to that antibiotic.

The LIBS apparatus must be an appropriate size and easy to use if it is to be implemented in a clinical setting. Ideally, the LIBS device would be located in the clinic itself so that a clinician can identify a pathogen within minutes after a sample is taken

from a patient. The apparatus currently used by our group is not practical for this purpose; it occupies an optical table approximately 1 m by 3 m, contains a system of precisely placed mirrors and lenses (making it difficult for any clinician to use), and requires laser safety goggles to be worn while in use. However, portable and bench-top LIBS devices have been made. A portable or bench-top LIBS device that is easy to use in terms of data acquisition, only requires the simple placement/loading of a sample in the device, and does not require wearing laser safety goggles is the ultimate goal for a clinical LIBS device.

To sum up, the sample preparation methods developed in this work utilize materials and equipment that are either already common or would be easy to implement in a clinical setting, and the research presented in this thesis suggests that LIBS is a promising technique for rapid pathogen identification in a clinical setting. To date, research in this field has mostly demonstrated the feasibility of the LIBS technique to rapidly identify pathogens. Further work remains in the development of this technique as a useful diagnostic tool. It has come a long way from discrimination of high concentrations of pure bacteria in the early 2000's to addressing the issues related to clinical specimens retrieved from a patient. The ongoing efforts in this field continue to bring the LIBS technology closer to its use as a tool for rapid pathogen identification.

Vita Auctoris

NAME: Alexandra E. Paulick

PLACE OF BIRTH: Windsor, Ontario

YEAR OF BIRTH: 1994

EDUCATION: B. Sc. [Honours] Physics, 2016
University of Windsor, Windsor, Ontario

M. Sc. Physics, 2018
University of Windsor, Windsor, Ontario